

EVALUATING BIOFLAVONOID INDUCED DNA DOUBLE-STRAND BREAKS
AND CHROMOSOMAL TRANSLOCATIONS

by

Donna Goodenow

A dissertation submitted to the faculty of
The University of North Carolina at Charlotte
in partial fulfillment of the requirements
for the degree of Doctor of Philosophy in
Biology

Charlotte

2020

Approved by:

Dr. Christine Richardson

Dr. Andrew Truman

Dr. Ian Marriott

Dr. Shan Yan

Dr. Jun-Tao Guo

ABSTRACT

DONNA GOODENOW. Evaluating bioflavonoid induced DNA double-strand breaks and chromosomal translocations.
(Under the direction of DR. CHRISTINE RICHARDSON)

Dietary bioflavonoids are a class of chemical compounds found in soy, fruits, vegetables, tea, coffee, wine, and dietary supplements. They are separated into 12 different sub-classes based upon their structure, however only six are dietarily relevant: flavanols, flavonols, flavones, isoflavones, flavanones, and anthocyanidins. Similar to the chemotherapeutic etoposide, bioflavonoids are characterized by multiple phenolic rings. Etoposide is a chemotherapeutic drug that causes extensive DNA double-strand breaks (DSBs) through the poisoning of the enzyme topoisomerase II (Top2). The Top2 enzyme's normal function is to relax supercoiled DNA and to do this the enzyme catalyzes a transient DSB. However, Top2 poisons, such as etoposide, interrupt Top2 and prevent the enzyme from religating the normally transient DSB. These DSBs must be legitimately repaired by the cells, otherwise chromosomal translocations may occur. Etoposide treatment is associated with the development of therapy-related leukemia due to chromosomal translocations involving the *MLL* gene. These translocations have been linked to etoposide's Top2 poisoning capabilities. Infant leukemia, which is characterized by aggressive symptoms and a low survival rate, are characterized by *MLL* translocations which may be linked to maternal ingestion of bioflavonoids while pregnant.

The purpose of my dissertation research was to investigate the mechanisms by which bioflavonoids may cause DNA DSBs and chromosomal translocations involving the *MLL* gene. I hypothesized that bioflavonoids would cause DNA DSBs similarly to

etoposide and that bioflavonoids of the same sub-class would resolve these breaks with similar kinetics. I also hypothesized that combination treatments of bioflavonoids would show similar resolution kinetics to the individual bioflavonoid treatments. Next, I hypothesized that bioflavonoids would cause DNA DSBs and chromosomal translocations through poisoning of Top2. Finally, I hypothesized that chronic, low dose treatments of bioflavonoids would cause sustained chromosomal translocations. Utilizing γ -H2AX, a marker of DNA DSBs, and a chromosomal translocation reporter cell line I tested these hypotheses with a panel of bioflavonoids. I determined that while bioflavonoids do cause DNA DSBs similar to etoposide, the mechanism by which these DSBs are resolved is not dependent on their sub-class, but instead is dependent upon their classification as a traditional or covalent Top2 poison. Additionally, I determined that while bioflavonoids do utilize Top2 to cause DNA damage and translocations, bioflavonoids also cause damage and translocation through Top2-independent mechanisms, that may be more mutagenic for specific bioflavonoids. Finally, I determined that chronic, low dose bioflavonoids do appear to cause small populations containing translocation events, but further research is needed to verify these observations.

DEDICATION

I dedicate my doctoral dissertation work to my mother, Marsha Goodenow. Without her, I would not have grown to be the person I am today. Thank you for all your love, support and encouragement throughout my lifetime, especially during this dissertation process.

ACKNOWLEDGEMENTS

To Dr. Christine Richardson, I would like to extend my most sincerely gratitude for all she has done for me throughout my graduate experience. Dr. Richardson has been a spectacular mentor to me with her endless patience, words of wisdom, and guiding hand in writing and the lab. Through her my skills both within and outside of the lab have grown and I hope to always be as dedicated to my work as she is to hers.

To my committee members Dr. Jun-Tao Gou, Dr. Ian Marriott, Dr. Andrew Truman, and Dr. Shan Yan, thank you all for your guidance and feedback throughout my research. Additionally, Dr. Marriott, thank you for your wonderful immunology class. I hope to integrate the knowledge gained from you into my future research. Dr. Truman, thank you for your wonderful support through the many classes I have taken with you. I have learned countless lab techniques from you that I hope to utilize in the future. To Dr. Shan Yan, thank you for your mentorship and it was a pleasure to learn from you and spend time together at the EMGS conferences. Also, I owe Dr. Jennifer Weller and Dr. Robert Reid for their collaboration and knowledgeable insights to my research project.

I would like to also thank Kiran Lalwani for her support in the lab and through this writing process. Kiran, you have been an amazing friend and colleague and I know you will do well in your future endeavors. To my other lab mates, past and current, Symonne Martin, Ami Changela, McKenna Williams, Rachel Sielaty, Chelsea Wright, Anindita Ghosh, Chase Berman, Mark Sahyouni, and Faith Emmanuel thank you all for your companionship and support of my research.

Thank you to my friends and colleagues in the department for your support and companionship through both fun and difficult times. Thanks especially to Austin Jefferies,

Dr. Amanda Burmeister, Dr. Whitney Leach, Dr. Priyanka Grover, Jill Waller, Laura Knighton, and Minnie Webster. To those outside of the department, Casey Hurst, Coren O'Hara, Dr. Julie Goodliffe, and Dr. Katherine Hall-Hertel, thank you for your support in my endeavors in the graduate student community.

Thank you to Dr. Rebecca Powell, Dr. Iain McKillop, Dr. Patricia Koplas, Dr. Jeffery Thomas, and Dr. Jennifer Easterwood, for their support as a post-baccalaureate and undergraduate, which lead me to graduate school.

Finally, I also owe my mother and long-time friend, Amanda Seagroves, a huge thanks for their constant support throughout my time at UNC Charlotte.

TABLE OF CONTENTS

LIST OF FIGURES	xii
LIST OF TABLES	xvi
FREQUENTLY USED ABBREVIATIONS	xviii
CHAPTER 1: INTRODUCTION	1
1.1 DNA Double-Strand Breaks: Causes and Repair	1
1.2 Double-Strand Break Repair: Homologous Recombination	3
1.3 Double-Strand Break Repair: End-Joining	9
1.4 Consequences of Illegitimate DNA Repair: Chromosomal Translocations	10
1.5 Infant Leukemia and the <i>MLL</i> gene	13
1.6 Topoisomerase II	15
1.7 Dietary Bioflavonoids	18
1.7.1 Compounds Used in this Research: Isoflavones	19
1.7.2 Compounds Used in this Research: Flavonols	20
1.7.3 Compounds Used in this Research: Flavones	21
1.8 Pleiotropic Bioflavonoid Effects	23
1.9 Aims of This Research	25
CHAPTER 2: MATERIALS AND METHODS	27
2.1 Cell Lines	27
2.2 Treatment Compounds	28
2.3 Treatment of Cells and Detection of γ -H2AX Foci	29
2.3.1 Experimental Design: Do Bioflavonoids Induce Prolonged DSBs?	29

2.3.2	Experimental Design: Do Bioflavonoids Induce DSBs through Top2 Poisoning?	30
2.3.3	γ -H2AX Staining Protocol and Scoring of Foci	31
2.4	Quantification of Chromosomal Translocations	31
2.5	Chronic, Low Dose Bioflavonoid Treatment	32
CHAPTER 3: BIOFLAVONOIDS INDUCE PROLONGED DNA DSBS		34
3.1	Results for No Treatment, Negative Controls, and Etoposide	34
3.2	Bioflavonoids Induce Persistent DNA DSBs that are Resolved with Differential Kinetics	38
3.2.1	Genistein	39
3.2.2	Quercetin	42
3.2.3	Kaempferol	44
3.2.4	Myricetin	46
3.2.5	Luteolin	48
3.2.6	Genistein and Quercetin Combination Treatment	50
3.2.7	Genistein, Quercetin, and Luteolin Combination Treatment	55
3.3	Results for Chemical Control: Dipyrone	57
3.4	Conclusions	61
CHAPTER 4: BIOFLAVONOIDS INDUCE DNA DSBS THROUGH TOP2- DEPENDENT AND INDEPENDENT MECHANISMS		66
4.1	Impact of DEX Pre-Treatment on Etoposide Induced DNA Damage	66
4.2	DNA Damage in Cells Treated with DEX Prior to Etoposide Exposure	69

4.3	Dexrazoxane Partially Reduces DNA Damage Induced by Genistein or Quercetin	71
4.4	Dexrazoxane Minimally Reduces DNA Damage Induced by Luteolin	73
4.5	Dexrazoxane Does Not Reduce DNA Damage Induced by Kaempferol	74
4.6	Dexrazoxane Cannot Reduce DNA Damage Induced by Combined Treatment of Bioflavonoids	75
4.7	Dexrazoxane Minimally Reduces DNA Damage Induced by Dipyron	78
4.8	Conclusions	79
CHAPTER 5: BIOFLAVONOIDS INDUCE CHROMOSOMAL TRANSLOCATIONS THROUGH TOP2- DEPENDENT AND INDEPENDENT MECHANISMS		81
5.1	Chromosomal Translocations Promoted by Bioflavonoid Exposure and Reduced by Dexrazoxane	81
5.2	Conclusions	84
CHAPTER 6: CHRONIC, LOW DOSE EXPOSURE TO BIOFLAVONOIDS		86
6.1	Detection of Chromosomal Translocations Induced by Chronic, Low Dose Bioflavonoid Treatment: Analysis of Cells After Paraformaldehyde Fixation	86
6.2	Detection of Chromosomal Translocations Induced by Chronic, Low Dose Bioflavonoid Treatment: Analysis of Cells without Fixation	89
6.3	Conclusions	93
CHAPTER 7: DISCUSSION AND FUTURE DIRECTIONS		95
7.1	Mechanistic Insights on Bioflavonoids as Top2 Poisons	95
7.2	Proposed Future Directions	102
7.2.1	Investigate Bioflavonoids that are Covalent Top2 Poisons	103

7.2.2	Investigate Bioflavonoids that are Proposed Covalent Top2 Poisons	103
7.2.3	Investigate Bioflavonoids Top2-Independent Mechanisms of DNA Damage	104
7.2.4	Determine Potential Mechanisms Bioflavonoids Use to Cause Translocations	106
7.3	Implications of this Research	107
	REFERENCES	109
	APPENDIX I: CURRENT CURRICULUM VITAE	121
	APPENDIX II: END-SEQ PRELIMINARY PROTOCOL	124

LIST OF FIGURES

FIGURE 1.1: Summarization of DSB Repair Outcomes by Homologous Recombination and End-Joining	2
FIGURE 1.2: Summarization of Causes, Repair and Outcomes of DNA Double-Strand Breaks	3
FIGURE 1.3: Basic Schematic Representation of the DNA Damage Response	4
FIGURE 1.4: DNA Damage Response to Ionizing Radiation Leading to Homologous Recombination	5
FIGURE 1.5: Double-Strand Break Repair: Homologous Recombination	8
FIGURE 1.6: Double-Strand Break Repair: End-Joining	10
FIGURE 1.7: Nuclear Proximity is Essential for Translocation Events	13
FIGURE 1.8: The Mixed Lineage Leukemia Gene and Translocation Partners	14
FIGURE 1.9: The MLL Breakpoint Cluster Region	15
FIGURE 1.10: Mechanism of Topoisomerase II	16
FIGURE 1.11: Removal of Stabilized Top2 Cleavage Complex from DNA	17
FIGURE 1.12: Basic Chemical Structures of Dietary Bioflavonoids	18
FIGURE 1.13: Chemical Structure of Isoflavone: Genistein	20
FIGURE 1.14: Chemical Structure of Flavonols: Quercetin, Kaempferol, and Myricetin	21
FIGURE 1.15: Chemical Structure of Flavone: Luteolin	22
FIGURE 1.16: Osheroff's Proposed Rules for Top2 Poison Classification of Bioflavonoids	23
FIGURE 2.1: <i>MLL-AF9-GFP</i> Translocation Reporter Cell Line	28
FIGURE 2.2: Experimental Design for Evaluation of DNA Damage Repair Kinetics Post-Exposure to Bioflavonoid	29

FIGURE 2.3: Experimental Design for Evaluation of DNA Damage Repair with Top2 Inhibited by Dexrazoxane (DEX)	30
FIGURE 2.4: Experimental Design for Evaluation of Chromosomal Translocations with Top2 Inhibited by Dexrazoxane (DEX)	32
FIGURE 2.5: Experimental Design for Chronic, Low Dose Bioflavonoid Treatments	33
FIGURE 3.1: DNA Damage in a Negative Control Panel at 4h Post-Exposure	35
FIGURE 3.2: DNA Damage Repair Kinetics Over 8h with Etoposide Treatment	37
FIGURE 3.3: DNA Damage Repair Kinetics Over 8h with Genistein Treatment	40
FIGURE 3.4: DNA Damage Repair Kinetics Over 8h with Quercetin Treatment	42
FIGURE 3.5: DNA Damage Repair Kinetics Over 8h with Kaempferol Treatment	44
FIGURE 3.6: DNA Damage Repair Kinetics Over 8h with Myricetin Treatment	47
FIGURE 3.7: DNA Damage Repair Kinetics Over 8h with Luteolin Treatment	49
FIGURE 3.8: DNA Damage Repair Kinetics Over 8h with Genistein/Quercetin Treatment	52
FIGURE 3.9: Generalized Repair Kinetics for Single and Combination Treatments	54
FIGURE 3.10: DNA Damage Repair Kinetics Over 8h with Genistein/Quercetin/Luteolin Treatment	56
FIGURE 3.11: DNA Damage Repair Kinetics Over 8h with Dipyrone Treatment	59
FIGURE 4.1: Preliminary DNA Damage Results to Determine DEX Dosing	67
FIGURE 4.2: DNA Damage in Cells Treated with DEX Prior to Etoposide Exposure	69

FIGURE 4.3: DNA Damage in Cells Treated with DEX Prior to Myricetin Exposure	70
FIGURE 4.4: DNA Damage in Cells Treated with DEX Prior to Genistein Exposure	71
FIGURE 4.5: DNA Damage in Cells Treated with DEX Prior to Quercetin Exposure	73
FIGURE 4.6: DNA Damage in Cells Treated with DEX Prior to Luteolin Exposure	74
FIGURE 4.7: DNA Damage in Cells Treated with DEX Prior to Kaempferol Exposure	75
FIGURE 4.8: DNA Damage in Cells Treated with DEX Prior to Genistein/Quercetin Exposure	76
FIGURE 4.9: DNA Damage in Cells Treated with DEX Prior to Genistein/Quercetin/Luteolin Exposure	77
FIGURE 4.10: DNA Damage in Cells Treated with DEX Prior to Dipyrone Exposure	78
FIGURE 5.1: Quantification of Translocations in Bioflavonoid Treated Cells with Top2 Inhibited with Dexrazoxane	83
FIGURE 6.1: Percent of Fixed MAG Cells with Translocations in Control Groups Over 20 Cycles	87
FIGURE 6.2: Percent of Fixed MAG Cells with Translocations in Genistein, Genistein/Quercetin and Dipyrone Groups Over 20 Cycles	88
FIGURE 6.3: Percent of Fixed MAG Cells with Translocations in Quercetin, Luteolin, and Genistein/Quercetin/Luteolin Groups Over 20 Cycles	88
FIGURE 6.4: Percent of Fixed MAG Cells with Translocations in Myricetin and Kaempferol Groups Over 20 Cycles	89
FIGURE 6.5: Percent of MAG Cells with Translocations in No Treatment and Luteolin Over 20 Cycles	91
FIGURE 6.6: Percent of MAG Cells with Translocations in DMSO and Dipyrone Groups Over 20 Cycles	91

FIGURE 6.7: Percent of MAG Cells with Translocations in Genistein, Kaempferol, Myricetin, and G/Q/L Groups Over 20 Cycles	92
FIGURE 6.8: Percent of MAG Cells with Translocations in Quercetin and G/Q Groups Over 20 Cycles	93
FIGURE 6.9: Representative Images of Morphological Changes in Cells with 20 Cycles of Bioflavonoid Treatment	94

LIST OF TABLES

TABLE 3.1: DNA Damage in a Negative Control Panel at 4h Post-Exposure Data Analysis	36
TABLE 3.2: DNA Damage Repair Kinetics Over 8h with Etoposide Treatment Data Analysis	38
TABLE 3.3: DNA Damage Repair Kinetics Over 8h with Genistein Treatment Data Analysis	41
TABLE 3.4: DNA Damage Repair Kinetics Over 8h with Quercetin Treatment Data Analysis	43
TABLE 3.5: DNA Damage Repair Kinetics Over 8h with Kaempferol Treatment Data Analysis	46
TABLE 3.6: DNA Damage Repair Kinetics Over 8h with Myricetin Treatment Data Analysis	48
TABLE 3.7: DNA Damage Repair Kinetics Over 8h with Luteolin Treatment Data Analysis	50
TABLE 3.8: DNA Damage Repair Kinetics Over 8h with Genistein/ Quercetin Treatment Data Analysis	53
TABLE 3.9: DNA Damage Repair Kinetics Over 8h with Genistein/ Quercetin/ Luteolin Treatment Data Analysis	57
TABLE 3.10: DNA Damage Repair Kinetics Over 8h with Dipyrone Treatment Data Analysis	60
TABLE 4.1: Preliminary DNA Damage Results to Determine DEX Dosing Data Analysis	68
TABLE 4.2: DNA Damage in Cells Treated with DEX Prior to Etoposide Exposure Data Analysis	69
TABLE 4.3: DNA Damage in Cells Treated with DEX Prior to Myricetin Exposure Data Analysis	70
TABLE 4.4: DNA Damage in Cells Treated with DEX Prior to Genistein Exposure Data Analysis	72

TABLE 4.5: DNA Damage in Cells Treated with DEX Prior to Quercetin Exposure Data Analysis	73
TABLE 4.6: DNA Damage in Cells Treated with DEX Prior to Luteolin Exposure Data Analysis	74
TABLE 4.7: DNA Damage in Cells Treated with DEX Prior to Kaempferol Exposure Data Analysis	75
TABLE 4.8: DNA Damage in Cells Treated with DEX Prior to Genistein/ Quercetin Exposure Data Analysis	77
TABLE 4.9: DNA Damage in Cells Treated with DEX Prior to Genistein/ Quercetin/Luteolin Exposure Data Analysis	78
TABLE 4.10: DNA Damage in Cells Treated with DEX Prior to Dipyrone Exposure Data Analysis	79
TABLE 5.1: Inhibition of Top2 with Dexrazoxane Pre-treatment and Frequency of Bioflavonoid-induced Translocations	83
TABLE 7.1: Visual Summarization of Hypothesized Mechanisms Bioflavonoids Utilize to Damage DNA	102

FREQUENTLY USED ABBREVIATIONS

DSB: Double strand break

Top2: Topoisomerase II

HR: Homologous recombination

NHEJ: Non-homologous end-joining

Alt-EJ: Alternative end-joining

ES cells: Embryonic stem cells

GFP: Green Fluorescent Protein

bcr: breakpoint cluster region

MAG: *MLL-AF9-GFP*

γ -H2AX: Gamma (phosphorylated) histone variant 2AX

DEX: Dexrazoxane

CHAPTER 1: INTRODUCTION

1.1 DNA Double-Strand Breaks: Causes and Repair

The integrity of DNA is essential to genome stability and proper cellular function. DNA damage when repaired improperly can result in hazardous mutations that alter cellular phenotype or lead to cell death. DNA double-strand breaks (DSBs) are one type of DNA damage, these are caused by endogenous factors like reactive oxygen species and replication fork collapse or by exogenous factors like radiation or chemotherapeutics¹⁻³.

However, DSBs are not always hazardous to a cell, though DNA damage in any form can lead to mutations, some mutations are beneficial to cells. DSBs in particular are key to genetic diversity and evolution. DSBs are utilized within immune cells to promote antigen receptor diversity and in meiosis DSBs induce crossing over which promotes gamete diversity. In addition, DSBs are used in normal cell function to relax supercoiled DNA for transcription and replication. Though DSBs are useful for cell function and genetic diversity, DSBs must be carefully regulated by specialized enzymes within the cell to ensure they do not lead to hazardous mutations. Enzymes such as RAG1/2 in immune cells and topoisomerase II in all cells, follow strict processes to create and repair DSBs. This means that any DSB caused by these specialized enzymes is transient; the DSB is generated quickly for a specific purpose, then religated. When the process of these proteins is interfered with, these transient DSBs can become stable DSBs, which must then be properly repaired, or hazardous mutations may occur.

DSBs are repaired through two main pathways; homologous recombination (HR) and end-joining (EJ). Furthermore, EJ can be separated into canonical non-homologous end-joining (NHEJ) and alternative end-joining (alt-EJ) (also known as microhomology

mediated end-joining). HR is the most accurate type of DSB repair as it uses a nearby homologous DNA sequence as a template to repair the damage, but this pathway requires the coordination of over 20 proteins, the broken ends must be heavily processed, and this type of repair typically only occurs in S/G2 phases of the cell cycle. Both forms of EJ are relatively quick compared to HR, as they require little to no end processing and these can both occur throughout the cell cycle. Though classical NHEJ and alt-EJ are quicker, they cause slight deletions or insertions to the sequence. Additionally, while HR can deal with protein blocked, two-ended, and one-ended breaks (caused by ssDNA breaks that are converted to DSBs through DNA replication), NHEJ and alt-EJ can only deal with two-ended breaks that are protein free (clean breaks). In addition, if there are multiple DSBs in the cell there is an increased risk of a chromosomal translocations occurring. Research shows that alt-EJ is the most mutagenic form of DSB repair^{1,4} (Figure 1.1).

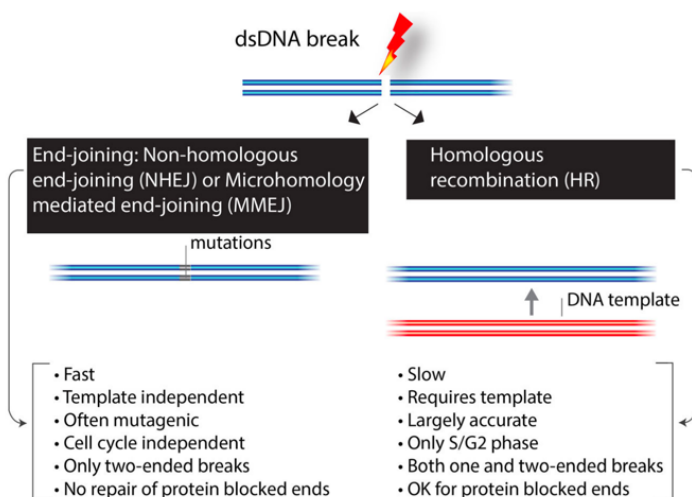


Figure 1.1: Summarization of DSB Repair Outcomes by Homologous Recombination and End-Joining. Microhomology mediated end-joining is another term for alternative end-joining (alt-EJ). Figure modified from Ranjha, Howard, and Cejka, 2018.

Much is still unknown about what directs DNA repair pathway choice, particularly alt-EJ, but there is strong evidence that the levels of DNA repair proteins and pattern of histone

modifications direct the repair pathway choice for DSBs⁵⁻⁷. For a visual summary of the causes, mechanisms of repair, and outcomes of repair for DSBs, see Figure 1.2.

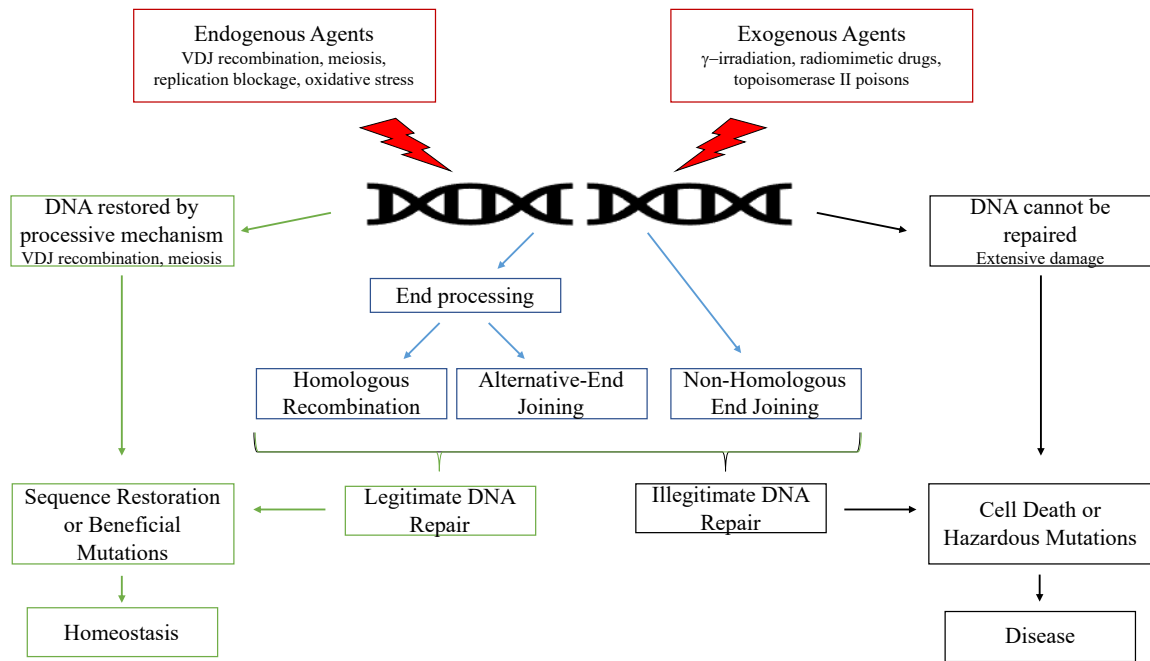


Figure 1.2: Summarization of Causes, Repair and Outcomes of DNA Double-Strand Breaks. Red, causes of DSBs, blue, mechanisms of DSB repair, green, positive repair outcomes, black, negative repair outcomes.

1.2 Double-Strand Break Repair: Homologous Recombination

HR is the most accurate type of DNA repair; however, HR has the most protein involvement, the most regulations, and takes the most time of the three repair pathways. For a DSB to be repaired by HR or either of the EJ pathways, first the damage must be sensed, then signal transduction pathways must be activated to bring in the proteins necessary to repair the damage, this is called the DNA damage response (DDR)^{2,3,8-11} (Fig. 1.3).

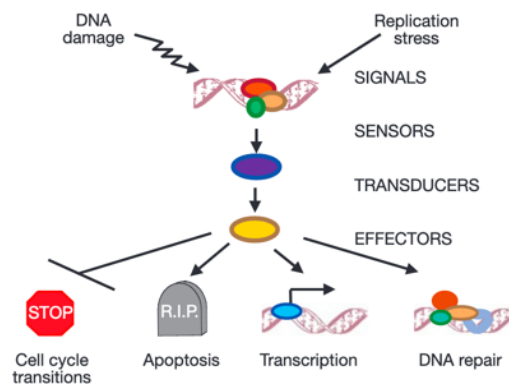


Figure 1.3: Basic Schematic Representation of the DNA Damage Response. After damage, the sensors recognize the damage and activate the transducers which call in and activate the effectors. Effectors are the DNA repair proteins, that prime the cell to respond to and fix the damage. Effectors are also proteins that can halt the cell cycle, begin apoptotic programming, and induce transcription of needed proteins. Figure from Zhou and Elledge, 2000.

After a DSB has occurred in order to initiate HR, first poly(ADP-ribose) polymerase 1 (PARP1) must recognize the break. PARP1 immediately adds branched poly(ADP-ribose) (PAR) groups to itself and nearby histones. The branched PAR recruits the Mre11-Rad50-Nbs1 (MRN) complex and inactive ATM kinase dimers with TIP60, an acetyltransferase, attached. PARG quickly removes the PAR groups allowing the MRN complex to bind to the DSB. MRN allows ATM to bind at the DSB site and activate through acetylation by TIP60 and auto-phosphorylation by ATM, thereby allowing TIP60 to separate from ATM. Once active, ATM begins phosphorylating everything it can^{1,3,11-13}.

One of the initial targets is the MRN complex, which upon phosphorylation can then begin to process the DSB ends with CtIP that is also ATM phosphorylated. Another primary target is the H2AX histone. Upon phosphorylation (and acetylation from TIP60) H2AX, now called γ -H2AX, has some chromatin remodeling functions necessary for DNA repair and γ -H2AX acts as a signal to recruit a number of other proteins as well as. The first protein recruited is MDC1 which helps with chromatin remodeling and becomes phosphorylated by ATM which thereby recruits RNF6 dimers that have ubiquitination (Ub)

functions. HERC2 associates with this phosphorylated RNF6 complex and appears to recruit PIAS4 which has sumoylation capabilities. RNF6 becomes SUMOylated and mono-Ub's histones in the area, which recruits RNF168, another ubiquitin ligase, that gets SUMOylated and poly-Ub's nearby histones. The poly-Ub trees call in BRCA1-A complexes by RAP80 mediators. These complexes cause histone modifications that bring in 53BP1, which has more histone remodeling functions and can inhibit end resection that occurs through the MRN and CtIP^{1,11,13,14} (Fig. 1.4).

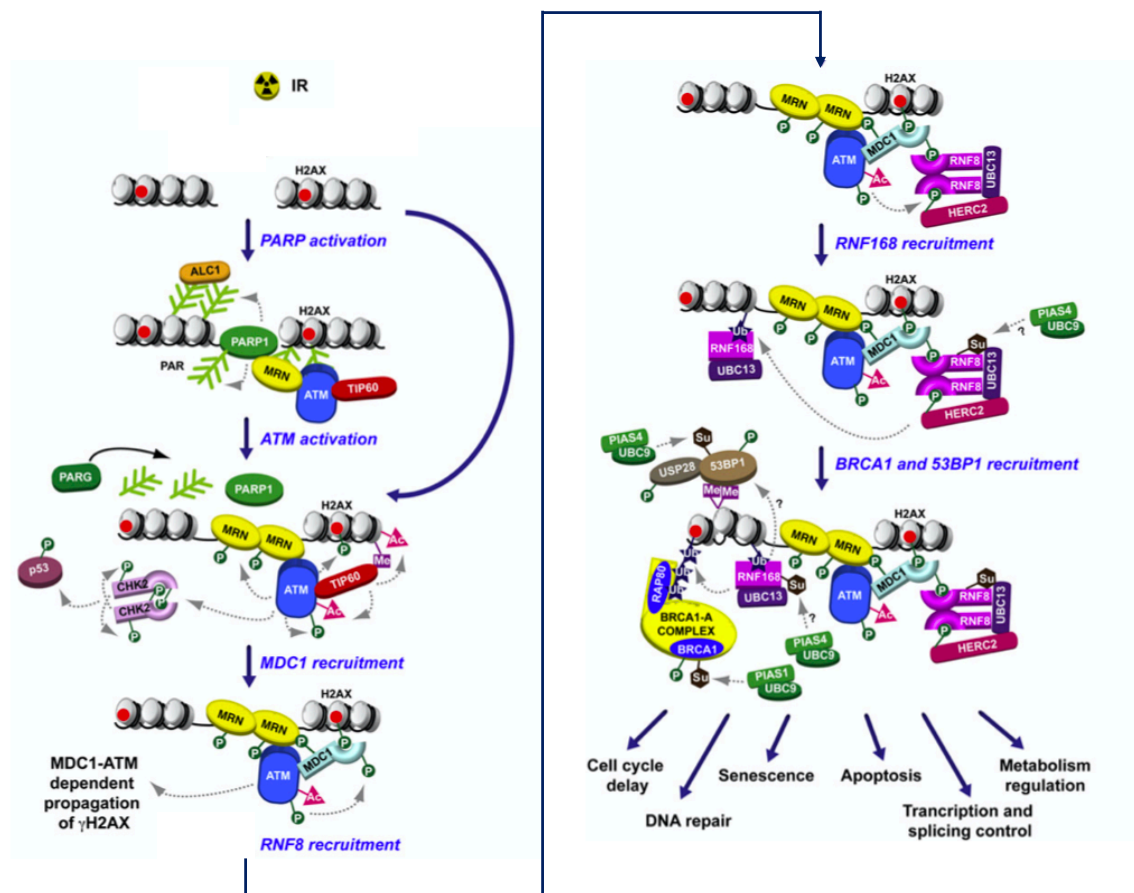


Figure 1.4: DNA Damage Response to Ionizing Radiation Leading to Homologous Recombination. Figure modified from Ciccia and Elledge, 2010.

In addition to all the histone remodeling, other proteins become phosphorylated and activated by ATM. Chk2 is one such protein, and it has protein kinase abilities also allowing it to phosphorylate a number of effector proteins in the cell cycle regulation like

p53 which can be modified by either Chk2 or ATM (or ATR or Chk1). Also, ARF protein (p14) seems to stabilize TIP60 interactions with ATM for better activation and promoted genome stability¹¹.

While the histone remodeling is occurring and other proteins are being recruited, the MRN (Mre11 has nuclease function and Rad50-Nbs1 have ATPase functions) works with CtIP to resect the DSB ends in a 3' to 5' fashion, termed short range end resection. Upon completion of short-range end resection, Exo1 or Dna2 nucleases work on long range end resection in a 5' to 3' direction (bidirectional resection). Exo1 has dsDNA nuclease function, while Dna2 must work with a helicase like BLM or WRN to unwind DNA for its ssDNA nuclease abilities^{3,12,13,15}. While long range end resection is occurring, RPA is binding to the 3' ssDNA overhang to protect it from nucleases. After this resection, one type of HR can occur called single strand annealing (SSA), where the two pieces of RPA coated DNA associate with one another with the help of Rad52 and if regions of homology are found they anneal to one another. Non-homologous flaps are cleaved off by enzymes like XPF-ERCC1 and ligated by LigIII (Fig. 1.5). This type of HR can cause large deletions and therefore has similarities to both NHEJ and HR^{1,11-13,16}.

Other forms of HR, break-induced replication (BIR), synthesis-dependent strand annealing (SDSA) and canonical HR (cHR), all use BRCA 1 and 2 with Rad51 for homology searches that cause strand-invasion, D-loop formation and resolution/dissolution. First for these, RPA must be dissociated from the ssDNA for Rad51 binding, this is mediated by DSS1 and BRCA2, which help displace RPA and stabilize ATP on Rad51 increasing its binding affinity for the ssDNA. Once Rad51 is on the DNA and the nucleofilament has formed, it can search for homology, BRCA1 may help with this

search^{1,11,13}. Any homology less than 7nt is a weak interaction and Rad51 moves on, 7nt and more allows the strand to search for further homology¹³. If found, the ATP on Rad51 is hydrolyzed causing the dsDNA to dissociate and the nucleofilament anneals with the template strand. RPA stabilizes this D-loop formation by binding to the displaced strand. DNA Polymerase δ or ϵ uses the invading strand as a primer to start synthesis^{12-14,17}.

In BIR, DNA Pol δ is used and the synthesis continues until the end of the chromosome causing definite gene conversion that can be very mutagenic, however this is the only option for one-side DSBs. With SDSA and cHR synthesis only goes part way down the strand instead of to the end of the chromosome. If the D-loop destabilizes by branch migration or helicases like RTEL1 the invading strand leaves the D-loop and religates back to its partner. If it does not destabilize, the other end of the DSB comes into the D-loop (no Rad51 involved) and religates to its former partner causing a double Holliday Junction (dHJ) and resolution or dissolution must occur^{1,11,13}.

Dissolution is the preferred mechanism in mitotic cells as it causes no crossing over. This is mediated by the BTRR complex, with the BLM helicase which cause branch migration of the two junctions towards one another until they form a hemicatane, which is where they cannot move any further, because they have run into each other¹. And the RMI1 and RMI2 mediate their unwinding through top3 α activity^{1,13}. If they are not dissolved, resolution must occur. Resolution can happen with crossover or non-crossover products and different sets of resolvases mediate this. There is the Gen1 resolvase which forms a dimer and can cause two nicks in the dHJ giving two religatable products, or you can have SM complex formation. The SM complex is made up of SLX1 and SLX4 which

make a 5' cut on one side of the HJ and the MUS81-EME1 proteins make a 3' cut on the other side, allowing for resolution^{1,3,8,11-13}.

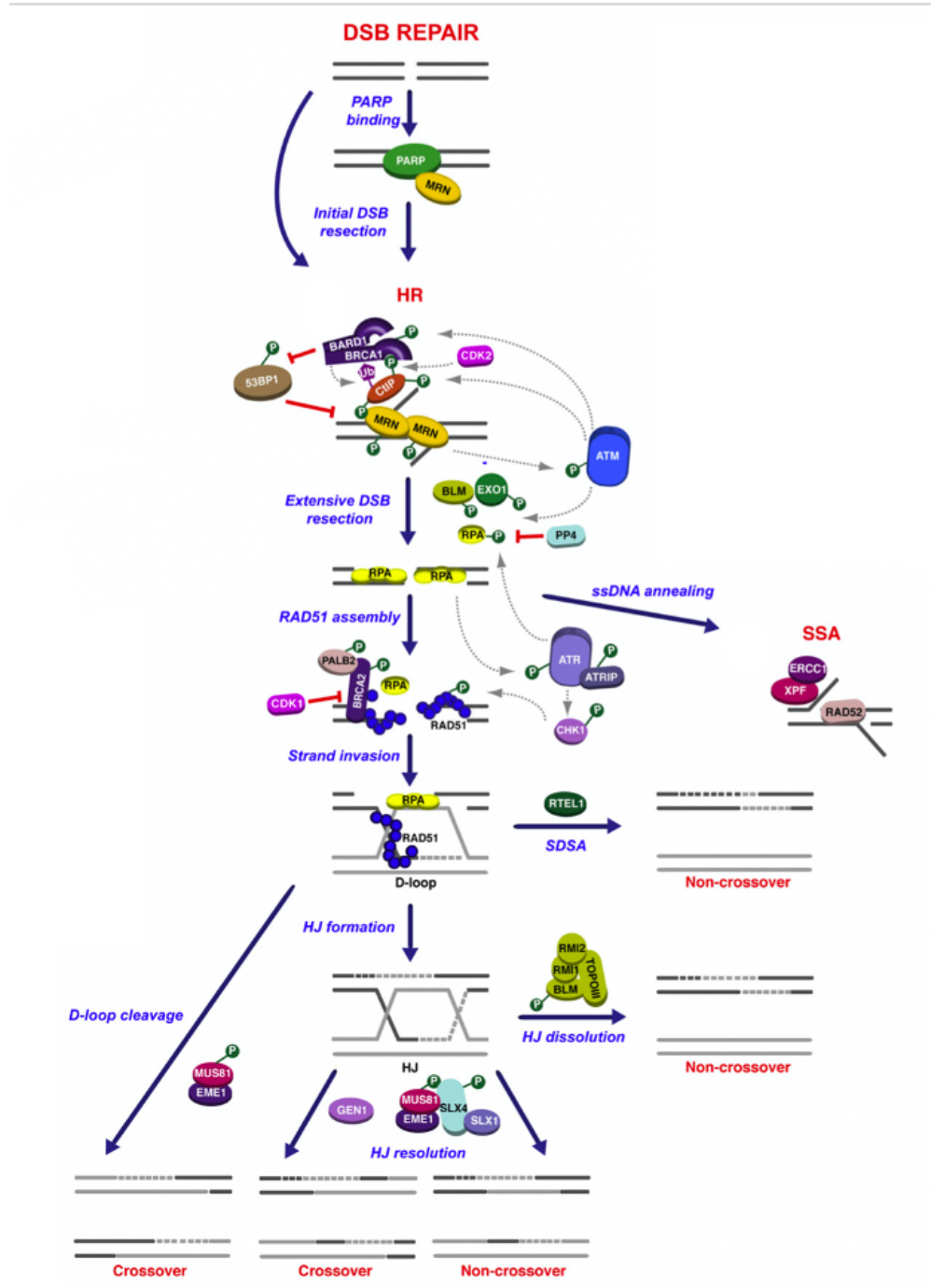


Figure 1.5: Double-Strand Break Repair: Homologous Recombination. Figure modified from Ciccia and Elledge, 2010.

1.3 Double-Strand Break Repair: End-Joining

End-joining is the second method of DSB repair. There are many considerations when the cell uses this pathway compared to HR, such as is the DSB one or two sided, is it clean or dirty (are there chemical groups or proteins attached to the DSBs) and what phase of the cell cycle it is in. With EJ, cell cycle is not a major factor and does not limit the pathway, but EJ typically needs clean DSBs and can only handle two sided, not one sided, breaks. The first step of NHEJ is that Ku70-80 dimers need bind to the DSB ends. Ku70-80 competes with PARP1 for binding to the DSB, if Ku70-80 binds first there is minimal end processing and NHEJ is used^{1,3,14,18-20}. Next DNA-PK is recruited to the Ku complex. DNA-PK can determine if the ends are blunt, like from a nuclease cleavage or RAG from VDJ recombination, or if there are overhangs or protein/group additions. If the break is clean, DNA-PK recruits XRCC4-XLF and LigIV, and these proteins work together to seal the DNA break^{3,14,15}. However, if there is an overhanging end or proteins are attached to the break site, DNA-PK recruits the ARTEMIS complex for end processing. ARTEMIS can normally move around protein groups and with its nuclease abilities it can digest the DSBs ends until they are blunt. After processing, the process follows the same scheme as before with XRCC4-XLF and LigIV recruitment to seal the DSB^{1,3,11,14,15,17,21} (Fig. 1.6A).

However, if PARP1 binds to the DSB before Ku70-80, the MRN complex will be recruited to process the ends for either HR or alt-EJ. Alt-EJ is a more recently discovered method of DSB repair and little is known about it. Alt-EJ seems to be a back-up repair mechanism for when HR and NHEJ are not an option. It is likely that alt-EJ occurs when processing for HR has begun, perhaps because PARP1 bound to the break first, or Ku70-80 is depleted in the cell, or because the DSB ends have proteins bound or the cell is in G1

phase of the cell cycle with no homologous chromosome to use as an HR template. For whichever reason alt-EJ begins, the process starts with minimal end processing (5-25 nucleotides) by the MRN complex working with CtIP to create short DNA overhangs with small regions of homology. After processing, XRCC1 and Lig3 work in complex to religate the ends and remove the overhanging bases. Alt-EJ is considered a quick and dirty method of DSB repair that is more mutagenic than HR or NHEJ^{18,22-24} (Fig. 1.6B).

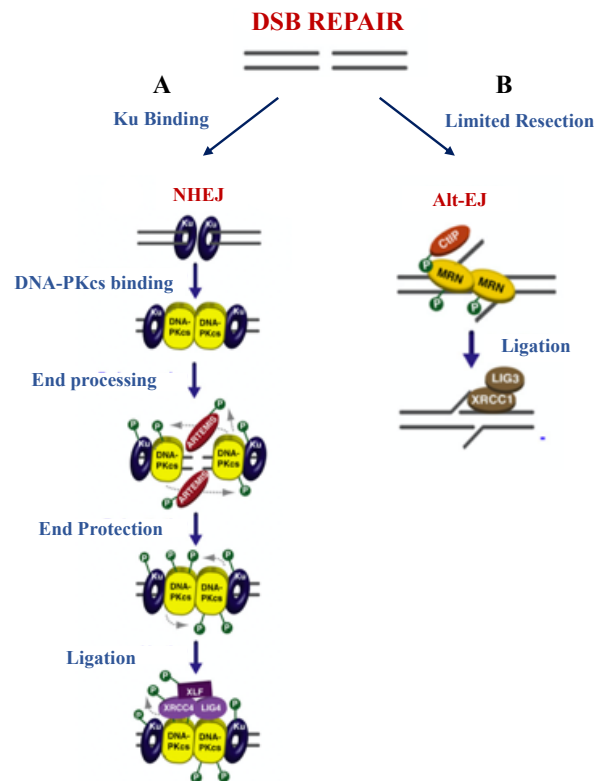


Figure 1.6: Double-Strand Break Repair: End-Joining. A, Classical non-homologous end-joining (NHEJ) occurs when Ku70-80 dimer binds to the DSB. B, Alternative end-joining occurs when PARP1 binds to DSB first thereby recruiting the MRN complex. Figure modified from Ciccia and Elledge, 2010.

1.4 Consequences of Illegitimate DNA Repair: Chromosomal Translocations

When HR, NHEJ, or alt-EJ repair mechanisms fail to restore DNA to its original sequence, this is considered a mutational event. NHEJ and alt-EJ frequently cause minor mutations in the form of small insertions or deletions to the DNA sequence, which typically

do not cause major cellular effects. However, large insertions, deletions, and even chromosomal translocations can occur and have hazardous effects on cellular function. My studies in particular focus on the formation of chromosomal translocations given their relevance to the etiology of infant leukemia (discussed in following section). Translocations frequently cause cancer and other diseases due to interference with normal protein expression²⁵. Translocations can lead to a protein coding gene being controlled by a different promoter or enhancer elements, or to the fusion of two different protein coding genes, which leads to the over or under expression of a protein or the expression of a chimeric protein with modified function^{15,25-27}.

One of the most well studied examples of a translocation that causes disease is the translocation that occurs between the BCR gene on the chromosome 22 and the ABL gene on the chromosome 9, which causes Chronic Myeloid Leukemia (CML). The normal function of the BCR gene is not completely understood, but it is known that BCR has kinase functions and GTPase relations. ABL is a protein tyrosine kinase that is associated with the cellular membrane and phosphorylates cell cycle proteins, including Mdm2, and DNA repair proteins, like BRCA1 and Rad51. ABL normally has an SH3 domain that regulates its function causing it to be activated only when its functions are needed^{14,15,17,25,27}.

To generate the BCR-ABL oncogenic translocation, a DSB in the ABL gene between its first two exons leaves a large portion of the gene intact, with all its protein kinase ability, but the regulatory domain, SH3, is rendered non-functional. This DSB is then repaired by ligation of the ABL gene with a segment of the BCR, which also had a DSB occur, thereby creating what is known as the Philadelphia chromosome. When this protein is transcribed, the ABL segment of the protein is now constitutively activated and can phosphorylate any

of its targets. This causes decreased cell cycle regulation and inhibited DNA repair, creating a cell that can divide without cell cycle control and that has a decreased ability to repair DNA damage leading to a mutator phenotype^{14,15,17,25,27}.

A translocation event can occur due to NHEJ, alt-EJ, or rarely SSA. In order for a translocation to occur, at least two DSBs must occur on separate chromosomes and the chromosomes with the DSBs must be in close proximity to one another within the nucleus. Typically, translocations occur between genes that are contained within the same transcription factory (Fig. 1.7)^{15,27,28}. If the two DSBs are blunt and free, with their backbone no longer attached to the original chromosome, Ku70/80 can attach to the blunt ends that have migrated together and begin NHEJ, which will result in a translocation event. If the ends have proteins attached or have slight overhangs, alt-EJ can be utilized and regions of microhomology (2-25nt) between the two chromosomes can be brought together. This likely occurs with free DSBs also. Rarely SSA, which is another intermediate of HR and NHEJ similar to alt-EJ with more resection and less mutagenicity, can mediate homology searches to find larger regions of homology to ligate together^{1,15,17,25}. SSA is thought to be the cause of the BCR-ABL translocation since Alu repetitive elements are found at the breakpoints of these genes, this is similar to the MLL translocations seen in patients with leukemia which is discussed in the next subsection^{1,11,14,15,18,22,23,27,29}.

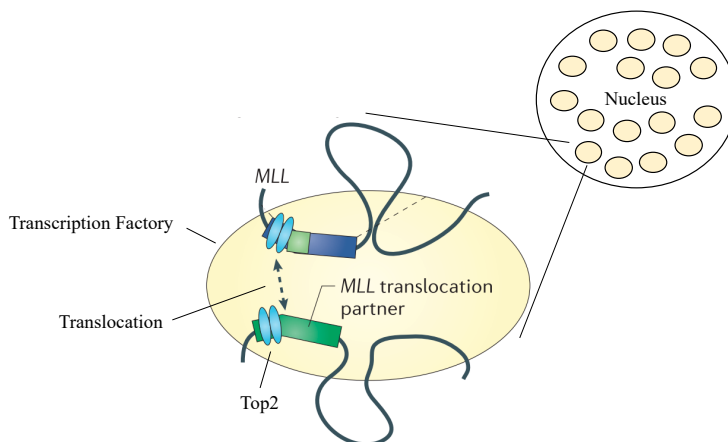


Figure 1.7: Nuclear Proximity is Essential for Translocation Events. Modified from Ashour, Atteya, and El-Khamisy, 2015.

1.5 Infant Leukemia and the *MLL* gene

Leukemia impacts approximately 36 in one million infants under one year old annually. A majority of these cases are classified as acute lymphoblastic leukemia (ALL) and acute myeloblastic leukemia (AML) (50% and 30% respectively) ³⁰. Infant leukemia typically presents with more aggressive symptoms and a lower survival rate than childhood or adult leukemia. In infants diagnosed with ALL and AML, approximately 80% harbor chromosomal translocations in the leukemic cells involving the mixed lineage leukemia (*MLL*) gene at chromosome position 11q23 ^{4,30-32}.

The *MLL* gene shows high homology with the trithorax gene, a *Drosophila* homeobox gene, which plays an important role in hematopoiesis ³⁰. The *MLL* gene contains multiple domains critical to its function in the survival of hematopoietic stem cells and progenitor cells. These components include a Menin interaction domain, AT-Hooks, a CxxC-RD2 domain, PhD fingers and a SET transactivation domain. Menin is a tumor suppressor protein that interacts with the MLL protein. The AT-Hooks and CxxC domains are essential for DNA binding, particularly the CxxC domain which binds to unmethylated CpG islands. RD2 interacts with the Polymerase Associated Factor complex (PAFc) which

is essential to MLL's transcriptional activity. The PhD fingers and SET domain are essential to MLL's methyltransferase abilities (Fig. 1.8A)³³.

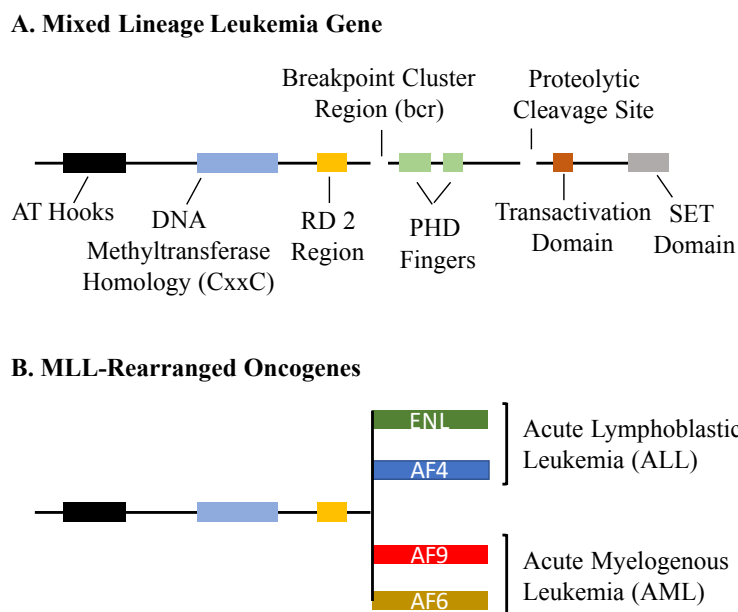


Figure 1.8: The *Mixed Lineage Leukemia* Gene and Translocation Partners. A, schematic diagram showing the domains of the *MLL* gene. B, the 4 most common *MLL* gene rearrangements.

Chromosomal rearrangements of the *MLL* gene with over 80 partner genes have been detected in neonatal blood spots of infants who later developed leukemia suggesting formation of the initiating rearrangement in utero (Fig 1.8B)^{27,30,31,33-35}. Sequenced breakpoints in the *MLL* gene involved in translocations are almost exclusively concentrated in an 8.3-kb region named the breakpoint cluster region (bcr), which contains exons 8-14 (Fig. 1.9)^{4,31,33,36,37}. The Phd fingers and SET domain are consistently deleted upon *MLL* translocation as they are located on the 3' end of the gene after the breakpoint cluster region. The PAFc-*MLL* interaction remains intact after translocation due to the *MLL* oncoprotein retention of the CxxC-RD2 domains. Therefore, it is hypothesized that the PAFc protein complex has an essential role in the transformation of hematopoietic stem cells and progenitor cells. This is supported by research showing *MLL*-AF9 fusion protein

interaction with PAFc increases the MLL-AF9 transcriptional activity and that increased levels of CDC73 and PAF1, components of the PAFc complex, are associated with other diseases such as breast, renal, gastric and prostate cancers^{33,36}.

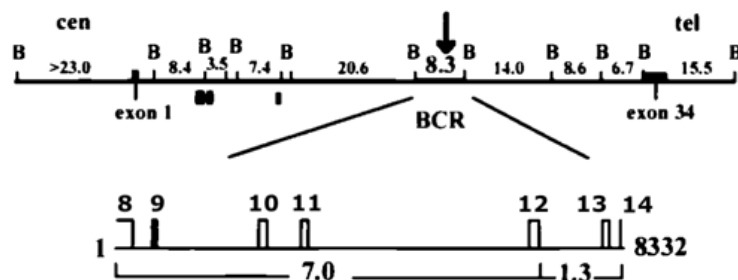


Figure 1.9: The *MLL* Breakpoint Cluster Region. Schematic of the *MLL* gene with the 8.3 kb bcr showing exons 8-14. Modified from Strick et. al, 2000.

Within this bcr, most of the rearrangements seen in patients with *de novo* leukemia are clustered in the 5' region of the bcr, but most of the rearrangements in patients with therapy-related leukemia (tAML) as well as infant leukemia are clustered together in the 3' region of the bcr. This difference in breakpoint localization suggests a different mechanism of initiation for these translocation events³¹. tAML is a secondary form of cancer that develops after a cancer patient has been treated with a chemotherapeutic that acts by "poisoning" the enzyme topoisomerase II (Top2), such as etoposide or doxorubicin^{4,31,32}. A number of previous research articles support the hypothesis that chemotherapeutic Top2 poisoning leads to DNA damage and chromosomal translocations that can lead to tAML. However, infant leukemia with similarly mapped breakpoints develops *in utero* without chemotherapeutic exposure, which has led researchers to investigate if there are other potential natural Top2 poisons that mothers are exposed to^{30,31}.

1.6 Topoisomerase II

Top2 is a regulatory enzyme that relaxes supercoiled DNA for transcription (Top2 β) and replication (Top2 α). Top2 acts in a multistep cleavage and religation reaction: (1) Top2

binds to two dsDNA molecules at Top2 recognition sequences; (2) a transient DSB is made in the first DNA helix (G-segment) creating a cleavage complex; (3) ATP hydrolysis drives a conformational change allowing the second dsDNA helix to pass through the DSB; (4) Top2 mediates religation of the DSB (Fig. 1.10). A catalytic Top2 inhibitor, like dexrazoxane, works to prevent DNA from binding to Top2 at step 1 preventing any part of this catalytic cycle³⁸⁻⁴².

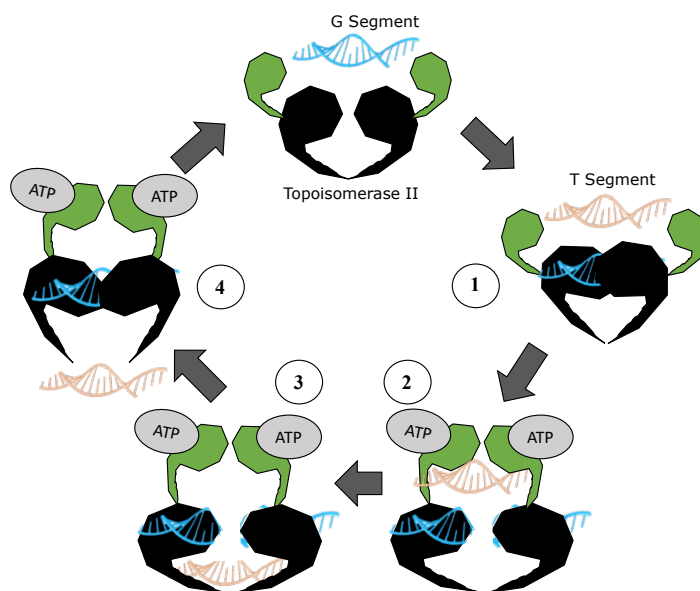


Figure 1.10: Mechanism of Topoisomerase II. 1, G and T DNA Segments bind to Top2. 2, a DSB is made by Top2 in the G DNA segment. 3, the T DNA segment passes through the DSB. 4, Top2 religates the DSB in the G segment and DNA is released from the enzyme.

In contrast to a Top2 inhibitor, other chemicals can work as Top2 “poisons”. A Top2 poison acts on the Top2 enzyme after it has already bound DNA and prevents the normal function of Top2. A traditional, or interfacial, Top2 poison stalls the enzyme in step 2 by binding to the active site of the enzyme preventing religation, thereby resulting in the formation of a stabilized cleavage complex (SCC)^{4,43}. On the other hand, a covalent Top2 poison works in a redox-dependent manner, binding to a distal site on the Top2 enzyme and increasing its ability to cause a DSB in step 2 through conformational changes to the

enzyme. Removal of the SCCs made by Top2 poisons is done by the small ubiquitin-related modifier ligase ZNF45/tyrosyl-DNA phosphodiesterase 2 (ZATT/TDP2) complex in order for NHEJ to repair the DSB. Removal of the SCC is required for DSB repair, and if ZATT/TDP2 does not remove the SCC, nucleases such as the MRN protein complex or CtIP may resect the DNA ends with the SCC attached to allow for HR or alt-EJ (Fig. 1.11)^{28,38,52–54,44–51}. SCCs may be destabilized over time or by replication or transcription machinery collision with the SCC^{4,20,43,47,51,53–55}. Upon SCC destabilization, the two ends of the DSB may separate and migrate throughout the nucleus promoting illegitimate DNA repair and chromosomal translocation formation⁴. In support of this, functional ZATT/TDP2 complexes have been shown to suppress chromosomal translocations^{20,54}.

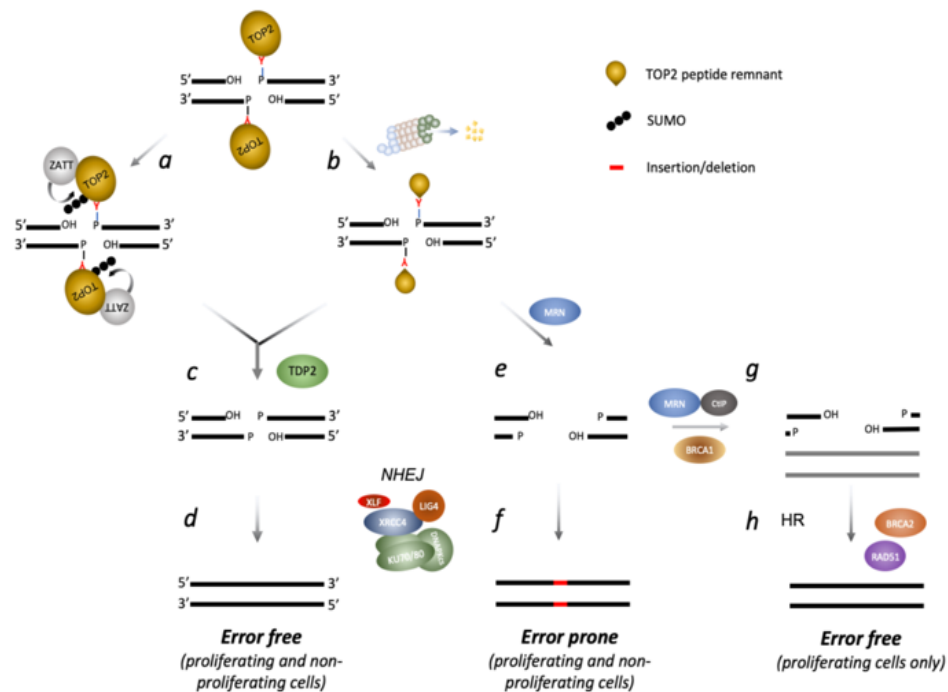


Figure 1.11: Removal of Stabilized Top2 Cleavage Complex from DNA. ZATT or Ubiquitination works with TDP2 to remove Top2 for DSB to be repaired by NHEJ. If not removed, nucleases resect ends for HR, NHEJ or alt-EJ to repair DSB. From Zagnoli-Vieira and Caldecott, 2020 prior to publication.

1.7 Dietary Bioflavonoids

A class of chemical compounds called bioflavonoids are found in soy, fruits, vegetables, tea, coffee, wine, and supplements. Similar to the chemotherapeutic etoposide, bioflavonoids are characterized by multiple phenolic rings. They are separated into 12 different sub-classes based upon their structure, however only six are dietarily relevant: flavanols, flavonols, flavones, isoflavones, flavanones, and anthocyanidins (Fig. 1.12)^{56,57}. In the subsequent sub-sections, further information will be given on the isoflavone, flavonol, and flavone sub-classes that were focused on in these studies. Few studies have compared the effects of different sub-classes with the same set of experiments and even fewer studies have studied combination treatments of bioflavonoids containing different sub-classes.

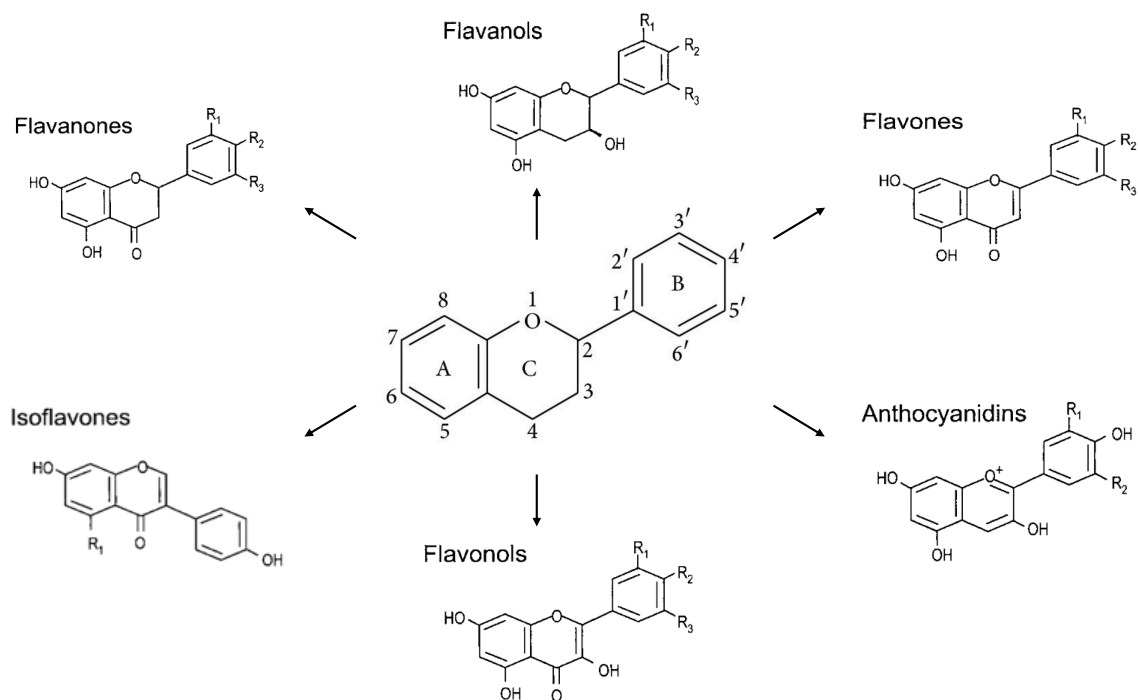


Figure 1.12: Basic Chemical Structures of Dietary Bioflavonoids. The middle backbone represents the general bioflavonoid poly-phenol ring structure. The six structures surrounding show the general structural differences between the sub-groups.

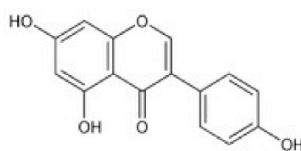
1.7.1 Compounds Used in this Research: Isoflavones

Isoflavones are polyphenolic secondary plant metabolites produced through the flavonoid-producing phenyl-propanoid synthesis pathway. In order for isoflavones to be produced the plant must express the isoflavone synthase enzyme, which converts flavanone precursors into isoflavones. This isoflavone synthase is only expressed in legumes and a few other select species. Plants with the highest concentrations of isoflavones are soy, red clover, and kudzu. The amount of isoflavone in these plants is dependent upon the conditions the plants were reared in and the final concentration of isoflavones in food products (including dietary supplements) depends upon the processing methods the plants undergo, and which part of the plant is used. Genistein, daidzein, glycitein, formononetin, biochanin A and irilone are the main isoflavones isolated from plants^{56,58,59}.

Interest in isoflavones has spiked in the past 20 years. This is due to the attribution of the consumption of isoflavone containing products with lower occurrences of coronary heart disease, breast and prostate cancer. This hypothesis came from the observations that citizens of Asian countries had less incidence of coronary heart disease, breast and prostate cancer compared to citizens of Western countries, and citizens in Asian countries typically ingest approximately 8-50mg/day of isoflavones compared to citizens in Western countries who ingest only 0.1-3.3 mg/day. Due to this potential health relevance, research has been conducted on high intake of isoflavones. Genistein (Fig. 1.13) in particular has been a focus of study since it is the main isoflavone found in soy products⁵⁹.

In animal models, increased genistein intake resulted in increased rates of pituitary and mammary gland tumors and stimulated MCF-7 tumor growth. Additionally, while increased genistein intake in post-menopausal women in Asian countries decreased breast

cancer risk, this decreased risk was not sustained in post-menopausal women in Western countries, including both native inhabitants and Asian immigrants. In fact, some studies, particularly of British women, showed that increased serum genistein levels in women with early stage breast cancer had increased transcription of cell cycle progression and cell proliferation genes⁵⁹. Given these results and the interest in isoflavones, genistein was one bioflavonoid selected as a focus for these studies.



Genistein

Figure 1.13: Chemical Structure of Isoflavone: Genistein.

1.7.2 Compounds Used in this Research: Flavonols

Flavonols are primarily found in fruits, vegetables, red wine, and tea and they compose the largest portion of humans' bioflavonoid intake given their distribution across a wide number of plant species⁵⁷. Within plants it has been shown that flavonols have the ability to protect the plant against UV-B damage and with their compacity as antioxidants they can protect the plants against oxidative damage also^{60,61}. Scientists and physicians want to determine ways to utilize the antioxidant capability of flavonols in human populations as a protectant against cardiovascular disease, neurological disease and potentially in smokers and athletes to protect against exercise induced oxidation^{62,63}.

The most common flavonols found in foods are quercetin, kaempferol, myricetin, and fiestin, with a majority of published literature focusing upon the first three though there are many others contained in foods. Similar to isoflavones the concentration of flavonol in the food product depends upon the plant in question, the conditions it was grown in, and the

part of the plant that was used. Flavonols are most frequently found in highest concentrations in the leaves, flowers, and fruits, which are exposed to sunlight; the exception to this being in onions, which grow below ground^{60,61}. The human dietary source of flavonols is dependent on culture and region. Humans residing in Asian countries typically get their flavonols from green tea, while the Netherlands, US and Denmark inhabitants mainly receive them from onions, apples, and tea. Citizens of Mediterranean areas get their flavonols from green vegetables. Within Italy, red wine is the main source of flavonols, though inhabitants of Northern villages also have a high intake from salads, soups, fruits, and vegetables⁶¹. Given that flavonols are highly present in the human diet and the large amount of previous literature to reference that focuses on multiple aspects of quercetin, kaempferol, and myricetin, these bioflavonoids were selected for these studies.

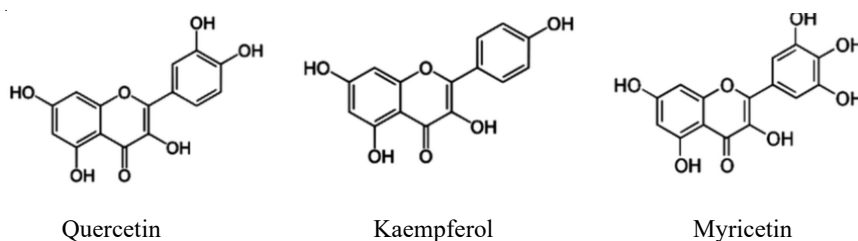


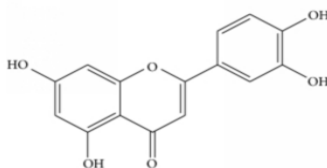
Figure 1.14: Chemical Structure of Flavonols: Quercetin, Kaempferol, and Myricetin.

1.7.3 Compounds Used in this Research: Flavones

Flavones are the end product of a complex multi-step synthetic pathway that occurs within a wide variety of plants. This pathway begins with phenylalanine that is converted through the generalized phenylpropanoid pathway that synthesizes most flavonoids. After this pathway, p-coumaroyl-CoA must be synthesized into chalcone with chalcone synthase. At this point, chalcone can be isomerized into a flavanone by chalcone isomerase (CHI). Finally, flavone synthase class I or II enzymes can catalyze the synthesis of a flavone from

flavanones. Flavones, similar to flavonols, can protect the plant from UV-B radiation. Flavones have the additional ability to provide protection against biological attacks in the form of pathogenic microbes. Flavones can act as signaling molecules to activate differential gene transcription to prevent the growth of microorganisms after invasion. Additionally, flavones can be expressed to deter insects and nematodes from eating the plants and they can be expressed to interfere with the growth and reproduction of other plants⁵⁶.

Flavones are found across a variety of plant species and expression of flavones appears to be widespread within the plant, from the roots to the leaves. However, though flavones are found throughout the plant kingdom, they are found much less commonly in fruits and vegetables as compared to flavonols. Apigenin and luteolin are the main flavonols found in food sources. The main food sources of flavones are celery, parsley, thyme, red peppers, and fruit skins^{57,64}. In humans, flavones, much like isoflavones and flavonols, appear to have antioxidant and anti-tumor capabilities, and they appear to effect signal transduction pathways. These studies selected luteolin (Fig. 1.15) as a focus from the flavone sub-group given it is the most consumed flavone and the most studied.



Luteolin

Figure 1.15: Chemical Structure of Flavone: Luteolin.

1.8 Pleiotropic Bioflavonoid Effects

Due to their antioxidant capacity, bioflavonoids are utilized in the form of dietary supplements for their presumed health benefits, such as protection against cardiovascular diseases, cancer, and inflammation⁶⁵. Bioflavonoids have been shown to have pleiotropic effects on cells⁶⁶ including as a potential poison of Top2^{4,31,32,66,67}. Bandele, Clawson, and Osheroff studied bioflavonoids in cell-free systems and have observed that the structure of the bioflavonoid determines if Top2 is poisoned in a traditional or redox-dependent manner^{32,68}. Bioflavonoids that act as a traditional/interfacial poison (including genistein, quercetin, and kaempferol) by inserting into the DSB and preventing its religation (step 4 of the Top2 mechanism), have an aromatic, planar C ring with a C4-keto group and a C5-OH that allows for the formation of a proposed pseudo ring and on the phenolic B ring there is a C4'-OH. Other bioflavonoids such as epigallocatechin gallate (EGCG) poison Top2 as a covalent (or redox) poison that attaches to a residue distal to the active site of Top2 and increases the DNA cleavage (step 2) of the Top2 enzyme and therefore need C3', C4' and C5' -OH groups attached to the phenolic B ring. In addition, some bioflavonoids such as myricetin have been demonstrated the ability to use both mechanisms to induce DNA damage and therefore have all of the groups described above (Fig. 1.16)^{4,32}.

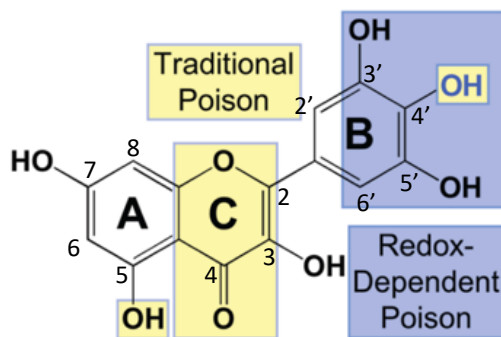


Figure 1.16: Osheroff's Proposed Rules for Top2 Poison Classification of Bioflavonoids. The structure of myricetin is shown to display the proposed rules for a traditional/interfacial Top2 poison and for the covalent/redox-dependent Top2 poison. Figure modified from Bandele, Clawson, and Osheroff, 2008.

Research has shown that select bioflavonoids can impact DSB repair and potentially repair pathway choice. Myricetin and EGCG stimulate the efficiency of NHEJ, while others such as silibinin, apigenin, and curcumin inhibit NHEJ protein localization to the nucleus and reduce NHEJ repair rates,^{21,65,69}. Data from the Richardson lab also shows genistein alters NHEJ and HR pathway-specific protein levels (in preparation, Ghosh, Lalwani, and Richardson).

Since bioflavonoids cause DSBs, and potentially impact DNA repair pathway choice, researchers hypothesize that bioflavonoid ingestion during pregnancy leads to *in utero* formation of chromosomal translocations in developing fetal hematopoietic stem cells and infant leukemia^{4,31,32,66,67}. To support this, research shows multiple bioflavonoids cross the placental barrier, and are detected in fetal tissue. Bioflavonoids are likely more damaging to fetuses due to differences in metabolic and excretion rates between the mother and fetus and because rapidly developing and proliferating cells are more sensitive to Top2 poisons^{65,70,71}. Interestingly, epidemiological data show that countries with populations with higher soy intake such as Japan have a two- to three- fold increase in the incidence of infant leukemia further supporting this hypothesis^{4,32}.

Additional pleiotropic effects of bioflavonoids include altering epigenetic markers and activating signal transduction MAP, NF-KB and EGFR pathways leading to altered expression of genes involved in cytokine expression, cell survival, cell cycle regulation and DNA repair. However, those studies were performed in cancer or differentiated cell lines; therefore further research is needed to demonstrate if the effects seen are relevant to wildtype stem and early hematopoietic progenitor cells that are the known initiating cells of leukemia phenotype^{4,16,79–86,69,72–78}.

The detailed mechanism of how bioflavonoids promote oncogenic translocation events is still undetermined. Current research indicates there is likely a multiple step pathway involved in producing these leukemia-initiating translocations: (1) DSBs are formed from Top2 poisoning, (2) DNA damage response (DDR) is activated, (3) DSBs are illegitimately repaired causing oncogenic translocations, and (4) cells with rearrangements survive, sustain further mutations, and proliferate. The ability to form a stable translocation may be dependent on the number of DNA damage sites, the stability of the breaks incurred by Top2 poisoning compounds, kinetics of removal of SCCs, or a favored mechanism of repair due to the DDR or epigenetic factors.

1.9 Aims of This Research

The primary goal of my studies is to investigate a panel of bioflavonoids from different sub-groups to determine their potential to cause DNA damage and chromosomal translocations, as well as to investigate the mechanism by which this DNA damage is caused. In addition, some combinations of bioflavonoids from different sub-groups were studied, since ingestion of bioflavonoids comes from multiple food sources. DNA damage was studied through immunocytochemistry (ICC), where cells were stained for phosphorylated histone 2AX (γ -H2AX), which is a marker of DNA DSBs. To study chromosomal translocations, a reporter cell line developed by the Richardson lab to quantify *MLL-AF9* translocations was utilized (see Chapter 2 for more information). In order to investigate the mechanism by which the DNA damage was caused, the catalytic Top2 inhibitor dexrazoxane (DEX) was used. DEX prevents Top2 from binding to DNA, thereby preventing any DNA damage and translocations that may be caused by the

poisoning of Top2. Therefore, any DNA damage or translocations observed after bioflavonoid treatment following DEX pretreatment, is likely caused through Top2-independent mechanisms.

For the first studies on DNA damage and mechanism of damage, bioflavonoids were studied with acute, high dose treatments, focused around the LD50's for these bioflavonoids. While these doses are likely not physiologically relevant, studies such as these are important for determining the potential of these compounds to cause DNA damage and chromosomal translocations and to understand the mechanisms by which bioflavonoids cause these effects. Additionally, bioflavonoids are bio-accumulative with a typical half-life of 23 hours, which can increase plasma concentrations, especially if consumed in large doses in the form of dietary supplements⁸⁷⁻⁸⁹. Finally, because of the potential of these bioflavonoids to cause infant leukemia due to *in utero* exposure, these high doses may be relevant given the difference in fetal vs maternal metabolism and the susceptibility of rapidly proliferating cells to bioflavonoid exposure. Prolonged, low-dose treatments of bioflavonoids were also examined in the last study to simulate a typical, physiologically relevant biological setting, versus a one-time, high-dose treatment used in most studies.

CHAPTER 2: MATERIALS AND METHODS

2.1 Cell Lines

Mouse embryonic stem (ES) cell lines D3⁹⁰ and EtG2a⁹¹ were obtained from ATCC, Old Town Manassas, VA. D3 cells are a wild type cell line, while EtG2a cells are deficient of the HPRT gene^{90,91} both cell lines were derived from male mice. Cells were authenticated by ATCC. Mycoplasma testing occurred yearly using InvivoGen Mycoplasma Detection kit according to manufacturer instructions. The MAG⁶⁵ cell line was genetically engineered in the Richardson lab (see below) from the parental EtG2a line. ES cells were maintained at 37°C 5% CO₂ on tissue culture dishes pre-treated with 0.2% gelatin (Sigma). Cells were passaged and expanded 3-8 times, and then frozen in liquid nitrogen as stocks. Stocks were thawed for each replicate experiment. Cells were maintained in non-selective medium consisting of Dulbecco's Modified Eagle Medium (DMEM; Gibco, Waltham, MA), 15% ES qualified STASIS fetal bovine serum (FBS; Gemini, Sacramento, CA), 100U/mL penicillin/streptomycin (Gemini), 2mM L-glutamine (Gemini), 0.1 mM non-essential amino acids (Gibco), 1000U/ml ESGRO® leukemia inhibitory factor (LIF; Gemini), 100 μ M β -mercaptoethanol (Sigma).

The *MLL-AF9-GFP* (MAG) cell line was genetically engineered by the Richardson lab as a Reporter for chromosomal translocations between the hu*MLL* bcr and the hu*AF9* bcr, which contain mapped breakpoints that have been identified in infant- and t-AML. In the MAG Reporter cell line, two engineered GFP exons, upstream (GFPe1) and downstream (GFPe2), were added hu*MLL* and hu*AF9* bcr transgene inserts. DNA DSBs in each of chromosome transgene inserts may be repaired to ligate the GFPe1 exon and the GFPe2 exon onto the same DNA duplex, generate a chromosomal translocation, and

generate a functional GFP gene (Fig. 2.1). The Reporter cell line previously demonstrated that exposure to etoposide, a panel of bioflavonoids, or ROS was sufficient to promote the formation of DSB-induced chromosomal translocations^{65,92}.

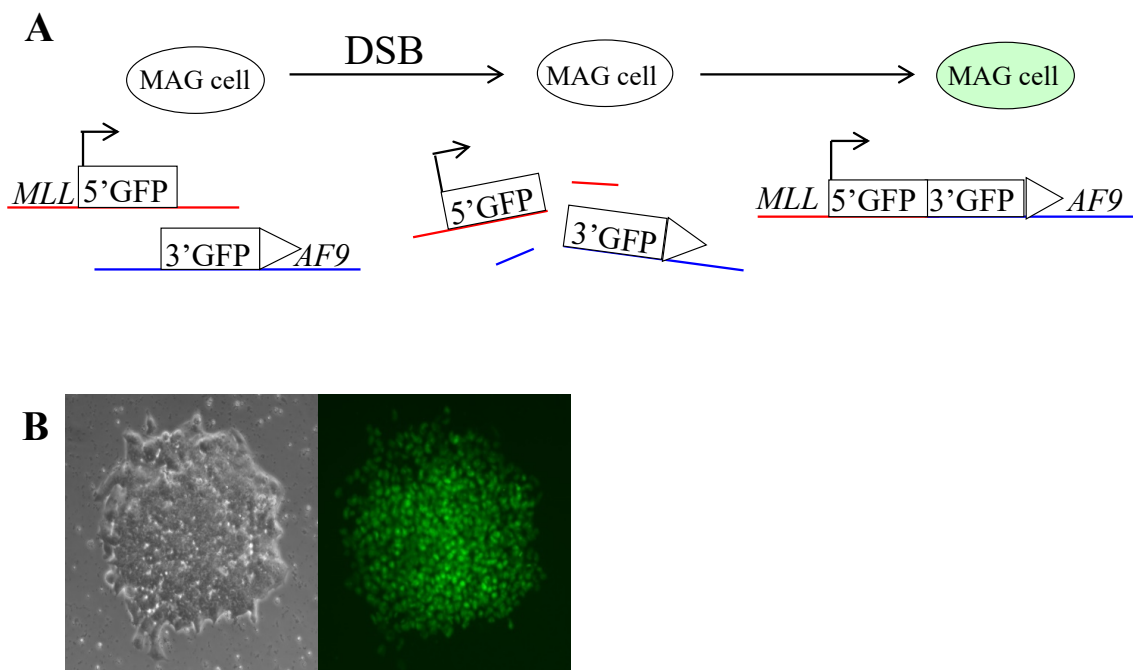


Figure 2.1: *MLL-AF9-GFP* Translocation Reporter Cell Line. A, Schematic diagram showing the two engineered *GFP* gene segments that when translocated form a full length *GFP* coding sequence. B, Representative images of GFP+ colony under microscopy, brightfield (left) fluorescence (right).

2.2 Treatment Compounds

Etoposide and bioflavonoids were obtained from LKT Laboratories (St Paul, MN). Dipyrone and dexrazoxane were obtained from Sigma (St. Louis, MO). Compounds were diluted in dimethyl sulfoxide (DMSO; Sigma) and stored as 20 mM stock solutions. Stock solutions were diluted in 1X phosphate buffered saline pH 7 (PBS; Fisher, Hampton, NH) prior to each experiment. Bioflavonoids used in this study include genistein, quercetin, luteolin, kaempferol, and myricetin. All treatment doses were based upon LD50 data and previous experiments performed by the Richardson lab⁶⁵.

2.3 Treatment of Cells and Detection of γ -H2AX Foci

To begin all experiments that assessed γ -H2AX foci, 1×10^6 stem cells were plated on 15 mm gelatin-coated coverslips (Neuvitro Corporation, Vancouver, WA) with 4 mL non-selective medium and incubated 12 h at 37°C 5% CO₂.

2.3.1 Experimental Design: Do Bioflavonoids Induce Prolonged DSBs?

In these experiments, no treatment was used as a negative control since DMSO, the vehicle control, showed similar numbers to untreated cells (For results see Chapter 3). Etoposide was used as a positive control. Dipyrone, a pain killer with anti-inflammatory effects, that causes *MLL* translocations through a different mechanism of action compared to etoposide was used as a chemical control to compare bioflavonoids to ⁶⁵. A panel of bioflavonoids were used at different doses and in combinations. Figure 2.2 describes the treatment design (A) and includes the main treatments and doses used (B).

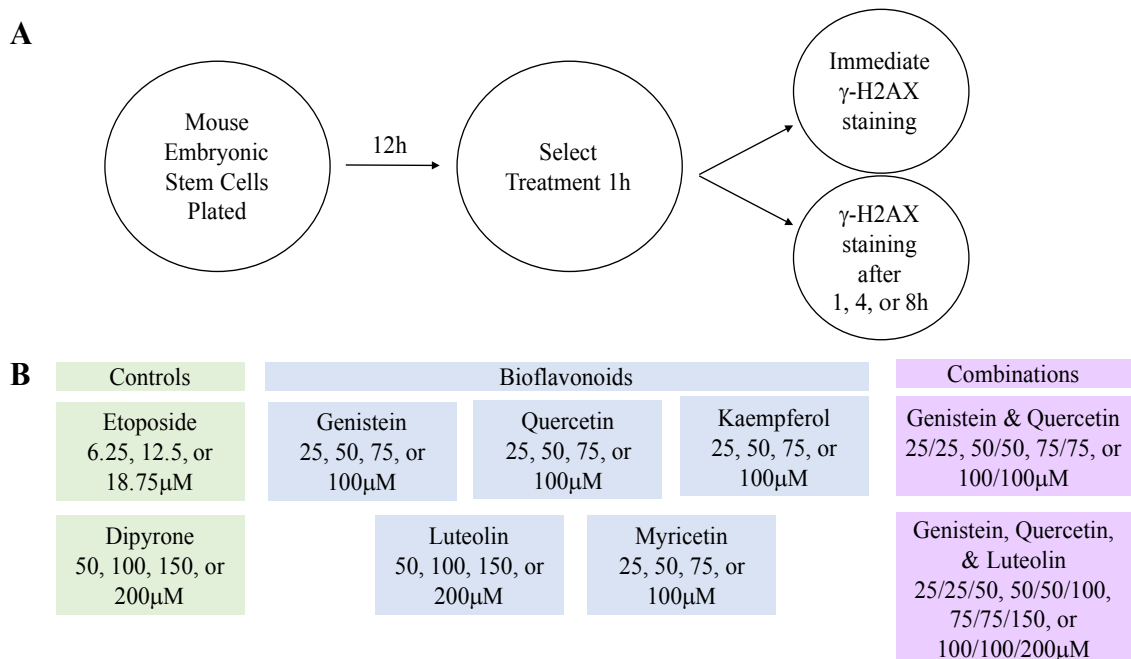


Figure 2.2: Experimental Design for Evaluation of DNA Damage Repair Kinetics Post-Exposure to Bioflavonoid. (A) Basic experimental design for control/bioflavonoid exposure and γ -H2AX staining. (B) Treatments as referred to by “Select Treatment” in A. Doses were determined based upon LD50 doses.

2.3.2 Experimental Design: Do Bioflavonoids Induce DSBs through Top2 Poisoning?

In these experiments, cells were treated with the catalytic Top2 inhibitor dexrazoxane (DEX). Dexrazoxane prevents Top2 from binding to DNA, therefore etoposide and other Top2 poisons should be limited in their ability to cause DNA DSBs. An hour of DEX pre-treatment prevents both Top2 α and Top2 β from binding to DNA, whereas 5 hour DEX pre-treatment causes degradation of the Top2 β isoform only⁹³⁻⁹⁵. To test both of these functions, cells were treated with DEX (see 2.2) at concentrations of 50 or 200 μ M for 1 or 5h before the 1h etoposide, dipyrone, or bioflavonoid treatment. After 1h of select treatment, the cells were immediately stained for γ -H2AX (Fig 2.3). For results, see Chapter 4.

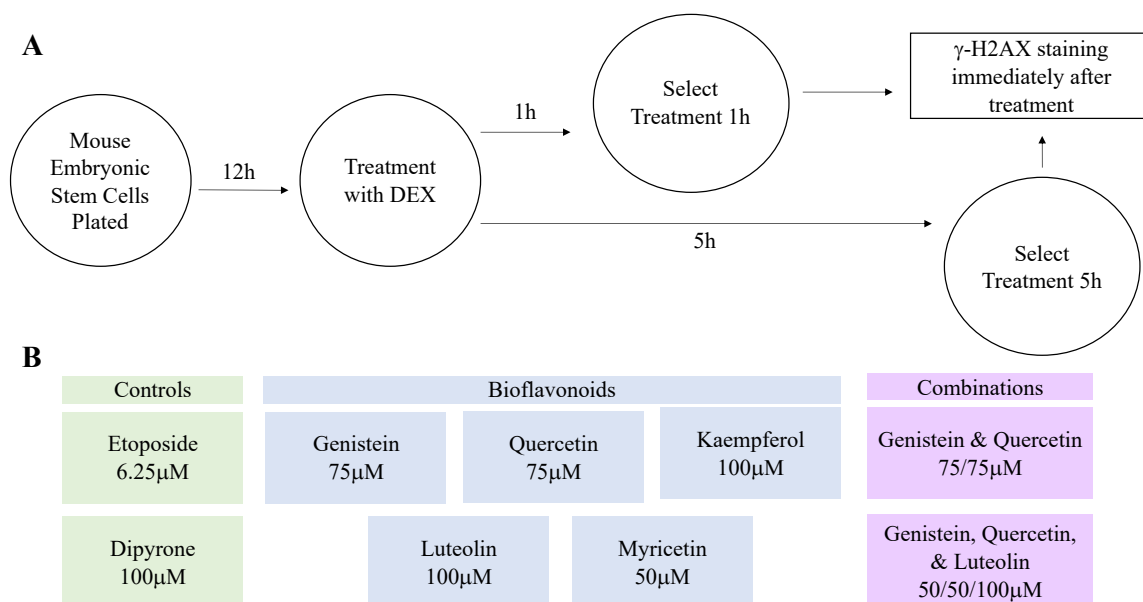


Figure 2.3: Experimental Design for Evaluation of DNA Damage Repair with Top2 Inhibited by Dexrazoxane (DEX). (A) Basic experimental design for DEX treatment prior to control/bioflavonoid exposure and γ -H2AX staining. (B) Treatments as referred to by “Select Treatment” in A. Doses were determined based upon LD50 doses.

2.3.3 γ -H2AX Staining Protocol and Scoring of Foci

After treatment, as described in section 2.3.1 or 2.3.2, compound was aspirated off cells and cells were washed with 1X PBS. Cells were fixed with 3% paraformaldehyde (Sigma) for 15 min at room temperature with rocking. Then coverslips were incubated with 0.2% Triton-X (Sigma) for 15 min at room temperature. Next, coverslips were blocked with 5% non-fat milk resuspended in 1x Tris-Buffered Saline-Tween 20 (TBS-T, Fisher, Waltham, MA) for 30 min at room temperature with rocking. Anti-phospho-Histone H2A.X antibody conjugated to Alexa Fluor 488 (15mg/ml; Millipore, Burlington, MA) was diluted 1:100 in 5% non-fat milk/TBS-T and applied to coverslips for 1h at room temperature in the dark. Coverslips were washed thrice with 1X PBS and mounted to slides (VWR, Radnor, PA) with a drop (~50-60 μ L) of ProLong Gold Antifade Mountant with DAPI (Life Technologies, Carlsbad, CA). Slides were stored at -20°C until confocal images were recorded with an Olympus FV1000 microscope. Each treatment/slide had 5 images taken from distributed areas on the slide, upper left and right quadrants, center, and lower left and right quadrants generally. After acquisition of the images, the number of γ -H2AX foci, green, per cell nuclei, stained with DAPI, was counted manually a minimum of 100 cells were counted for each treatment. One-way ANOVA with Sidak's multiple comparisons test was used for statistical analysis.

2.4 Quantification of Chromosomal Translocations

MAG ES translocation Reporter cells⁶⁵ were plated at a density of 2×10^7 cells per 10 cm tissue culture plate. Treatment was added to the culture medium after 5h treatment with DEX. Cells were treated with etoposide or a select bioflavonoid for 1h (Fig. 2.4).

Following exposure, cells were washed with 1X PBS before trypsinization. Cells were washed with 1X PBS again following trypsinization and plated on 96 well culture dishes with ES media. All treatment cohorts were washed with 1X PBS on the first 2 d after treatment, then incubated in ES media 37°C 5% CO₂. For each experiment, all cells on all plates in all treatment groups were screened at days 5-7 post-treatment for GFP+ fluorescence at 400X magnification on an inverted Zeiss Axiovert25 microscope with images recorded by Zeiss AxioCam MRc digital camera. GFP+ cell colonies represent a translocation between two engineered GFP exons within hu*MLL* and hu*AF9* bcr transgene inserts (Fig. 2.1B)⁶⁵. Each complete experiment including controls was repeated a minimum of three independent times (n = 3). One-way ANOVA using Bonferroni post-hoc tests were used for statistical analysis.

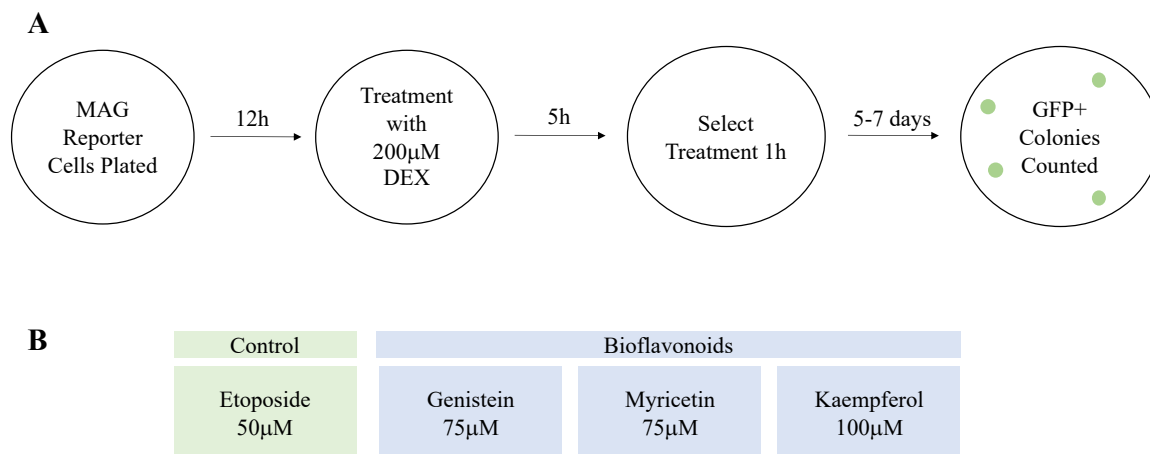


Figure 2.4: Experimental Design for Evaluation of Chromosomal Translocations with Top2 Inhibited by Dexrazoxane (DEX). (A) Basic experimental design for DEX treatment prior to control/bioflavonoid exposure and. (B) Treatments as referred to by “Select Treatment” in A. Doses were determined based upon doses from Bariar et. al 2018.

2.5 Chronic, Low Dose Bioflavonoid Treatment

MAG ES translocation Reporter cells⁶⁵ were plated at a density of 1×10^7 cells per 10 cm tissue culture plate and were incubated overnight at 37°C 5% CO₂. After approximately 24 hours cells were treated with low doses of bioflavonoids as described in

Figure 2.5A for 48hours. After treatment, the medium containing treatment was aspirated and cells were washed with 1X PBS. Cells were then trypsinized, collected, and counted. 1×10^7 cells from each group were plated on 10 cm tissue culture plates. The remaining cells were either fixed with 3% paraformaldehyde to be sorted at a later date and frozen as pellets (experiment a), or immediately run through the flow cytometer (experiment b). This treatment cycle was repeated with the same cells for 20 cycles (Fig. 2.5B).

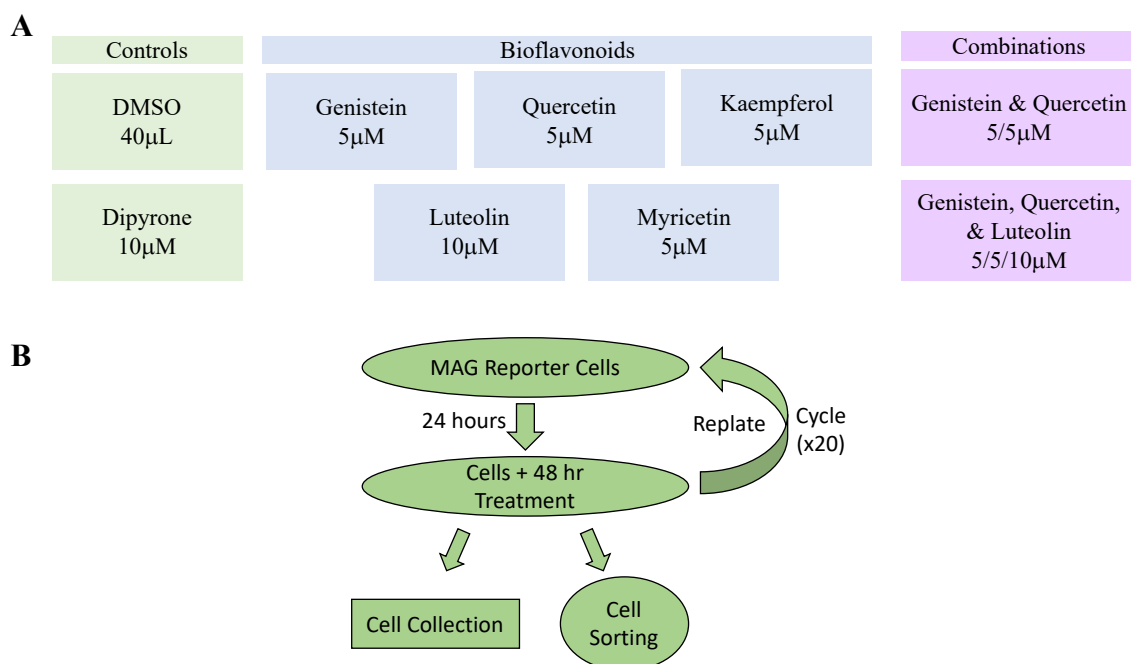


Figure 2.5: Experimental Design for Chronic, Low Dose Bioflavonoid Treatments. (A) Treatments as referred to by “Treatment” in B. (B) Basic experimental treatment schedule for chronic, low dose bioflavonoid exposure.

CHAPTER 3: BIOFLAVONOIDS INDUCE PROLONGED DNA DSBS

The purpose of the experiments described in this chapter was to examine if bioflavonoids cause DNA DSBs and if this DNA damage was repaired over time in a manner similar to etoposide. The potential of bioflavonoids to directly induce DNA DSBs was determined by the appearance of γ -H2AX foci immediately after bioflavonoid treatment and was assessed 1, 4 and 8 hours after treatment to understand the persistence of DSBs due to bioflavonoid exposure over time. Additionally, trends in the kinetics of DNA repair that occurred over time between treatment groups was assessed.

3.1 Results for No Treatment, Negative Controls, and Etoposide

As expected, untreated asynchronous cultures of ES cells contained few, if any, spontaneous γ -H2AX foci across all experiments and timepoints. The few DSBs observed in these untreated cells are likely due to normal cellular processes, such as replication, where replication stress can lead to replication fork collapse and DSBs. A panel of other compounds were tested including; DMSO, vitamin A and B, epigallocatechin gallate, flavanone, biochanin A, daidzen, hesperidin, naringenin, 3-3 diindolylmethane, and fiestin. Vitamin A and B are natural plant compounds that do not have a polyphenol ring structure. The panel of other bioflavonoids tested have been less studied and are thought to be less hazardous to humans based upon their limited concentrations in food sources. These cells were treated with each respective compound at a dose of 200 μ M (except fiestin, which is highly cytotoxic, at 25 μ M) for 1h, after treatment the cells were washed with PBS and fresh media was added for 4h, after which γ -H2AX staining was performed and foci counted. DMSO, the vehicle control, had an average of 3.07 foci/cell and all Vitamins and bioflavonoids on average contained 1.39 to 2.87 foci/cell, except flavanone with 4.61

foci/cell (Fig. 3.1). Statistically (Table 3.1) all treatments were significantly elevated compared to control cells except biochanin A, 3-3 diindolylmethane, and fisetin. However, each group (except flavanone) when compared to control cells had only approximately 2 (or less) more foci on average. Given the high doses of bioflavonoids and the low absolute number of foci on average in these treatments, the plausible conclusion is that these bioflavonoids do not cause DSBs at a biologically significant level. Flavanone did have 3.5 more foci/cell than the no treatment group. This is comparable to quercetin treatment shown in Fig. 3.1 with almost 4 more foci than control, but this quercetin treatment was only at a dose of 25 μM compared to the 200 μM dose of flavanone. Therefore, while flavanone may be of interest to further studies, a dose of 200 μM is not physiologically relevant, leading to the conclusion that flavanone is seemingly non-hazardous to cells.

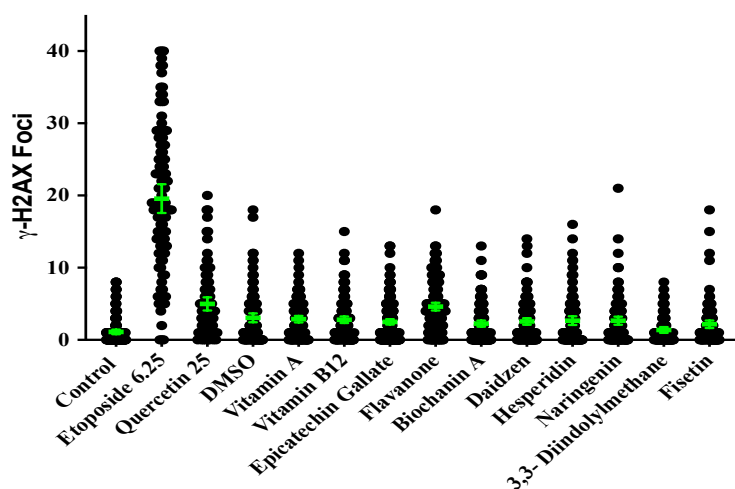


Figure 3.1: DNA Damage in a Negative Control Panel at 4h Post-Exposure. Control cells were left untreated for the treatment period. Etoposide and quercetin at 4h post-exposure and their lowest respective doses (6.25 and 25 μM) have been included for reference. For statistical analysis, see Table 3.1.

Table 3.1: DNA Damage in a Negative Control Panel at 4h Post-Exposure Data Analysis. Cells were treated with a panel of compounds at 200 μ M (except etoposide, 6.25, quercetin, 25, and fisetin, 25) for 1h. At 4h post-exposure, all treatments were significantly elevated compared to control cells except biochanin A, 3-3 diindolylmethane, and fisetin. A one-way ANOVA was used with Sidak's multiple comparisons test (**** $p < 0.0001$, *** $p < 0.001$, ** $p < 0.01$, * $p < 0.05$).

Compound	Comparison		Average Values	Difference	p-value	Significant		
Control	Etoposide	Control 4h	Eto 6.25 4h	1.1	19.57	18.47	<0.0001	****
	Quercetin	Control 4h	Quer 25 4h	1.1	4.989	3.886	<0.0001	****
	DMSO	Control 4h	DMSO 4h	1.1	3.065	1.961	0.0002	***
	Vitamin A	Control 4h	Vit A 200 4h	1.1	2.871	1.768	0.001	**
	Vitamin B12	Control 4h	Vit B12 200 4h	1.1	2.793	1.69	0.0014	**
	Epicatechin Gallate	Control 4h	Epi Gal 200 4h	1.1	2.497	1.394	0.0072	**
	Flavanone	Control 4h	Flav 200 4h	1.1	4.614	3.511	<0.0001	****
	Biochanin A	Control 4h	Bioch A 200 4h	1.1	2.255	1.152	0.0802	ns
	Daidzen	Control 4h	Daid 200 4h	1.1	2.551	1.448	0.0128	*
	Hesperidin	Control 4h	Hes 200 4h	1.1	2.667	1.563	0.0093	**
	Nargenin	Control 4h	Nar 200 4h	1.1	2.661	1.558	0.0074	**
	3-3 Diindolylmethane	Control 4h	3-3 Di 200 4h	1.1	1.385	0.2812	0.9992	ns
	Fisetin	Control 4h	Fise 25 4h	1.1	2.169	1.066	0.1746	ns

As a positive control, cells were exposed to the potent Top2 poison etoposide. Given the potency of etoposide as a Top2 poison, it was expected that etoposide would induce a robust number of DNA DSBs even at low doses. Increasing the dose of etoposide was expected to create an increase in the number of DSBs observed. Over the time points it was expected that a decrease in the number of DSBs observed would reflect their repair. By examining the number of DSBs induced by etoposide immediately after treatment and again at 1, 4, and 8h post-treatment, a pattern of the repair kinetics was expected to be observable to compare to the bioflavonoid treatments.

An increasing number of γ -H2AX foci were scored immediately following exposure to etoposide with an average of 19.3, 20.9, and 26.0 foci/cell at 6.25, 12.5, 18.75 μ M doses, respectively (Fig. 3.2B). All averages and p-values can be found in Table 3.2. These data support that etoposide has a clearly defined dose dependent increase in the amount of DNA damage seen (Fig. 3.2A) and will provide a clear reference point for the other treatments.

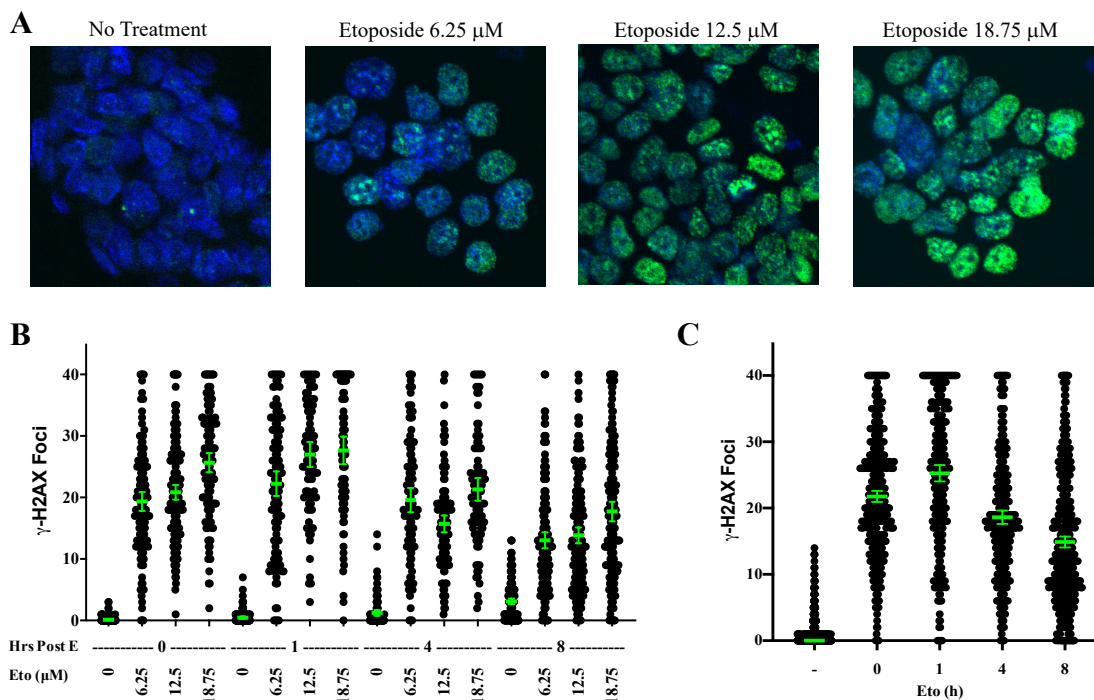


Figure 3.2: DNA Damage Repair Kinetics Over 8h with Etoposide Treatment. After 1h etoposide treatment at 6.25, 12.5, or 18.75 μ M, cells were stained for γ -H2AX immediately after treatment, or following 1, 4, or 8h recovery. (A) Representative confocal images from all etoposide doses immediately after treatment and staining. (B) Each point represents the number of γ -H2AX foci in a cell. Averages are represented in green with error bars showing the 95% confidence interval. At least 100 cells were counted for each treatment group/time point. (C) The average number of γ -H2AX foci are shown for each timepoint, all doses were combined to show the general trend of DNA damage recovery over 8h. For statistical analysis, see Table 3.2.

A similar pattern of persistence of DNA damage over time and kinetics of DSB repair was observed for all doses of etoposide tested. The average number of γ -H2AX foci persisted or slightly increased 1h post-exposure and then gradually declined over the total 8h period. For example, 6.25 μ M etoposide immediately induced an average of 19.3 foci/cell that persisted and slightly increased at 1h post-treatment (avg. 22.2 foci/cell). At 4h post-treatment the average number of foci slightly declined (avg. 19.6 foci/cell), followed by a significant decline in the number of foci at 8h (avg 13.0 foci/cell) consistent with DSB repair, although still elevated above baseline untreated cells (Fig. 3.2B). Considering all three treatment doses, etoposide-induced DNA DSBs appear and

statistically increase over 1h post-exposure before decreasing significantly after 4 and 8h (Fig. 3.2C).

Table 3.2: DNA Damage Repair Kinetics Over 8h with Etoposide Treatment Data Analysis. The average number of γ -H2AX foci of the treatments being compared are shown with the p-value from the comparison. A one-way ANOVA was used with Sidak's multiple comparisons test (**** p<0.0001, *** p<0.001, ** p<0.01, * p<0.05).

Compound	Comparison	Average Values		p-value	Significant		
Control (C)	0 hr vs 1 hr	0.11	0.46	>0.9999	ns		
	1 hr vs 4 hr	0.46	1.24	>0.9999	ns		
	4 hr vs 8 hr	1.24	3.11	0.0596	ns		
Etoposide (Eto)	To Control	C 0 hr vs Eto 6.25 0 hr	0.11	19.34	<0.0001	****	
		C 0 hr vs Eto 12.5 0 hr	0.11	20.85	<0.0001	****	
		C 0 hr vs Eto 18.75 0 hr	0.11	25.66	<0.0001	****	
		C 1 hr vs Eto 6.25 1 hr	0.46	22.23	<0.0001	****	
		C 1 hr vs Eto 12.5 1 hr	0.46	26.99	<0.0001	****	
		C 1 hr vs Eto 18.75 1 hr	0.46	27.66	<0.0001	****	
		C 4 hr vs Eto 6.25 4 hr	1.24	19.57	<0.0001	****	
		C 4 hr vs Eto 12.5 4 hr	1.24	15.7	<0.0001	****	
		C 4 hr vs Eto 18.75 4 hr	1.24	21.32	<0.0001	****	
		C 8 hr vs Eto 6.25 8 hr	3.11	13.04	<0.0001	****	
		C 8 hr vs Eto 12.5 8 hr	3.11	13.84	<0.0001	****	
		C 8 hr vs Eto 18.75 8 hr	3.11	17.72	<0.0001	****	
		By Time	Eto 6.25 0 hr vs 1 hr	19.34	22.23	0.4246	ns
		Eto 6.25 1 hr vs 4 hr	22.23	19.57	0.8241	ns	
		Eto 6.25 4 hr vs 8 hr	19.57	13.04	<0.0001	****	
		Eto 12.5 0 hr vs 1 hr	20.85	26.99	<0.0001	****	
		Eto 12.5 1 hr vs 4 hr	26.99	15.7	<0.0001	****	
		Eto 12.5 4 hr vs 8 hr	15.7	13.84	0.9967	ns	
		Eto 18.75 0 hr vs 1 hr	25.66	27.66	>0.9999	ns	
		Eto 18.75 1 hr vs 4 hr	27.66	21.32	<0.0001	****	
		Eto 18.75 4 hr vs 8 hr	21.32	17.72	0.0435	*	
Etoposide Doses Combined	To Control	C vs Eto 0 hr All	1.337	21.76	<0.0001	****	
		C vs Eto 1 hr All	1.337	25.25	<0.0001	****	
		C vs Eto 4 hr All	1.337	18.63	<0.0001	****	
		C vs Eto 8 hr All	1.337	14.88	<0.0001	****	
		By Time	Eto All 0 hr vs 1 hr	21.76	25.25	<0.0001	****
			Eto All 1 hr vs 4 hr	25.25	18.63	<0.0001	****
			Eto All 4 hr vs 8 hr	18.63	14.88	<0.0001	****

3.2 Bioflavonoids Induce Persistent DNA DSBs that are Resolved with Differential Kinetics

Etoposide is a known Top2 poison that at low doses can cause robust amounts of DNA damage and therefore is used as a chemotherapeutic agent. Since bioflavonoids have

structural similarity to etoposide and can induce DSBs, it was uncertain if the DSBs caused by bioflavonoids are sensed and repaired with kinetics similar to those induced by etoposide. To quantify the persistence and repair of bioflavonoid-induced DNA damage, cells were exposed to increasing doses of bioflavonoids, and γ -H2AX foci scored at immediately after exposure and 1, 4, and 8h post-exposure. All bioflavonoids induced the robust appearance of γ -H2AX foci, though the damage did not reach the levels observed with etoposide treatment.

3.2.1 Genistein

Genistein (25, 50, 75, 100 μ M; LD50 =75 μ M) induced an average of 7.6, 13.3, 15.6, and 18.4 foci/cell immediately following treatment. The average number of γ -H2AX foci/cell persisted at 1h post-exposure as compared to the 0h timepoint, although it was observed that one dose (50 μ M) led to a further statistically significant decrease in the average number foci/cell (avg. 8.3 foci/cell). The presence of γ -H2AX foci decreased at 4h and 8h post-exposure following all doses. By 4h post-exposure, the average number of foci/cell with 25 μ M treatment decreased to baseline and remained at baseline after 8h (avg. 0.9 & 4.8 foci/cell). By 8h post-exposure, 50 μ M treatment decreased to baseline also (avg. 3.9 foci/cell). A slight but statistically insignificant increase was observed in foci/cell at 8h post-exposure of 25 μ M (4.8 foci/cell) compared to 4h post-exposure (avg. 0.9 foci/cell) (Fig. 3.3 & Table 3.3).

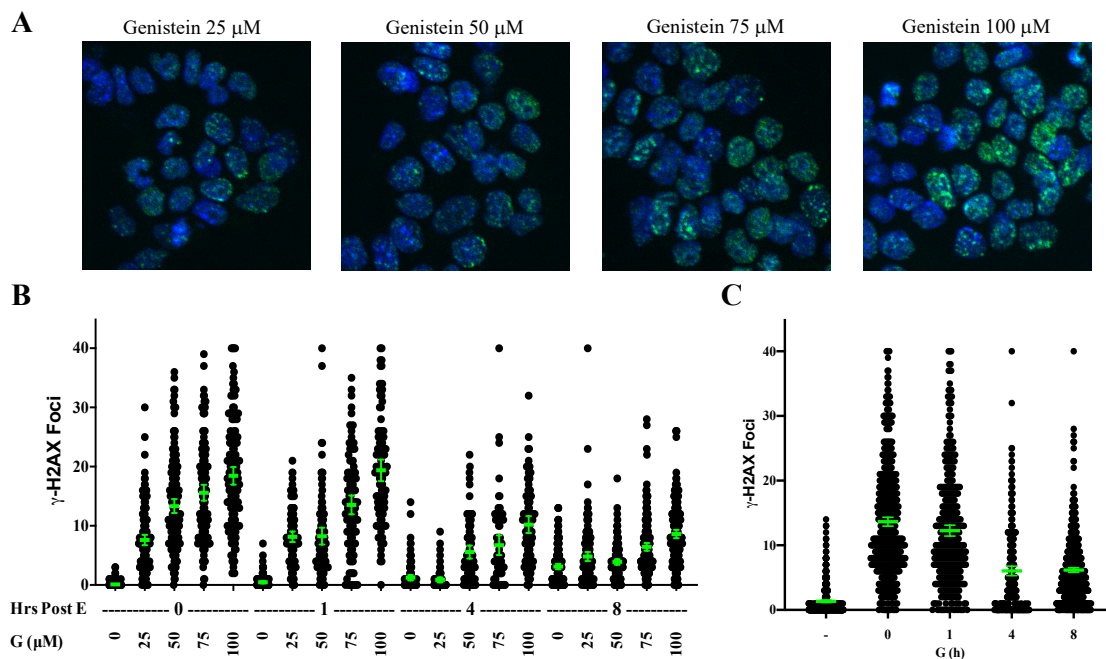


Figure 3.3: DNA Damage Repair Kinetics Over 8h with Genistein Treatment. After 1h genistein treatment at 25, 50, 75, or 100 μ M, cells were stained for γ -H2AX immediately after treatment, or following 1, 4, or 8h recovery. (A) Representative confocal images from all genistein doses immediately after treatment and staining. (B) Each point represents the number of γ -H2AX foci in a cell. Averages are represented in green with error bars showing the 95% confidence interval. At least 100 cells were counted for each treatment group/time point. (C) The average number of γ -H2AX foci are shown for each timepoint, all doses were combined to show the general trend of DNA damage recovery over 8h. For statistical analysis, see Table 3.3.

Table 3.3: DNA Damage Repair Kinetics Over 8h with Genistein Treatment Data Analysis. The average number of γ -H2AX foci of the treatments being compared are shown with the p-value from the comparison. A one-way ANOVA was used with Sidak's multiple comparisons test (**** p<0.0001, *** p<0.001, ** p<0.01, * p<0.05).

Compound	Comparison	Average Values	p-value	Significant		
Genistein (G)	To Control	C 0 hr vs G 25 0 hr	0.11 7.61	<0.0001	****	
		C 0 hr vs G 50 0 hr	0.11 13.34	<0.0001	****	
		C 0 hr vs G 75 0 hr	0.11 15.59	<0.0001	****	
		C 0 hr vs G 100 0 hr	0.11 18.44	<0.0001	****	
		C 1 hr vs G 25 1 hr	0.46 8.14	<0.0001	****	
		C 1 hr vs G 50 1 hr	0.46 8.26	<0.0001	****	
		C 1 hr vs G 75 1 hr	0.46 13.52	<0.0001	****	
		C 1 hr vs G 100 1 hr	0.46 19.37	<0.0001	****	
		C 4 hr vs G 25 4 hr	1.24 0.85	>0.9999	ns	
		C 4 hr vs G 50 4 hr	1.24 5.56	<0.0001	****	
		C 4 hr vs G 75 4 hr	1.24 6.73	<0.0001	****	
		C 4 hr vs G 100 4 hr	1.24 10.2	<0.0001	****	
		C 8 hr vs G 25 8 hr	3.11 4.81	0.2111	ns	
		C 8 hr vs G 50 8 hr	3.11 3.9	>0.9999	ns	
		C 8 hr vs G 75 8 hr	3.11 6.45	<0.0001	****	
		C 8 hr vs G 100 8 hr	3.11 8.61	<0.0001	****	
	By Time	G 25 0 hr vs 1 hr	7.61 8.14	>0.9999	ns	
		G 25 1 hr vs 4 hr	8.14 0.85	<0.0001	****	
		G 25 4 hr vs 8 hr	0.85 4.81	<0.0001	****	
		G 50 0 hr vs 1 hr	13.34 8.26	<0.0001	****	
G 50 1 hr vs 4 hr		8.26 5.56	0.0508	ns		
G 50 4 hr vs 8 hr		5.56 3.9	0.6972	ns		
G 75 0 hr vs 1 hr		15.59 13.52	0.1617	ns		
G 75 1 hr vs 4 hr		13.52 6.73	<0.0001	****		
G 75 4 hr vs 8 hr		6.73 6.45	>0.9999	ns		
G 100 0 hr vs 1 hr		18.44 19.37	>0.9999	ns		
G 100 1 hr vs 4 hr		19.37 10.2	<0.0001	****		
G 100 4 hr vs 8 hr		10.2 8.61	0.7117	ns		
Genistein Doses Combined		To Control	C vs G 0 hr All	1.337 13.64	<0.0001	****
			C vs G 1 hr All	1.337 12.26	<0.0001	****
	C vs G 4 hr All		1.337 6.039	<0.0001	****	
	C vs G 8 hr All		1.337 6.171	<0.0001	****	
	By Time	G All 0 hr vs 1 hr	13.64 12.26	0.0054	**	
		G All 1 hr vs 4 hr	12.26 6.039	<0.0001	****	
		G All 4 hr vs 8 hr	6.039 6.171	>0.9999	ns	

Overall, when accounting for all four concentrations of genistein, the average number of DNA DSBs decreased slightly 1h post-exposure, before drastically and significantly decreasing at 4h and remaining low or undetectable by 8h post-exposure (Fig. 3.3C and Table 3.3).

3.2.2 Quercetin

Quercetin (25, 50, 75, 100 μM ; LD50 =75 μM) induced an average of 12.0, 15.8, 15.4, and 20.2 foci/ cell. Cells exposed to quercetin showed significant number of $\gamma\text{-H2AX}$ foci immediately following exposure at all doses, that rapidly significantly decreased within 1h at all concentrations. At 1h post-exposure with 25 μM , the average number foci/cell decreased by half (avg. 12.0 to 6.5 foci/cell). The average foci/cell remained constant or further decreased by 4h post-exposure. Interestingly, by 8h post-exposure of higher 75 and 100 μM concentration, we observed a significant increase in the average number of foci/cell compared to the 4h with (avg. 7.1 to 14.2 & 3.9 to 13.0 foci/cell respectively) (Fig. 3.4B & Table 3.4).

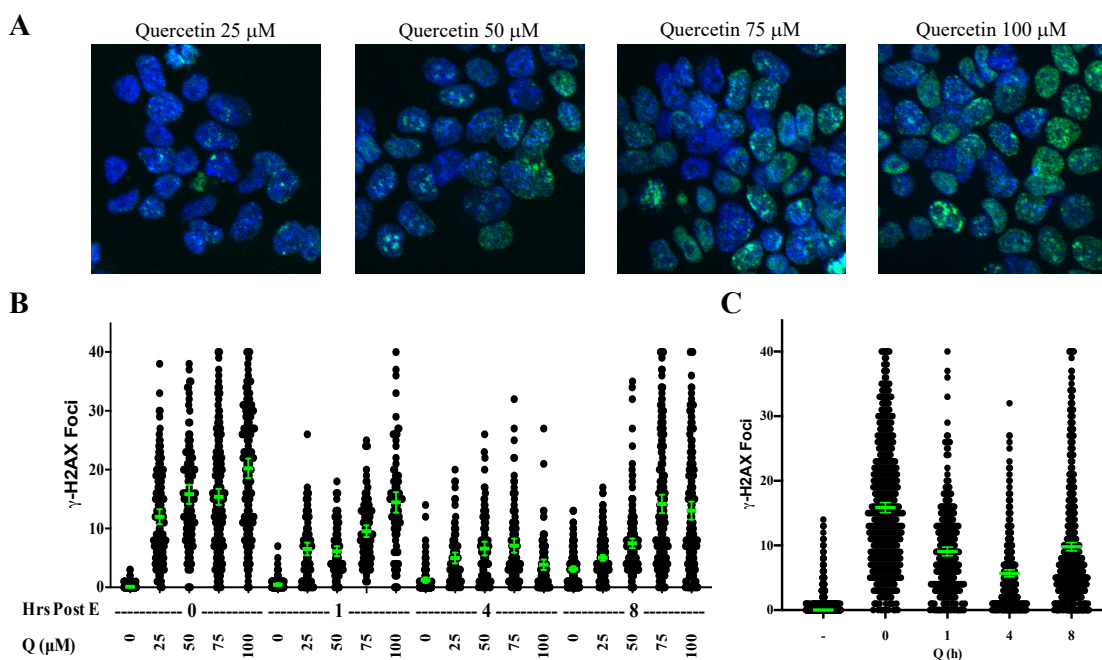


Figure 3.4: DNA Damage Repair Kinetics Over 8h with Quercetin Treatment. After 1h quercetin treatment at 25, 50, 75, or 100 μM , cells were stained for $\gamma\text{-H2AX}$ immediately after treatment, or following 1, 4, or 8h recovery. (A) Representative confocal images from all quercetin doses immediately after treatment and staining. (B) Each point represents the number of $\gamma\text{-H2AX}$ foci in a cell. Averages are represented in green with error bars showing the 95% confidence interval. At least 100 cells were counted for each treatment group/time point. (C) The average number of $\gamma\text{-H2AX}$ foci are shown for each timepoint, all doses were combined to show the general trend of DNA damage recovery over 8h. For statistical analysis, see Table 3.4.

When all quercetin concentration treatments are considered, there was a significant decline in DSBs by 1 and 4h post-exposure, with a significant increase 8h post-exposure (Fig. 3.4C and Table 3.4).

Table 3.4: DNA Damage Repair Kinetics Over 8h with Quercetin Treatment Data Analysis. The average number of γ -H2AX foci of the treatments being compared are shown with the p-value from the comparison. A one-way ANOVA was used with Sidak's multiple comparisons test (**** p<0.0001, *** p<0.001, ** p<0.01, * p<0.05).

Compound	Comparison		Average Values		p-value	Significant
Genistein (G)	To Control	C 0 hr vs G 25 0 hr	0.11	7.61	<0.0001	****
		C 0 hr vs G 50 0 hr	0.11	13.34	<0.0001	****
		C 0 hr vs G 75 0 hr	0.11	15.59	<0.0001	****
		C 0 hr vs G 100 0 hr	0.11	18.44	<0.0001	****
		C 1 hr vs G 25 1 hr	0.46	8.14	<0.0001	****
		C 1 hr vs G 50 1 hr	0.46	8.26	<0.0001	****
		C 1 hr vs G 75 1 hr	0.46	13.52	<0.0001	****
		C 1 hr vs G 100 1 hr	0.46	19.37	<0.0001	****
		C 4 hr vs G 25 4 hr	1.24	0.85	>0.9999	ns
		C 4 hr vs G 50 4 hr	1.24	5.56	<0.0001	****
		C 4 hr vs G 75 4 hr	1.24	6.73	<0.0001	****
		C 4 hr vs G 100 4 hr	1.24	10.2	<0.0001	****
		C 8 hr vs G 25 8 hr	3.11	4.81	0.2111	ns
		C 8 hr vs G 50 8 hr	3.11	3.9	>0.9999	ns
		C 8 hr vs G 75 8 hr	3.11	6.45	<0.0001	****
		C 8 hr vs G 100 8 hr	3.11	8.61	<0.0001	****
	By Time	G 25 0 hr vs 1 hr	7.61	8.14	>0.9999	ns
		G 25 1 hr vs 4 hr	8.14	0.85	<0.0001	****
		G 25 4 hr vs 8 hr	0.85	4.81	<0.0001	****
		G 50 0 hr vs 1 hr	13.34	8.26	<0.0001	****
G 50 1 hr vs 4 hr		8.26	5.56	0.0508	ns	
G 50 4 hr vs 8 hr		5.56	3.9	0.6972	ns	
G 75 0 hr vs 1 hr		15.59	13.52	0.1617	ns	
G 75 1 hr vs 4 hr		13.52	6.73	<0.0001	****	
G 75 4 hr vs 8 hr		6.73	6.45	>0.9999	ns	
G 100 0 hr vs 1 hr		18.44	19.37	>0.9999	ns	
G 100 1 hr vs 4 hr	19.37	10.2	<0.0001	****		
G 100 4 hr vs 8 hr	10.2	8.61	0.7117	ns		
Genistein Doses Combined	To Control	C vs G 0 hr All	1.337	13.64	<0.0001	****
		C vs G 1 hr All	1.337	12.26	<0.0001	****
		C vs G 4 hr All	1.337	6.039	<0.0001	****
		C vs G 8 hr All	1.337	6.171	<0.0001	****
	By Time	G All 0 hr vs 1 hr	13.64	12.26	0.0054	**
		G All 1 hr vs 4 hr	12.26	6.039	<0.0001	****
		G All 4 hr vs 8 hr	6.039	6.171	>0.9999	ns

3.2.3 Kaempferol

Kaempferol only weakly induced DSBs; 25, 50, 75, 100 μM induced an average of 4.2, 4.6, 5.6, and 5.6 foci/cell (LD50: 100 μM). Increasing concentrations of kaempferol led to an immediate, mild, but statistically significant increase in $\gamma\text{-H2AX}$ foci with 4.2, 4.6, 5.6, and 5.6 foci/cell, respectively. All doses of kaempferol caused a similar number of $\gamma\text{-H2AX}$ foci. The appearance of $\gamma\text{-H2AX}$ significantly increased by 1h post-exposure at all doses except 75 μM . For example, the average number foci/cell quadrupled 1h post-exposure with 25 μM treatment (avg. 16.9 foci/cell). By 4h and 8h post-exposure, $\gamma\text{-H2AX}$ foci decreased back to approximately the same amount observed immediately following treatment at the 0h timepoint (Fig. 3.5B and Table 3.5).

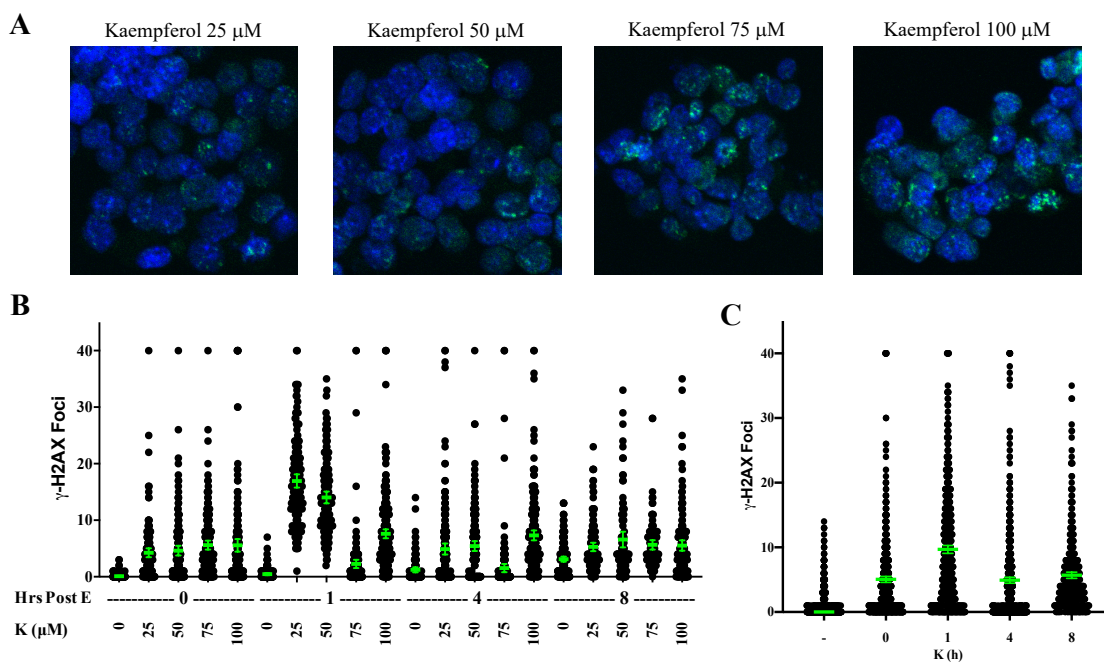


Figure 3.5: DNA Damage Repair Kinetics Over 8h with Kaempferol Treatment. After 1h kaempferol treatment at 25, 50, 75, or 100 μM , cells were stained for $\gamma\text{-H2AX}$ immediately after treatment, or following 1, 4, or 8h recovery. (A) Representative confocal images from all kaempferol doses immediately after treatment and staining. (B) Each point represents the number of $\gamma\text{-H2AX}$ foci in a cell. Averages are represented in green with error bars showing the 95% confidence interval. At least 100 cells were counted for each treatment group/time point. (C) The average number of $\gamma\text{-H2AX}$ foci are shown for each timepoint, all doses were combined to show the general trend of DNA damage recovery over 8h. For statistical analysis, see Table 3.5.

Overall, kaempferol showed a significantly elevated number of γ -H2AX foci immediately after treatment compared to control. This increased 1h post exposure when all doses were account for together, though it is the lower kaempferol doses (25 & 50 μ M) that mainly increased. After 4 and 8h post exposure the amount of damage significantly decreased again (Fig. 3.5C and Table 3.5).

Table 3.5: DNA Damage Repair Kinetics Over 8h with Kaempferol Treatment Data Analysis. The average number of γ -H2AX foci of the treatments being compared are shown with the p-value from the comparison. A one-way ANOVA was used with Sidak's multiple comparisons test (**** p<0.0001, *** p<0.001, ** p<0.01, * p<0.05).

Compound	Comparison	Average Values		p-value	Significant		
Kaempferol (K)	To Control	C 0 hr vs K 25 0 hr	0.11	4.24	<0.0001	****	
		C 0 hr vs K 50 0 hr	0.11	4.62	<0.0001	****	
		C 0 hr vs K 75 0 hr	0.11	5.6	<0.0001	****	
		C 0 hr vs K 100 0 hr	0.11	5.56	<0.0001	****	
		C 1 hr vs K 25 1 hr	0.46	16.94	<0.0001	****	
		C 1 hr vs K 50 1 hr	0.46	14.03	<0.0001	****	
		C 1 hr vs K 75 1 hr	0.46	2.28	0.2073	ns	
		C 1 hr vs K 100 1 hr	0.46	7.6	<0.0001	****	
		C 4 hr vs K 25 4 hr	1.24	4.9	<0.0001	****	
		C 4 hr vs K 50 4 hr	1.24	5.43	<0.0001	****	
		C 4 hr vs K 75 4 hr	1.24	1.55	>0.9999	ns	
		C 4 hr vs K 100 4 hr	1.24	7.32	<0.0001	****	
		C 8 hr vs K 25 8 hr	3.11	5.28	0.025	*	
		C 8 hr vs K 50 8 hr	3.11	6.59	<0.0001	****	
		C 8 hr vs K 75 8 hr	3.11	5.65	0.0075	**	
		C 8 hr vs K 100 8 hr	3.11	5.53	0.0033	**	
	By Time	K 25 0 hr vs 1 hr	4.24	16.94	<0.0001	****	
		K 25 1 hr vs 4 hr	16.94	4.9	<0.0001	****	
		K 25 4 hr vs 8 hr	4.9	5.28	>0.9999	ns	
		K 50 0 hr vs 1 hr	4.62	14.03	<0.0001	****	
K 50 1 hr vs 4 hr		14.03	5.43	<0.0001	****		
K 50 4 hr vs 8 hr		5.43	6.59	0.9843	ns		
K 75 0 hr vs 1 hr		5.6	2.28	<0.0001	****		
K 75 1 hr vs 4 hr		2.28	1.55	>0.9999	ns		
K 75 4 hr vs 8 hr		1.55	5.65	<0.0001	****		
K 100 0 hr vs 1 hr		5.56	7.6	0.0071	**		
K 100 1 hr vs 4 hr		7.6	7.32	>0.9999	ns		
K 100 4 hr vs 8 hr		7.32	5.53	0.0866	ns		
Kaempferol Doses Combined		To Control	C vs K 0 hr All	1.337	5.047	<0.0001	****
			C vs K 1 hr All	1.337	9.685	<0.0001	****
	C vs K 4 hr All		1.337	4.918	<0.0001	****	
	C vs K 8 hr All		1.337	5.688	<0.0001	****	
	By Time	K All 0 hr vs 1 hr	5.047	9.685	<0.0001	****	
		K All 1 hr vs 4 hr	9.685	4.918	<0.0001	****	
		K All 4 hr vs 8 hr	4.918	5.688	0.2038	ns	

3.2.4 Myricetin

Cells treated with increasing doses of myricetin led to an overall significant increase in the average number foci/cell, although not with dose dependent increases

observed with other bioflavonoids tested. Myricetin induced an average of 9.2 and 10.5 foci/cell, however, the number of observed foci peaked at 50 μ M (LD50) and at higher doses were quenched, although higher than untreated cells. 75 and 100 μ M myricetin induced an average of 3.7 and 4.8 foci/cell immediately after treatment, respectively. The appearance of γ -H2AX persisted or continued to significantly increase by 1h post-exposure, before significantly decreasing at 4 and 8h post-exposure (Fig. 3.6B and Table 3.6). Myricetin treatment showed the most similar trend to etoposide treatment with an increase in γ -H2AX foci after 1h, followed by decreases by 4 and 8h, with all doses returning to baseline by 8h post-exposure (Fig. 3.6C and Table 3.6).

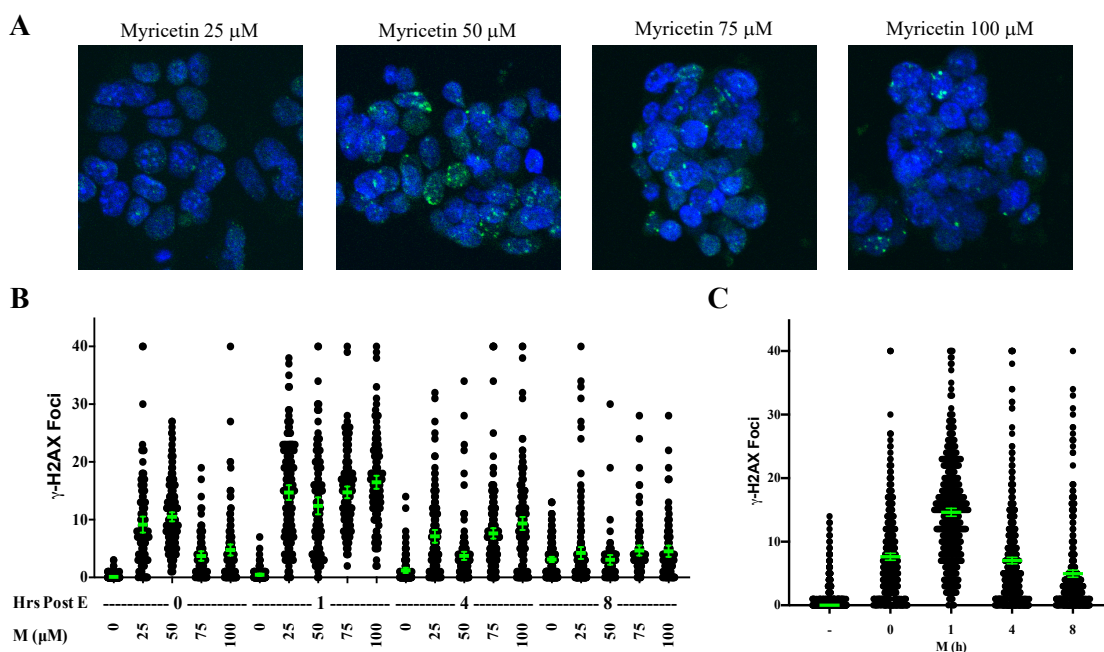


Figure 3.6: DNA Damage Repair Kinetics Over 8h with Myricetin Treatment. After 1h myricetin treatment at 25, 50, 75, or 100 μ M, cells were stained for γ -H2AX immediately after treatment, or following 1, 4, or 8h recovery. (A) Representative confocal images from all myricetin doses immediately after treatment and staining. (B) Each point represents the number of γ -H2AX foci in a cell. Averages are represented in green with error bars showing the 95% confidence interval. At least 100 cells were counted for each treatment group/time point. (C) The average number of γ -H2AX foci are shown for each timepoint, all doses were combined to show the general trend of DNA damage recovery over 8h. For statistical analysis, see Table 3.6.

Table 3.6: DNA Damage Repair Kinetics Over 8h with Myricetin Treatment Data Analysis. The average number of γ -H2AX foci of the treatments being compared are shown with the p-value from the comparison. A one-way ANOVA was used with Sidak's multiple comparisons test (**** p<0.0001, *** p<0.001, ** p<0.01, * p<0.05).

Compound	Comparison	Average Values		p-value	Significant		
Myricetin (M)	To Control	C 0 hr vs M 25 0 hr	0.11	9.15	<0.0001	****	
		C 0 hr vs M 50 0 hr	0.11	10.49	<0.0001	****	
		C 0 hr vs M 75 0 hr	0.11	3.71	0.0001	***	
		C 0 hr vs M 100 0 hr	0.11	4.76	<0.0001	****	
		C 1 hr vs M 25 1 hr	0.46	14.69	<0.0001	****	
		C 1 hr vs M 50 1 hr	0.46	12.39	<0.0001	****	
		C 1 hr vs M 75 1 hr	0.46	14.73	<0.0001	****	
		C 1 hr vs M 100 1 hr	0.46	16.48	<0.0001	****	
		C 4 hr vs M 25 4 hr	1.24	7.12	<0.0001	****	
		C 4 hr vs M 50 4 hr	1.24	3.74	0.0177	*	
		C 4 hr vs M 75 4 hr	1.24	7.63	<0.0001	****	
		C 4 hr vs M 100 4 hr	1.24	9.35	<0.0001	****	
		C 8 hr vs M 25 8 hr	3.11	4.23	0.9533	ns	
		C 8 hr vs M 50 8 hr	3.11	3.05	>0.9999	ns	
		C 8 hr vs M 75 8 hr	3.11	4.67	0.6952	ns	
		C 8 hr vs M 100 8 hr	3.11	4.53	0.8494	ns	
	By Time	M 25 0 hr vs 1 hr	9.15	14.69	<0.0001	****	
		M 25 1 hr vs 4 hr	14.69	7.12	<0.0001	****	
		M 25 4 hr vs 8 hr	7.12	4.23	0.0007	***	
		M 50 0 hr vs 1 hr	10.49	12.39	0.1227	ns	
M 50 1 hr vs 4 hr		12.39	3.74	<0.0001	****		
M 50 4 hr vs 8 hr		3.74	3.05	>0.9999	ns		
M 75 0 hr vs 1 hr		3.71	14.73	<0.0001	****		
M 75 1 hr vs 4 hr		14.73	7.63	<0.0001	****		
M 75 4 hr vs 8 hr		7.63	4.67	0.0008	***		
M 100 0 hr vs 1 hr		4.76	16.48	<0.0001	****		
M 100 1 hr vs 4 hr		16.48	9.35	<0.0001	****		
M 100 4 hr vs 8 hr		9.35	4.53	<0.0001	****		
Myricetin Doses Combined		To Control	C vs M 0 hr All	1.337	7.637	<0.0001	****
			C vs M 1 hr All	1.337	14.62	<0.0001	****
	C vs M 4 hr All		1.337	7.032	<0.0001	****	
	C vs M 8 hr All		1.337	4.970	<0.0001	****	
	By Time	M All 0 hr vs 1 hr	7.637	14.62	<0.0001	****	
		M All 1 hr vs 4 hr	14.62	7.032	<0.0001	****	
		M All 4 hr vs 8 hr	7.032	4.970	<0.0001	****	

3.2.5 Luteolin

Cells treated with increasing doses of luteolin led to an overall significant increase in the average number foci/cell, although not with dose dependent increases observed with other bioflavonoids tested. Luteolin induced an average of 10.8 and 17.0 foci/cell at 50 and

100 μ M, however, the number of observed foci peaked at 100 μ M and at higher doses were quenched, although these were still significantly higher than untreated cells. 150 and 200 μ M luteolin induced an average of 8.3 and 11.5 foci/cell immediately after treatment, respectively (LD50: 175 μ M). However, a lack of consistent dose-dependency and repair kinetics was observed across the timepoints and doses (Fig. 3.7B and Table 3.7). Considering all doses and timepoints of cells post-exposure to luteolin, samples consistently showed that by 8h post-exposure all samples had significantly decreased damage compared to the 0h timepoint (Fig. 3.7C and Table 3.7).

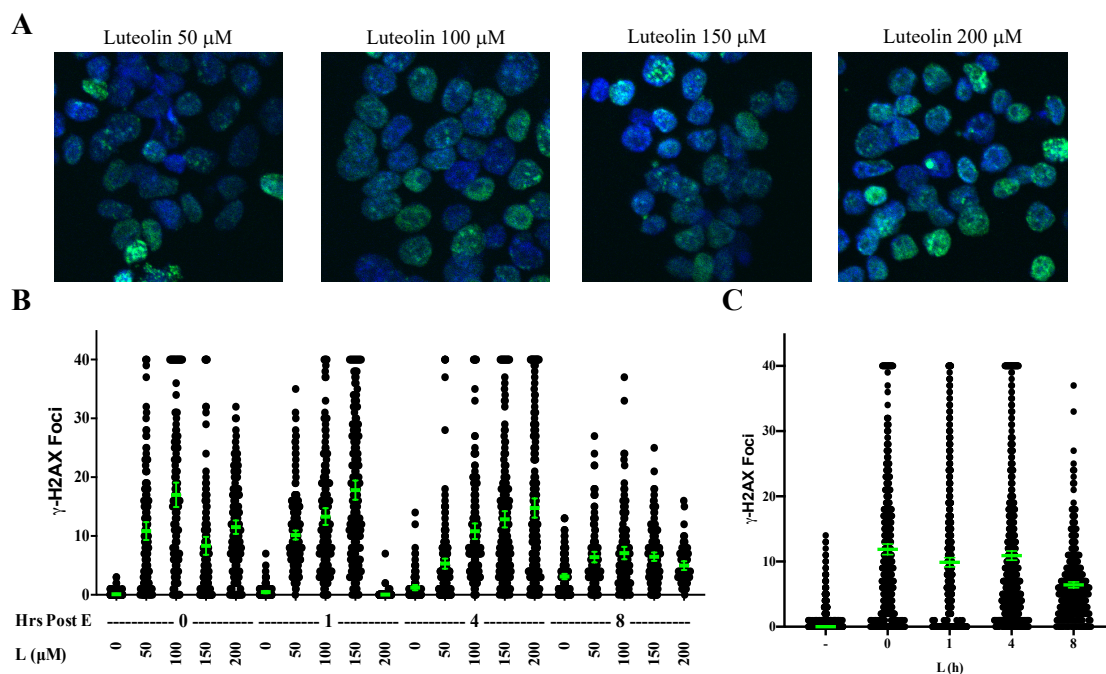


Figure 3.7: DNA Damage Repair Kinetics Over 8h with Luteolin Treatment. After 1h luteolin treatment at 50, 100, 150, or 200 μ M, cells were stained for γ -H2AX immediately after treatment, or following 1, 4, or 8h recovery. (A) Representative confocal images from all luteolin doses immediately after treatment and staining. (B) Each point represents the number of γ -H2AX foci in a cell. Averages are represented in green with error bars showing the 95% confidence interval. At least 100 cells were counted for each treatment group/time point. (C) The average number of γ -H2AX foci are shown for each timepoint, all doses were combined to show the general trend of DNA damage recovery over 8h. For statistical analysis, see Table 3.7.

Table 3.7: DNA Damage Repair Kinetics Over 8h with Luteolin Treatment Data Analysis. The average number of γ -H2AX foci of the treatments being compared are shown with the p-value from the comparison. A one-way ANOVA was used with Sidak's multiple comparisons test (**** p<0.0001, *** p<0.001, ** p<0.01, * p<0.05).

Compound	Comparison	Average Values		p-value	Significant	
Luteolin (L)	To Control	C 0 hr vs L 50 0 hr	0.11	10.84	<0.0001	****
		C 0 hr vs L 100 0 hr	0.11	17	<0.0001	****
		C 0 hr vs L 150 0 hr	0.11	8.34	<0.0001	****
		C 0 hr vs L 200 0 hr	0.11	11.51	<0.0001	****
		C 1 hr vs L 50 1 hr	0.46	10.17	<0.0001	****
		C 1 hr vs L 100 1 hr	0.46	13.3	<0.0001	****
		C 1 hr vs L 150 1 hr	0.46	17.81	<0.0001	****
		C 1 hr vs L 200 1 hr	0.46	0.06	>0.9999	ns
		C 4 hr vs L 50 4 hr	1.24	5.3	0.0003	***
		C 4 hr vs L 100 4 hr	1.24	10.82	<0.0001	****
		C 4 hr vs L 150 4 hr	1.24	12.84	<0.0001	****
		C 4 hr vs L 200 4 hr	1.24	14.77	<0.0001	****
		C 8 hr vs L 50 8 hr	3.11	6.42	0.0099	**
		C 8 hr vs L 100 8 hr	3.11	7.1	0.0003	***
		C 8 hr vs L 150 8 hr	3.11	6.48	0.0033	**
		C 8 hr vs L 200 8 hr	3.11	4.97	0.9769	ns
	By Time	L 50 0 hr vs 1 hr	10.84	10.17	>0.9999	ns
		L 50 1 hr vs 4 hr	10.17	5.3	<0.0001	****
		L 50 4 hr vs 8 hr	5.3	6.42	0.9998	ns
		L 100 0 hr vs 1 hr	17	13.3	0.001	***
L 100 1 hr vs 4 hr		13.3	10.82	0.1081	ns	
L 100 4 hr vs 8 hr		10.82	7.1	0.0013	**	
L 150 0 hr vs 1 hr		8.34	17.81	<0.0001	****	
L 150 1 hr vs 4 hr		17.81	13.84	<0.0001	****	
L 150 4 hr vs 8 hr	12.84	6.48	<0.0001	****		
Luteolin Doses Combined	To Control	C vs L 0 hr All	1.337	11.87	<0.0001	****
		C vs L 1 hr All	1.337	9.880	<0.0001	****
		C vs L 4 hr All	1.337	10.90	<0.0001	****
		C vs L 8 hr All	1.337	6.420	<0.0001	****
	By Time	L All 0 hr vs 1 hr	11.87	9.880	0.0002	***
		L All 1 hr vs 4 hr	9.880	10.90	0.1186	ns
		L All 4 hr vs 8 hr	10.90	6.420	<0.0001	****

3.2.6 Genistein and Quercetin Combination Treatment

Few previous studies have focused on combining bioflavonoids from different subgroups though combination treatments would better mimic dietary exposure to these compounds. Therefore, to determine if combinatorial exposure to bioflavonoids would an

promote additive or synergistic impact on the appearance, persistence, and repair of γ -H2AX foci, genistein and quercetin were both used in this section.

Cells were exposed to equal concentrations of both genistein and quercetin (G/Q) at the same concentrations used for single exposures to each. Therefore, these doses are still higher than most would experience through a normal diet. It was expected that bioflavonoids from different sub-groups would increase the amount of damage observed in these cells. However, by contrast, cells exposed to increasing concentrations of G/Q immediately after treatment produced a similar average number of foci/cell (9.2-17.9) compared to genistein (7.6-18.4) or quercetin (12-20.2) alone instead of increased amounts of damage. By 1h post-exposure, the observed kinetic trend of average foci/cell in the G/Q cells mirrored that of genistein alone with the amount of damage remaining consistent with the 0h timepoint (Fig. 3.8, 3.9 and Table 3.8). Overall, the amount of DNA DSBs in cells exposed to G/Q decreased slightly at 4h, then significantly decreased by 8h post-exposure, except in the 100/100 μ M group which showed a significant increase in average foci/cell from 1 to 4h post-exposure, before decreasing at 8h post-exposure (avg. 15.3 to 19.0 foci/cell) (Fig. 3.8 and Table 3.8).

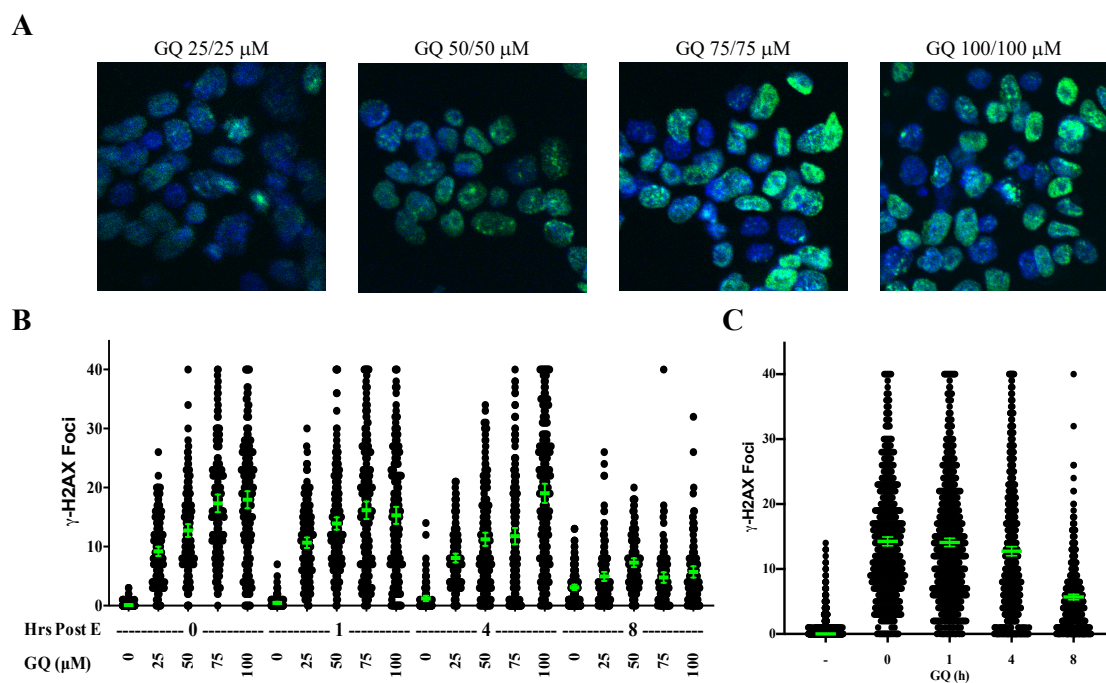


Figure 3.8: DNA Damage Repair Kinetics Over 8h with Genistein/Quercetin Treatment. After 1h genistein/quercetin treatment at 25/25, 50/50, 75/75, or 100/100 μM , cells were stained for $\gamma\text{-H2AX}$ immediately after treatment, or following 1, 4, or 8h recovery. (A) Representative confocal images from all genistein/quercetin doses immediately after treatment and staining. (B) Each point represents the number of $\gamma\text{-H2AX}$ foci in a cell. Averages are represented in green with error bars showing the 95% confidence interval. At least 100 cells were counted for each treatment group/time point. (C) The average number of $\gamma\text{-H2AX}$ foci are shown for each timepoint, all doses were combined to show the general trend of DNA damage recovery over 8h. For statistical analysis, see Table 3.8.

Table 3.8: DNA Damage Repair Kinetics Over 8h with Genistein/Quercetin Treatment Data Analysis. The average number of γ -H2AX foci of the treatments being compared are shown with the p-value from the comparison. A one-way ANOVA was used with Sidak's multiple comparisons test (**** p<0.0001, *** p<0.001, ** p<0.01, * p<0.05).

Compound	Comparison	Average Values		p-value	Significant	
Genistein/ Quercetin (GQ)	To Control	C 0 hr vs GQ 25 0 hr	0.11	9.21	<0.0001	****
		C 0 hr vs GQ 50 0 hr	0.11	12.73	<0.0001	****
		C 0 hr vs GQ 75 0 hr	0.11	17.32	<0.0001	****
		C 0 hr vs GQ 100 0 hr	0.11	17.94	<0.0001	****
	C 1 hr vs GQ 25 1 hr	0.46	10.67	<0.0001	****	
		C 1 hr vs GQ 50 1 hr	0.46	13.92	<0.0001	****
		C 1 hr vs GQ 75 1 hr	0.46	16.16	<0.0001	****
		C 1 hr vs GQ 100 1 hr	0.46	15.3	<0.0001	****
	C 4 hr vs GQ 25 4 hr	1.24	8.07	<0.0001	****	
		C 4 hr vs GQ 50 4 hr	1.24	11.25	<0.0001	****
		C 4 hr vs GQ 75 4 hr	1.24	11.77	<0.0001	****
		C 4 hr vs GQ 100 4 hr	1.24	19.04	<0.0001	****
	C 8 hr vs GQ 25 8 hr	3.11	4.95	0.6395	ns	
		C 8 hr vs GQ 50 8 hr	3.11	7.28	<0.0001	****
		C 8 hr vs GQ 75 8 hr	3.11	4.78	0.9105	ns
		C 8 hr vs GQ 100 8 hr	3.11	5.7	0.1193	ns
	By Time	GQ 25 0 hr vs 1 hr	9.21	10.67	0.9301	ns
		GQ 25 1 hr vs 4 hr	10.67	8.07	0.0551	ns
		GQ 25 4 hr vs 8 hr	8.07	4.95	0.0086	**
		GQ 50 0 hr vs 1 hr	12.73	13.92	0.995	ns
GQ 50 1 hr vs 4 hr		13.92	11.25	0.0096	**	
GQ 50 4 hr vs 8 hr		11.25	7.28	<0.0001	****	
GQ 75 0 hr vs 1 hr		17.32	16.16	0.9981	ns	
GQ 75 1 hr vs 4 hr		16.16	11.77	<0.0001	****	
GQ 75 4 hr vs 8 hr		11.77	4.78	<0.0001	****	
GQ 100 0 hr vs 1 hr		17.94	15.3	0.0237	*	
GQ 100 1 hr vs 4 hr		15.3	19.04	<0.0001	****	
GQ 100 4 hr vs 8 hr		19.04	5.7	<0.0001	****	
Genistein/ Quercetin Doses Combined	To Control	C vs GQ 0 hr All	1.337	14.25	<0.0001	****
		C vs GQ 1 hr All	1.337	14.10	<0.0001	****
		C vs GQ 4 hr All	1.337	12.74	<0.0001	****
		C vs GQ 8 hr All	1.337	5.690	<0.0001	****
	By Time	GQ All 0 hr vs 1 hr	14.25	14.10	0.9998	ns
		GQ All 1 hr vs 4 hr	14.10	12.74	0.0052	**
		GQ All 4 hr vs 8 hr	12.74	5.690	<0.0001	****

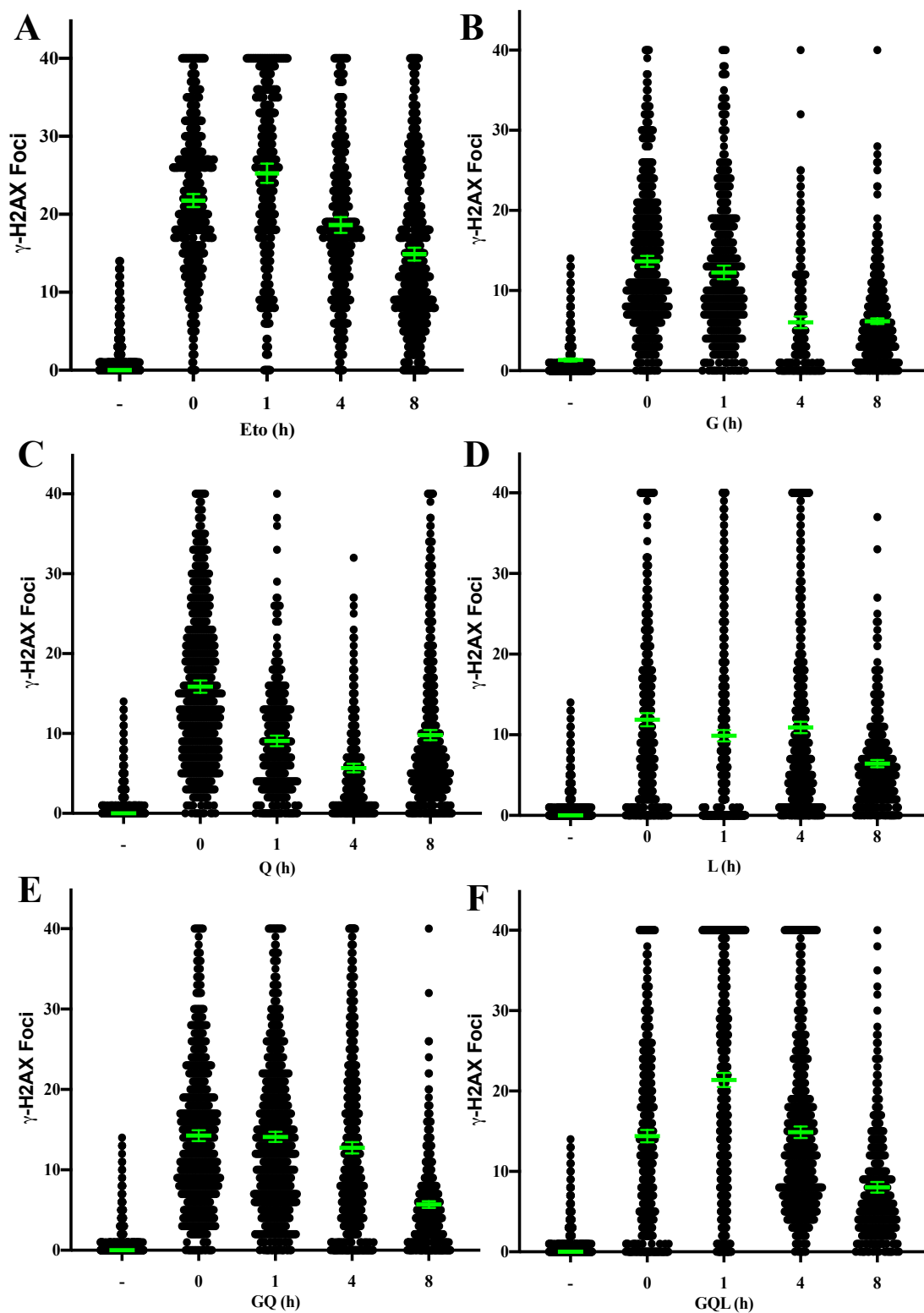


Figure 3.9: Generalized Repair Kinetics for Single and Combination Treatments. Each point represents the number of γ -H2AX foci in a cell. Averages are represented in green with error bars showing the 95% confidence interval. At least 100 cells were counted for each treatment group/time point. (A) Etoposide (B) Genistein (C) Quercetin (D) Luteolin (E) Genistein/Quercetin and (F) Genistein/Quercetin/Luteolin

3.2.7 Genistein, Quercetin, and Luteolin Combination Treatment

Similar to the 3.3.6 section, a triple treatment containing genistein, quercetin and luteolin was given to cells in this experiment. This treatment was selected because each of these bioflavonoids represents the most consumed bioflavonoid from the isoflavone, flavonol, and flavone sub-groups respectively. Cells were exposed to the same concentrations of genistein, quercetin, and luteolin (G/Q/L) as used for individual exposures. Given the large concentrations of bioflavonoids from different sub-groups these cells were exposed to, it was predicted similar levels of damage to etoposide would be present and the kinetics of DSB repair should mimic etoposide also.

Immediately after G/Q/L treatment, the number of γ -H2AX foci/cell was similar to what was observed in cells exposed to each individual bioflavonoid at 0h post-exposure (GQL: 12.8-17.7; G: 7.6-18.4; Q:12-20.2 & L: 8.3-17). γ -H2AX foci continued to appear over the first hour post-exposure to G/Q/L, for example the number of foci/cell in the lowest dose treatment increased from 12.8 to 21.9 on average. Since the G/Q treatment had 9.2 foci/cell and the luteolin had 10.2 foci on average, these numbers suggest an additive, rather than synergistic, impact of exposure to luteolin to the combination of G/Q, because though there was an increase to an average 12.8 foci/cell, the increase is not greater than what would be seen by adding their effects together.

The kinetics of repair of the G/Q/L DSBs was similar to single exposures with all doses showing a significant decrease in the number of foci/cell by 4h post-exposure as compared to 1h. The average number of foci/cell continued to significantly decrease 8h post-exposure (Fig. 3.10 and Table 3.9). The kinetics with all four doses is similar to the

trend observed with etoposide exposure, with an increase in DNA DSBs by 1h post-exposure followed by repair of DSBs by 4 and 8h post-exposure (Fig. 3.10 and Table 3.9).

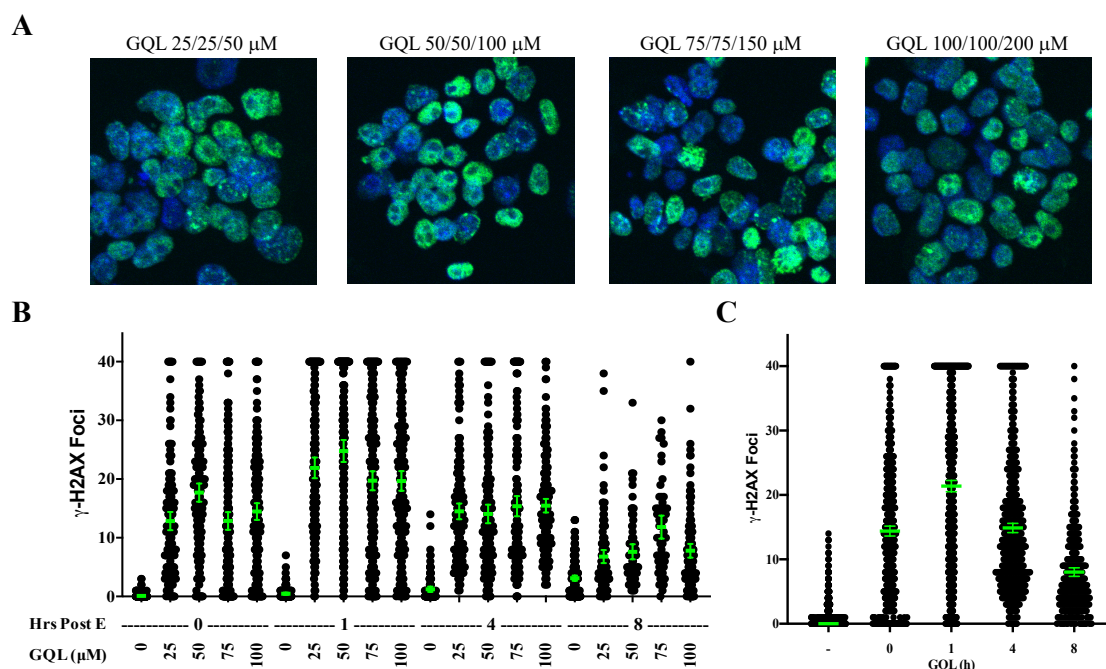


Figure 3.10: DNA Damage Repair Kinetics Over 8h with Genistein/Quercetin/Luteolin Treatment. After 1h genistein/quercetin/luteolin treatment at 25/25/50, 50/50/100, 75/75/150, or 100/100/200 μM , cells were stained for $\gamma\text{-H2AX}$ immediately after treatment, or following 1, 4, or 8h recovery. (A) Representative confocal images from all genistein/quercetin/luteolin doses immediately after treatment and staining. (B) Each point represents the number of $\gamma\text{-H2AX}$ foci in a cell. Averages are represented in green with error bars showing the 95% confidence interval. At least 100 cells were counted for each treatment group/time point. (C) The average number of $\gamma\text{-H2AX}$ foci are shown for each timepoint, all doses were combined to show the general trend of DNA damage recovery over 8h. For statistical analysis, see Table 3.9.

Table 3.9: DNA Damage Repair Kinetics Over 8h with Genistein/Quercetin/ Luteolin Treatment Data Analysis. The average number of γ -H2AX foci of the treatments being compared are shown with the p-value from the comparison. A one-way ANOVA was used with Sidak's multiple comparisons test (**** p<0.0001, *** p<0.001, ** p<0.01, * p<0.05).

Compound	Comparison	Average Values		p-value	Significant		
Genistein/ Quercetin/Luteolin (GQL)	To Control	C 0 hr vs GQL 25 0 hr	0.11	12.84	<0.0001	****	
		C 0 hr vs GQL 50 0 hr	0.11	17.69	<0.0001	****	
		C 0 hr vs GQL 75 0 hr	0.11	12.87	<0.0001	****	
		C 0 hr vs GQL 100 0 hr	0.11	14.47	<0.0001	****	
		C 1 hr vs GQL 25 1 hr	0.46	21.9	<0.0001	****	
		C 1 hr vs GQL 50 1 hr	0.46	24.78	<0.0001	****	
		C 1 hr vs GQL 75 1 hr	0.46	19.71	<0.0001	****	
		C 1 hr vs GQL 100 1 hr	0.46	19.68	<0.0001	****	
		C 4 hr vs GQL 25 4 hr	1.24	14.5	<0.0001	****	
		C 4 hr vs GQL 50 4 hr	1.24	14.05	<0.0001	****	
		C 4 hr vs GQL 75 4 hr	1.24	15.38	<0.0001	****	
		C 4 hr vs GQL 100 4 hr	1.24	15.46	<0.0001	****	
		C 8 hr vs GQL 25 8 hr	3.11	6.79	0.0441	*	
		C 8 hr vs GQL 50 8 hr	3.11	7.61	0.02	*	
		C 8 hr vs GQL 75 8 hr	3.11	11.82	<0.0001	****	
		C 8 hr vs GQL 100 8 hr	3.11	7.78	0.0009	***	
	By Time	GQL 25 0 hr vs 1 hr	12.84	21.9	<0.0001	****	
		GQL 25 1 hr vs 4 hr	21.9	14.5	<0.0001	****	
		GQL 25 4 hr vs 8 hr	14.5	6.79	<0.0001	****	
		GQL 50 0 hr vs 1 hr	17.69	24.78	<0.0001	****	
GQL 50 1 hr vs 4 hr		24.78	14.05	<0.0001	****		
GQL 50 4 hr vs 8 hr		14.05	7.61	<0.0001	****		
GQL 75 0 hr vs 1 hr		12.87	19.71	<0.0001	****		
GQL 75 1 hr vs 4 hr		19.71	15.38	0.0002	***		
GQL 75 4 hr vs 8 hr		15.38	11.82	0.4507	ns		
GQL 100 0 hr vs 1 hr		14.47	19.68	<0.0001	****		
GQL 100 1 hr vs 4 hr		19.68	15.46	0.0005	***		
GQL 100 4 hr vs 8 hr		15.46	7.78	<0.0001	****		
Genistein/ Quercetin/Luteolin Doses Combined		To Control	C vs GQL 0 hr All	1.337	14.39	<0.0001	****
			C vs GQL 1 hr All	1.337	21.37	<0.0001	****
	C vs GQL 4 hr All		1.337	14.87	<0.0001	****	
	C vs GQL 8 hr All		1.337	8.026	<0.0001	****	
	By Time	GQL All 0 hr vs 1 hr	14.39	21.37	<0.0001	****	
		GQL All 1 hr vs 4 hr	21.37	14.87	<0.0001	****	
		GQL All 4 hr vs 8 hr	14.87	8.026	<0.0001	****	

3.3 Results for Chemical Control: Dipyrone

Dipyrone is a pain reliever, and similar to bioflavonoids, has anti-inflammatory effects. However, dipyrone does not have the polyphenol ring structure of bioflavonoids

and is not a confirmed Top2 poison. Dipyron has been associated with *MLL* rearrangements in epidemiological studies in infant leukemia²⁶. Therefore, dipyron was selected as another compound to test. It was expected to cause DNA DSBs, but with damage and repair kinetics that would be different from those following etoposide and bioflavonoid exposure. Immediately after exposure to dipyron, an increased amount of γ -H2AX foci were scored compared to control. The amount of damage seen increased in a dose dependent manner except in the highest dose group with 3.3, 5.3, 11.0, and 7.9 foci/cell at 50, 100, 150 and 200 μ M doses respectively (LD50:100 μ M) (Fig. 3.11B). However, 1h after treatment the amount of DNA damage decreased or remained constant and at 4h post exposure all doses of dipyron decreased back to control levels. At 8h following exposure, the amount of γ -H2AX foci again increased significantly to 7.3, 9.1, 5.7, and 12.3 foci/cell. At 8h, all doses, except the 150 μ M, even exceeded the damage immediately after treatment.

Overall, dipyron treated cells had a significant amount of damage immediately after treatment, this damage decreased significantly 1h and 4h following treatment, before significantly increasing 8h post treatment (Fig. 3.11C). For all average foci/cell and significance see Table 3.10.

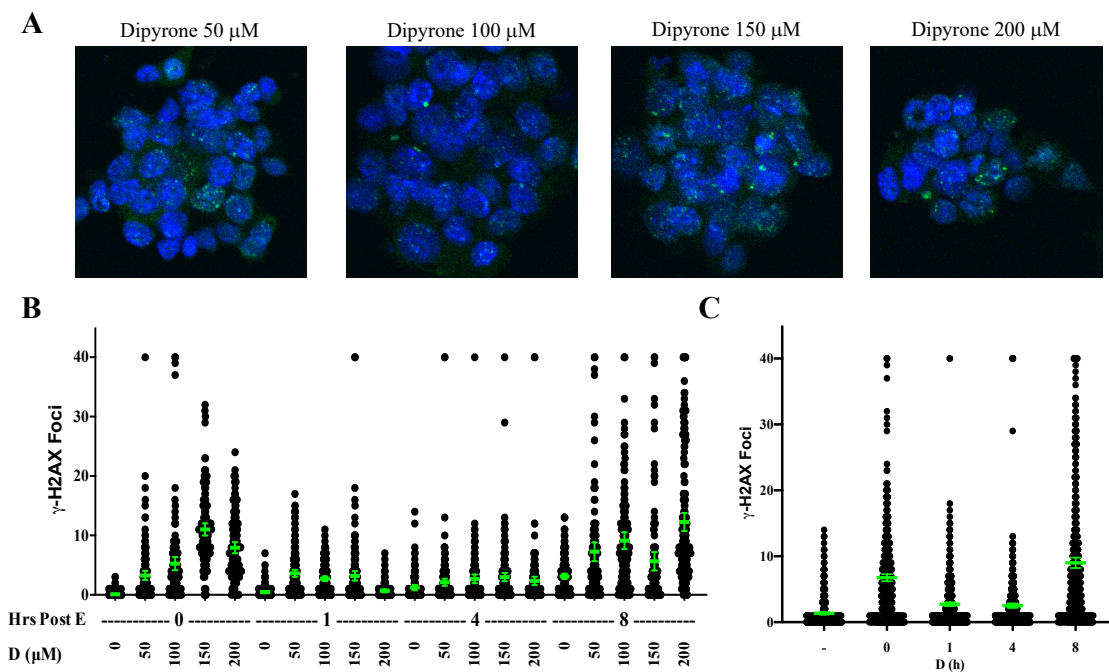


Figure 3.11: DNA Damage Repair Kinetics Over 8h with Dipyrene Treatment. After 1h dipyrene treatment at 50, 100, 150, or 200 μM , cells were stained for $\gamma\text{-H2AX}$ immediately after treatment, or following 1, 4, or 8h recovery. (A) Representative confocal images from all dipyrene doses immediately after treatment and staining. (B) Each point represents the number of $\gamma\text{-H2AX}$ foci in a cell. Averages are represented in green with error bars showing the 95% confidence interval. At least 100 cells were counted for each treatment group/time point. (C) The average number of $\gamma\text{-H2AX}$ foci are shown for each timepoint, all doses were combined to show the general trend of DNA damage recovery over 8h. For statistical analysis, see Table 3.10.

Table 3.10: DNA Damage Repair Kinetics Over 8h with Dipyrone Treatment Data Analysis. The average number of γ -H2AX foci of the treatments being compared are shown with the p-value from the comparison. A one-way ANOVA was used with Sidak's multiple comparisons test (**** p<0.0001, *** p<0.001, ** p<0.01, * p<0.05).

Compound	Comparison	Average Values		p-value	Significant	
Dipyrone (D)	To Control	C 0 hr vs D 50 0 hr	0.11	3.26	<0.0001	****
		C 0 hr vs D 100 0 hr	0.11	5.26	<0.0001	****
		C 0 hr vs D 150 0 hr	0.11	11.01	<0.0001	****
		C 0 hr vs D 200 0 hr	0.11	7.94	<0.0001	****
		C 1 hr vs D 50 1 hr	0.46	3.63	<0.0001	****
		C 1 hr vs D 100 1 hr	0.46	2.71	0.0205	*
		C 1 hr vs D 150 1 hr	0.46	3.21	0.0008	***
		C 1 hr vs D 200 1 hr	0.46	0.68	>0.9999	ns
		C 4 hr vs D 50 4 hr	1.24	2.13	0.9991	ns
		C 4 hr vs D 100 4 hr	1.24	2.69	0.7829	ns
		C 4 hr vs D 150 4 hr	1.24	2.99	0.2808	ns
		C 4 hr vs D 200 4 hr	1.24	2.35	0.9814	ns
		C 8 hr vs D 50 8 hr	3.11	7.26	<0.0001	****
		C 8 hr vs D 100 8 hr	3.11	9.13	<0.0001	****
		C 8 hr vs D 150 8 hr	3.11	5.65	0.0029	**
		C 8 hr vs D 200 8 hr	3.11	12.26	<0.0001	****
	By Time	D 50 0 hr vs 1 hr	3.26	3.63	>0.9999	ns
		D 50 1 hr vs 4 hr	3.63	2.13	0.2681	ns
		D 50 4 hr vs 8 hr	2.13	7.26	<0.0001	****
		D 100 0 hr vs 1 hr	5.26	2.71	0.0017	**
		D 100 1 hr vs 4 hr	2.71	2.69	>0.9999	ns
		D 100 4 hr vs 8 hr	2.69	9.13	<0.0001	****
		D 150 0 hr vs 1 hr	11.01	3.21	<0.0001	****
		D 150 1 hr vs 4 hr	3.21	2.99	>0.9999	ns
D 150 4 hr vs 8 hr	2.99	5.65	0.0015	**		
D 200 0 hr vs 1 hr	7.94	0.68	<0.0001	****		
D 200 1 hr vs 4 hr	0.68	2.35	0.3652	ns		
D 200 4 hr vs 8 hr	2.35	12.26	<0.0001	****		
Dipyrone Doses Combined	To Control	C vs D 0 hr All	1.337	6.733	<0.0001	****
		C vs D 1 hr All	1.337	2.724	0.0002	***
		C vs D 4 hr All	1.337	2.511	0.0021	**
		C vs D 8 hr All	1.337	9.011	<0.0001	****
	By Time	D All 0 hr vs 1 hr	6.733	2.724	<0.0001	****
		D All 1 hr vs 4 hr	2.724	2.511	0.9923	ns
		D All 4 hr vs 8 hr	2.511	9.011	<0.0001	****

3.4 Conclusions

The purpose of the experiments presented in this chapter was to determine if bioflavonoids cause DNA DSBs and how this DNA damage would be repaired over time. The appearance of γ -H2AX foci was used to score DNA DSBs that occurred immediately after bioflavonoid treatment and after 1, 4, and 8 hours post-treatment to understand the persistence of DSBs. It was expected that bioflavonoids would induce DNA damage in a dose dependent manner, and that the damage induced by bioflavonoids would be repaired over time post-treatment. It was also expected that the different bioflavonoid sub-groups would have different kinetics of DNA damage repair due to potential differences in their mechanisms of action, though it was unknown what difference in trends would be observable. Finally, the combination treatments containing bioflavonoids of different sub-groups, were expected to induce more damage, though it was unknown if this damage would be synergistic or additive.

The results from these experiments clearly demonstrate that bioflavonoid exposure induces DSBs and repairs these breaks with some similarities to etoposide exposure. Overall, agents induced a rapid appearance and significant average number of γ -H2AX foci/cell statistically higher than those observed in control cells immediately post-exposure in a dose-dependent manner. It was noted that high doses of myricetin and luteolin were outliers. As expected, since lower concentrations of bioflavonoids produced an absolute lower number of foci/cell, their repair led to a return to baseline levels at earlier timepoints post-exposure than higher concentrations.

Despite bioflavonoid treatments at high concentrations, they induced damage at lower absolute levels than etoposide. These findings are not unexpected, given the known

potency of the Top2 poison etoposide and its use as a chemotherapeutic agent. Exposure to myricetin showed the most similar overall kinetics of DNA damage and repair as etoposide. Etoposide and its metabolites act as both an interfacial (traditional) and as a covalent Top2 poison^{32,96}. Bandele *et al* demonstrated that myricetin also works through both mechanisms to poison Top2 in cell free systems. This suggests that, contrary to the initial hypothesis of sub-groups showing similar kinetics, the biochemical mechanism of Top2 poisoning may be more predictive of a bioflavonoid's potential to induce DNA DSBs³². Bandele *et al* also showed myricetin causes more DNA cleavage than traditional poisons but at a slower rate, this slower rate could allow the cell's repair proteins time to properly process with the amount of damage occurring. This could in part explain the significantly lower number of DSBs that form in cells exposed to myricetin as compared to cells exposed to genistein or quercetin that act exclusively as traditional poisons³². Genistein treated cells had some similarities to etoposide and myricetin treated cells, with resolution of DNA damage occurring at later timepoints. The only dissimilarity between these groups is at the early timepoint following treatment genistein showed a decrease instead of an increase in DNA damage. Given that genistein is an isoflavone, while myricetin is a flavonol, these data suggest that sub-groups are not the best predictive measure for the kinetics of DSB resolution. This lends further support to the new hypothesis that Top2 poison classification is more predictive of DNA resolution kinetics than bioflavonoid sub-class.

Kaempferol, which is in the flavonol sub-group with quercetin and myricetin, but is only a traditional Top2 poison, showed a trend of DNA damage resolution similar to etoposide at early timepoints post-exposure. Interestingly, at later times kaempferol treated cells showed a slight increase in the amount of DSBs, although not statistically significant.

In a similar manner, dipyrone, which was not expected to have similar mechanisms to bioflavonoids, demonstrated an increase in DNA damage at later timepoints with low levels of initial damage. Quercetin treated cells did not show a similar trend in DSB resolution to etoposide and myricetin but showed slight similarities to kaempferol. Quercetin treated cells rapidly and robustly repaired DNA damage readily observable at early timepoints post-treatment. Similar to kaempferol and dipyrone, quercetin, particularly at higher doses, induced a second wave of γ -H2AX foci at the latest timepoint, suggesting an alternative mechanism of DNA damage.

With both genistein and quercetin, a decrease in the amount of damage is observed at early timepoints post-treatment, though the decrease was much more rapid for quercetin, making genistein resemble etoposide more than quercetin. In the combined genistein and quercetin treatment, the trend observed demonstrated a pattern with closer similarity to genistein and etoposide than to quercetin. At early timepoints in this combined treatment, there was no resolution of DSBs though resolution did occur at later timepoints. It is possible that genistein and quercetin work through similar pathways to disrupt Top2 and that only a certain amount of DNA damage can be caused through this mechanism. This is supported by analyzing the combinatory effects of bioflavonoids using the program CompuSyn⁹⁷. Analysis of combination effects of genistein and quercetin treatment compared to genistein or quercetin individual treatments showed this combination have mostly antagonistic effects on the number of foci. This would explain the similar levels of damage seen at the earliest timepoint in the single and the combination groups. However, given the higher concentration of bioflavonoids in the combination treatments, damage may not be resolved as quickly, or there may be bioflavonoids still present in the cell to

cause damage at early timepoints post-treatment. This could explain why genistein and quercetin show significant resolution of DSBs early post-treatment, while G/Q treatment shows sustained damage at the early timepoints.

Cells treated with a combination of genistein, quercetin, and luteolin also showed a similar kinetic trend to etoposide and myricetin, with initial increases in damage at early timepoints before resolution. This opposes the initial hypothesis that combination treatments would resemble the kinetics of single treatments. It is possible that some metabolites of genistein, quercetin, and/or luteolin are less potent covalent Top2 poisons, that required combination treatments to see their effects. The antagonistic effect observed in the genistein and quercetin treatment was observed in the triple combination treatment also. Further supporting that these bioflavonoids in high concentrations probably compete for the Top2 active site, therefore if they do have a secondary covalent function they would in a saturated system bind to other sites available. If accurate these data provide support for the new hypothesis that Top2 poison classification is a better predictor of DSB resolution kinetics, but it would need to be verified that these bioflavonoids can work through covalent mechanisms.

When considering these data as a whole, this set of experiments clearly demonstrated that bioflavonoids cause DNA damage similar to etoposide as evidenced by the rapid appearance of γ -H2AX foci. Further, resolution of the DSBs induced by most of the bioflavonoids examined are also broadly similar to the timing of resolution of damage induced by etoposide. However, close examination of the persistence and kinetics of resolution of γ -H2AX foci leads to a new hypothesis that potency and prolonged activity as a DNA damaging agent is not correlated with a bioflavonoid's biochemical sub-class,

but instead on the mechanism that each bioflavonoid works as a poison of Top2. Therefore, the experiments described in the next chapter focus on determining if bioflavonoids cause DSBs through Top2-dependent or Top2-independent mechanisms.

CHAPTER 4: BIOFLAVONOIDS INDUCE DNA DSBS THROUGH TOP2-DEPENDENT AND INDEPENDENT MECHANISMS

Bioflavonoids kaempferol, quercetin and myricetin have been shown to directly inhibit Top2 in cell free systems.³² However, bioflavonoids also have pleiotropic effects such as modulation of genetic expression of cell cycle proteins and proliferation factors through signal transduction pathways or epigenetic marker modification, and direction of DSB repair pathway choice^{16,21,79–86,69,72–78}. Therefore, the aims of these experiments were (1) to determine if bioflavonoid-induced DNA DSBs are caused by poisoning of Top2 as etoposide is known to and (2) to determine if classification as a Top2 poison is more predictive of DNA damage potential than sub-class. To examine this, cells were treated with dexrazoxane (DEX) to inhibit Top2 from binding to DNA. Cells were then exposed to etoposide, bioflavonoids, or dipyrone and DNA damage quantified by scoring of γ -H2AX foci. It was expected that in compounds that act to damage DNA through Top2-dependent mechanisms there would be an observable reduction in the amount of damage with DEX pre-treatment, while those that act through Top2-independent mechanisms will not have an observed reduction of DSBs.

4.1 Impact of DEX Pre-Treatment on Etoposide Induced DNA Damage

In order to determine the ideal dose at which to pre-treat cells with DEX, 4 doses, 25, 50, 100, and 200 μ M were selected for testing based upon previous studies done in other cell types^{93–95}. As expected, asynchronous cultures +DEX alone contained few, if any, spontaneous γ -H2AX foci across all experiments and timepoints similar to untreated cells. Cells treated with DEX and a single 6.25 μ M dose of etoposide showed a significant

reduction in the average number of foci/cell observed at all DEX treatment doses (Fig. 4.1). The reduction in the number of foci/cell observed was dose dependent, with some reduction following 25 μM DEX and more reductions following 50 μM DEX. However, doses above 50 μM did not lead to any further reduction in observed foci/cell indicative of saturation of the system and the majority of available Top2 binding to DEX. Based on these data, 50 μM was used for future experiments. Though small in absolute numbers, it was noted that a slightly greater number of foci/cell was observed with 200 μM DEX treatment but overall the curve was flat at these higher doses (Table 4.1). Therefore, further experiments used 200 μM DEX as well.

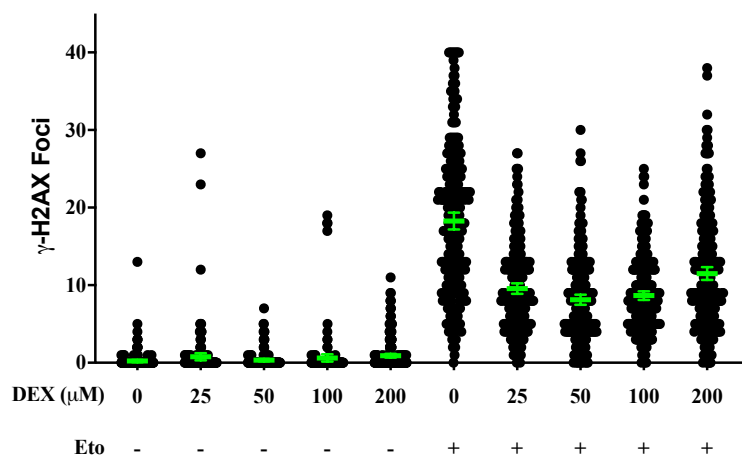


Figure 4.1: Preliminary DNA Damage Results to Determine DEX Dosing. Cells were treated with dexrazoxane for 1h at 25, 50, 100 or 200 μM . After 1h of dexrazoxane, cells were left for 1h or treated with 6.25 μM etoposide for 1h, before $\gamma\text{-H2AX}$ staining occurred. Each point represents the number of $\gamma\text{-H2AX}$ foci in a cell. Averages are represented in green with error bars showing the 95% confidence interval. At least 100 cells were counted for each treatment group/time point. For statistical analysis, see Table 4.1.

Table 4.1: Preliminary DNA Damage Results to Determine DEX Dosing Data Analysis. The average number of γ -H2AX foci of the treatments being compared are shown with the p-value from the comparison. A one-way ANOVA was used with Sidak's multiple comparisons test (**** p<0.0001, *** p<0.001, ** p<0.01, * p<0.05).

Compound	Comparison		Average Values		Difference	p-value	Significant
To Control	Control	DEX 25	0.22	0.76	0.54	0.9999	ns
	Control	DEX 50	0.22	0.34	0.12	>0.9999	ns
	Control	DEX 100	0.22	0.62	0.40	>0.9999	ns
	Control	DEX 200	0.22	0.91	0.69	0.9797	ns
	Control	Eto 25	0.22	18.26	18.04	<0.0001	****
	Control	Eto 25 + DEX 25	0.22	9.56	9.34	<0.0001	****
	Control	Eto 25 + DEX 50	0.22	8.12	7.90	<0.0001	****
	Control	Eto 25 + DEX 100	0.22	8.66	8.43	<0.0001	****
	Control	Eto 25 + DEX 200	0.22	11.50	11.28	<0.0001	****
Within DEX	DEX 25	DEX 50	0.76	0.34	-0.43	>0.9999	ns
	DEX 50	DEX 100	0.34	0.62	0.29	>0.9999	ns
	DEX 100	DEX 200	0.62	0.91	0.29	>0.9999	ns
	DEX 25	Eto 25 + DEX 25	0.76	9.56	8.80	<0.0001	****
	DEX 50	Eto 25 + DEX 50	0.34	8.12	7.78	<0.0001	****
	DEX 100	Eto 25 + DEX 100	0.62	8.66	8.03	<0.0001	****
	DEX 200	Eto 25 + DEX 200	0.91	11.50	10.59	<0.0001	****
To Eto	Eto 25	Eto 25 + DEX 25	18.26	9.56	-8.70	<0.0001	****
	Eto 25	Eto 25 + DEX 50	18.26	8.12	-10.14	<0.0001	****
	Eto 25	Eto 25 + DEX 100	18.26	8.66	-9.61	<0.0001	****
	Eto 25	Eto 25 + DEX 200	18.26	11.50	-6.76	<0.0001	****
Within Eto	Eto 25 + DEX 25	Eto 25 + DEX 50	9.56	8.12	-1.44	0.0409	*
	Eto 25 + DEX 50	Eto 25 + DEX 100	8.12	8.66	0.54	0.9983	ns
	Eto 25 + DEX 100	Eto 25 + DEX 200	8.66	11.50	2.85	<0.0001	****

Given the preliminary DEX results, it was decided that pre-treatment for cells would be with doses of 50 and 200 μ M and the pre-treatment times would be 1h and 5h before exposure to etoposide or bioflavonoids. Etoposide (6.25 μ M) alone induced an average 20.1 foci/cell that was significantly reduced by pre-treatment with DEX in a time and dose dependent manner. With 1h 50 μ M DEX treatment, the average of number of foci observed was reduced to 12.0 foci/cell. 1h 200 μ M DEX treatment saw a further reduction compared to the 1h 50 μ M treatment to 9.7 foci/cell. With 5h DEX treatment, these numbers were reduced to an average of 7.8 and 5.7 foci/cell in the 50 and 200 μ M DEX groups respectively (Fig. 4.2 and Table 4.2). These results support that etoposide causes DNA DSBs through poisoning Top2, not through Top2-independent mechanisms.

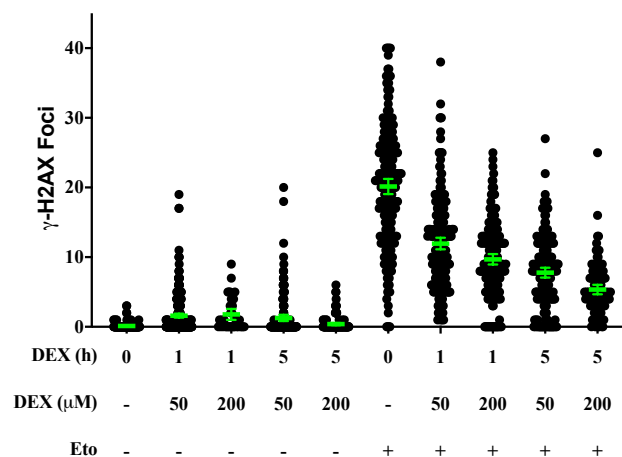


Figure 4.2: DNA Damage in Cells Treated with DEX Prior to Etoposide Exposure. Cells were treated with 50 or 200 μM DEX for 1 or 5h before etoposide exposure (6.25 μM) for 1h. Each point represents the number of $\gamma\text{-H2AX}$ foci in a cell. Averages are represented in green with error bars showing the 95% confidence interval. At least 100 cells were counted for each treatment group/time point. For statistical analysis, see Table 4.2.

Table 4.2: DNA Damage in Cells Treated with DEX Prior to Etoposide Exposure Data Analysis. The average number of $\gamma\text{-H2AX}$ foci of the treatments being compared are shown with the p-value from the comparison. A one-way ANOVA was used with Sidak's multiple comparisons test (**** $p < 0.0001$, *** $p < 0.001$, ** $p < 0.01$, * $p < 0.05$).

Compound	Comparison	Average Values	Difference	p-value	Significant			
Etoposide	To Control	0h, 0 DEX	Eto	0.11	20.14	20.03	<0.0001	****
		1h, 50 DEX	Eto+ 1h, 50 DEX	1.61	11.96	10.35	<0.0001	****
		1h, 200 DEX	Eto+ 1h, 200 DEX	1.78	9.69	7.91	<0.0001	****
		5h, 50 DEX	Eto+ 5h, 50 DEX	1.28	7.78	6.5	<0.0001	****
		5h, 200 DEX	Eto+ 5h, 200 DEX	0.39	5.37	4.97	<0.0001	****
		To Eto	Eto	Eto+ 1h, 50 DEX	20.14	11.96	-8.18	<0.0001
		Eto	Eto+ 1h, 200 DEX	20.14	9.69	-10.45	<0.0001	****
		Eto	Eto+ 5h, 50 DEX	20.14	7.78	-12.36	<0.0001	****
		Eto	Eto+ 5h, 200 DEX	20.14	5.37	-14.77	<0.0001	****
By DEX (h)		Eto+ 1h, 50 DEX	Eto+ 5h, 50 DEX	11.96	7.78	-4.18	<0.0001	****
		Eto+ 1h, 200 DEX	Eto+ 5h, 200 DEX	9.69	5.37	-4.32	<0.0001	****
By DEX (μM)		Eto+ 1h, 50 DEX	Eto+ 1h, 200 DEX	11.96	9.69	-2.27	<0.0001	****
		Eto+ 5h, 50 DEX	Eto+ 5h, 200 DEX	7.78	5.37	-2.41	0.0005	***

4.2 Dexrazoxane Significantly Reduces DNA Damage Induced by Myricetin

A significant portion of myricetin-induced DSBs were inhibited by the pre-treatment of cells with dexrazoxane consistent with a Top2-dependent mechanism of activity similar to the reduction observed in etoposide induced DNA damage. Myricetin (50 μM) exposure alone induced an average 10.5 foci/cell that was significantly reduced with DEX pre-treatment in a time (1 vs 5h) and dose (50 vs 200 μM) dependent manner.

After 1h 50 μM DEX and myricetin treatment, damage was reduced to 6.3 foci/cell. DEX 200 μM and/or 5h further reduced the average to 3.9, 2.2, and 2.0 foci/cell to baseline levels reducing the amount of damage by > 80% following 200 μM for 5h indicating that the significant majority of myricetin-induced DSBs were created via a Top2-dependent mechanism (Fig. 4.3 and Table 4.3).

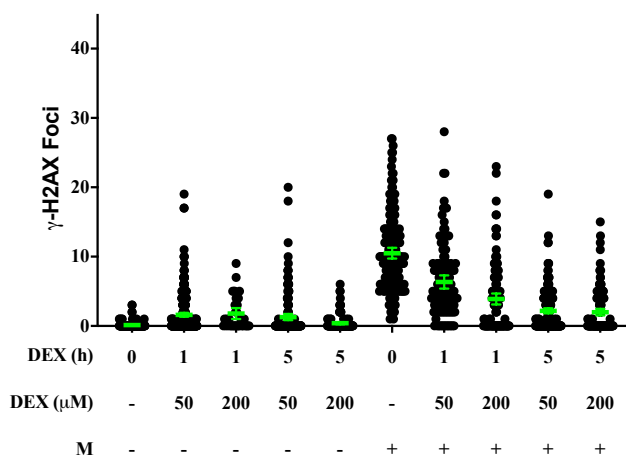


Figure 4.3: DNA Damage in Cells Treated with DEX Prior to Myricetin Exposure. Cells were treated with 50 or 200 μM DEX for 1 or 5h before myricetin exposure (50 μM) for 1h. Each point represents the number of $\gamma\text{-H2AX}$ foci in a cell. Averages are represented in green with error bars showing the 95% confidence interval. At least 100 cells were counted for each treatment group/time point. For statistical analysis, see Table 4.4.

Table 4.3: DNA Damage in Cells Treated with DEX Prior to Myricetin Exposure Data Analysis. The average number of $\gamma\text{-H2AX}$ foci of the treatments being compared are shown with the p-value from the comparison. A one-way ANOVA was used with Sidak's multiple comparisons test (**** $p < 0.0001$, *** $p < 0.001$, ** $p < 0.01$, * $p < 0.05$).

Compound	Comparison	Average Values	Difference	p-value	Significant			
Myricetin	To Control	0h, 0 DEX	M	0.11	10.49	10.38	<0.0001	****
		1h, 50 DEX	M+ 1h, 50 DEX	1.61	6.34	4.73	<0.0001	****
		1h, 200 DEX	M+ 1h, 200 DEX	1.78	3.87	2.09	0.0189	*
		5h, 50 DEX	M+ 5h, 50 DEX	1.28	2.17	0.89	0.1433	ns
		5h, 200 DEX	M+ 5h, 200 DEX	0.39	1.98	1.59	0.0013	**
To M	M	M+ 1h, 50 DEX	10.49	6.34	-4.15	<0.0001	****	
	M	M+ 1h, 200 DEX	10.49	3.87	-6.62	<0.0001	****	
	M	M+ 5h, 50 DEX	10.49	2.17	-8.32	<0.0001	****	
	M	M+ 5h, 200 DEX	10.49	1.98	-8.51	<0.0001	****	
By DEX (h)	M+ 1h, 50 DEX	M+ 5h, 50 DEX	6.34	2.17	-4.17	<0.0001	****	
	M+ 1h, 200 DEX	M+ 5h, 200 DEX	3.87	1.98	-1.89	<0.0001	****	
By DEX (μM)	M+ 1h, 50 DEX	M+ 1h, 200 DEX	6.34	3.87	-2.47	<0.0001	****	
	M+ 5h, 50 DEX	M+ 5h, 200 DEX	2.17	1.98	-0.19	>0.9999	ns	

4.3 Dexrazoxane Partially Reduces DNA Damage Induced by Genistein or Quercetin

Exposure to 75 μM genistein alone induced an average 15.6 foci/cell. Treatment with 50 μM DEX 1h did not reduce the amount of damage observed. However, increasing either the dose of DEX or the time of exposure to DEX did lead to a reduction in the number of foci observed. 200 μM treatment 1h reduced detectable damage by 48% to an average of 8.1 foci/cell. A similar amount of DNA damage was observed following DEX treatment 5h regardless of the dose of DEX used (Fig. 4.4 and Table 4.4). Overall, only half of the DNA damage induced by genistein was inhibited by DEX.

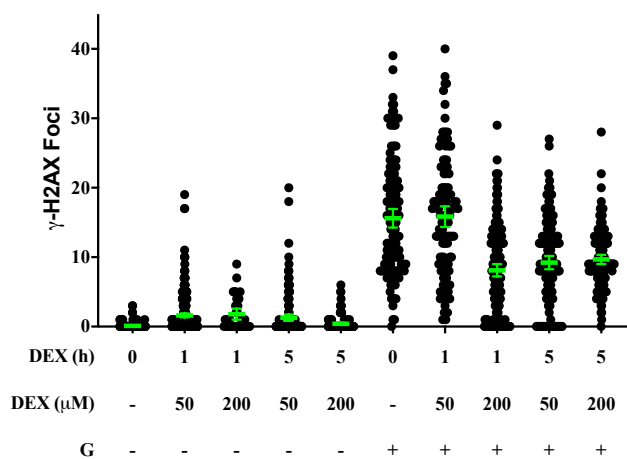


Figure 4.4: DNA Damage in Cells Treated with DEX Prior to Genistein Exposure. Cells were treated with 50 or 200 μM DEX for 1 or 5h before genistein exposure (75 μM) for 1h. Each point represents the number of $\gamma\text{-H2AX}$ foci in a cell. Averages are represented in green with error bars showing the 95% confidence interval. At least 100 cells were counted for each treatment group/time point. For statistical analysis, see Table 4.5.

Table 4.4: DNA Damage in Cells Treated with DEX Prior to Genistein Exposure Data Analysis. The average number of γ -H2AX foci of the treatments being compared are shown with the p-value from the comparison. A one-way ANOVA was used with Sidak's multiple comparisons test (**** p<0.0001, *** p<0.001, ** p<0.01, * p<0.05).

Compound	Comparison		Average Values		Difference	p-value	Significant	
Genistein	To Control	0h, 0 DEX	G	0.11	15.59	15.48	<0.0001	****
		1h, 50 DEX	G+ 1h, 50 DEX	1.61	15.83	14.22	<0.0001	****
		1h, 200 DEX	G+ 1h, 200 DEX	1.78	8.105	6.32	<0.0001	****
		5h, 50 DEX	G+ 5h, 50 DEX	1.28	9.2	7.92	<0.0001	****
		5h, 200 DEX	G+ 5h, 200 DEX	0.39	9.667	9.28	<0.0001	****
	To G	G	G+ 1h, 50 DEX	15.59	15.83	0.24	>0.9999	ns
		G	G+ 1h, 200 DEX	15.59	8.105	-7.48	<0.0001	****
		G	G+ 5h, 50 DEX	15.59	9.2	-6.39	<0.0001	****
		G	G+ 5h, 200 DEX	15.59	9.667	-5.92	<0.0001	****
	By DEX (h)	G+ 1h, 50 DEX	G+ 5h, 50 DEX	15.83	9.2	-6.63	<0.0001	****
G+ 1h, 200 DEX		G+ 5h, 200 DEX	8.105	9.667	1.56	0.0675	ns	
By DEX (μ M)	G+ 1h, 50 DEX	G+ 1h, 200 DEX	15.83	8.105	-7.73	<0.0001	****	
	G+ 5h, 50 DEX	G+ 5h, 200 DEX	9.2	9.667	0.467	>0.9999	ns	

Exposure to 75 μ M quercetin alone induced an average 15.4 foci/cell that was not reduced, and unexpectedly elevated, following 50 μ M DEX 1h to 19.3 foci/cell. However, similar to what was observed with genistein treatment, 200 μ M DEX 1h reduced detectable damage by 43% to an average of 8.8 foci/cell that remained relatively unchanged with 5h DEX exposure regardless of dose (Fig. 4.5 and Table 4.5). Overall, only half of the DNA damage induced by quercetin was inhibited by DEX. Taken together, these data suggest that genistein and quercetin generate DNA damage through mechanisms partially dependent on Top2, but at least half of the damage is induced through Top2-independent mechanisms.

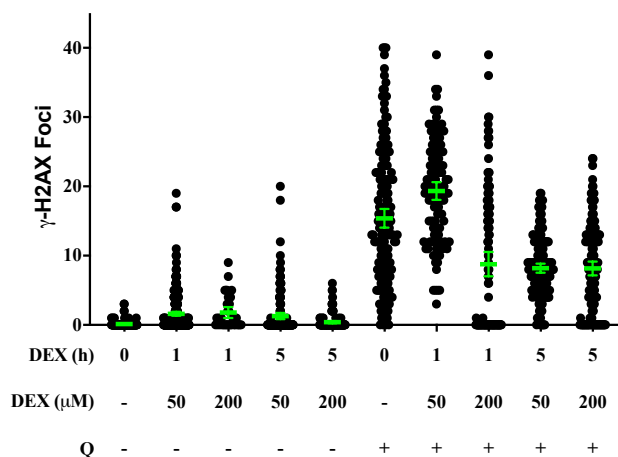


Figure 4.5: DNA Damage in Cells Treated with DEX Prior to Quercetin Exposure. Cells were treated with 50 or 200 μM DEX for 1 or 5h before quercetin exposure (75 μM) for 1h. Each point represents the number of $\gamma\text{-H2AX}$ foci in a cell. Averages are represented in green with error bars showing the 95% confidence interval. At least 100 cells were counted for each treatment group/time point. For statistical analysis, see Table 4.6.

Table 4.5: DNA Damage in Cells Treated with DEX Prior to Quercetin Exposure Data Analysis. The average number of $\gamma\text{-H2AX}$ foci of the treatments being compared are shown with the p-value from the comparison. A one-way ANOVA was used with Sidak's multiple comparisons test (**** $p < 0.0001$, *** $p < 0.001$, ** $p < 0.01$, * $p < 0.05$).

Compound	Comparison	Average Values	Difference	p-value	Significant			
Quercetin	To Control	0h, 0 DEX	Q	0.11	15.39	15.28	<0.0001	****
		1h, 50 DEX	Q+ 1h, 50 DEX	1.61	19.33	17.73	<0.0001	****
		1h, 200 DEX	Q+ 1h, 200 DEX	1.78	8.77	6.99	<0.0001	****
		5h, 50 DEX	Q+ 5h, 50 DEX	1.28	8.19	6.91	<0.0001	****
		5h, 200 DEX	Q+ 5h, 200 DEX	0.39	8.15	7.76	<0.0001	****
To G	Q	Q+ 1h, 50 DEX	15.39	19.33	3.95	<0.0001	****	
	Q	Q+ 1h, 200 DEX	15.39	8.77	-6.62	<0.0001	****	
	Q	Q+ 5h, 50 DEX	15.39	8.19	-7.19	<0.0001	****	
	Q	Q+ 5h, 200 DEX	15.39	8.15	-7.24	<0.0001	****	
By DEX (h)	Q+ 1h, 50 DEX	Q+ 5h, 50 DEX	19.33	8.19	-11.14	<0.0001	****	
	Q+ 1h, 200 DEX	Q+ 5h, 200 DEX	8.77	8.15	-0.62	0.9997	ns	
By DEX (μM)	Q+ 1h, 50 DEX	Q+ 1h, 200 DEX	19.33	8.77	-10.56	<0.0001	****	
	Q+ 5h, 50 DEX	Q+ 5h, 200 DEX	8.19	8.15	-0.04	>0.9999	ns	

4.4 Dexrazoxane Minimally Reduces DNA Damage Induced by Luteolin

Luteolin exposure induced an average 17.0 foci/cell. 1h DEX treatment significantly decreased the average by 49% to 8.7 foci/cell; however, 5h/+DEX led to a significant increase in the average to 20.0 foci/cell, which is significantly higher than luteolin only exposure (Fig. 4.6 and Table 4.6). Although 1h DEX significantly inhibited DNA DSBs induced by luteolin, increased pre-treatment time to 5h increased damage, supporting a Top2-independent mechanism for the remaining observed DSBs.

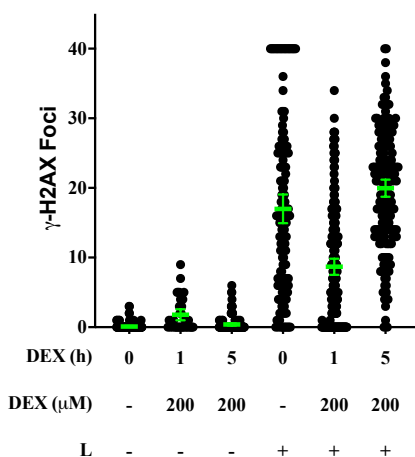


Figure 4.6: DNA Damage in Cells Treated with DEX Prior to Luteolin Exposure. Cells were treated with 200 μ M DEX for 1 or 5h before luteolin exposure (100 μ M) for 1h. Each point represents the number of γ -H2AX foci in a cell. Averages are represented in green with error bars showing the 95% confidence interval. At least 100 cells were counted for each treatment group/time point. For statistical analysis, see Table 4.7.

Table 4.6: DNA Damage in Cells Treated with DEX Prior to Luteolin Exposure Data Analysis. The average number of γ -H2AX foci of the treatments being compared are shown with the p-value from the comparison. A one-way ANOVA was used with Sidak's multiple comparisons test (**** $p < 0.0001$, *** $p < 0.001$, ** $p < 0.01$, * $p < 0.05$).

Compound	Comparison	Average Values	Difference	p-value	Significant			
Luteolin	To Control	0h, 0 DEX	L	0.11	17	16.89	<0.0001	****
		1h, 200 DEX	L+ 1h, 200 DEX	1.78	8.68	6.9	<0.0001	****
		5h, 200 DEX	L+ 5h, 200 DEX	0.39	19.96	19.57	<0.0001	****
		L	L+ 1h, 200 DEX	17	8.68	-8.32	<0.0001	****
		L	L+ 5h, 200 DEX	17	19.96	2.96	0.0028	**
By DEX (h)	L+ 1h, 200 DEX	L+ 5h, 200 DEX	8.68	19.96	11.28	<0.0001	****	

4.5 Dexrazoxane Does Not Reduce DNA Damage Induced by Kaempferol

Kaempferol exposure alone induced an average 5.6 foci/cell. This average increased significantly with 1hr DEX treatment to 9.2 foci/cell, and 5h DEX treatment showed a further significant increase compared to 1h DEX group with an average 16.2 foci/cell, an almost 3-fold elevation compared to exposure to kaempferol only (Fig. 4.7 and Table 4.7). This suggests that kaempferol works strongly through Top2 independent mechanisms to induce DNA damage.

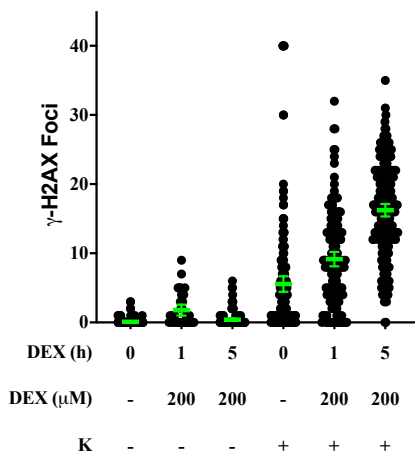


Figure 4.7: DNA Damage in Cells Treated with DEX Prior to Kaempferol Exposure. Cells were treated with 200 μ M DEX for 1 or 5h before kaempferol exposure (100 μ M) for 1h. Each point represents the number of γ -H2AX foci in a cell. Averages are represented in green with error bars showing the 95% confidence interval. At least 100 cells were counted for each treatment group/time point. For statistical analysis, see Table 4.10.

Table 4.7: DNA Damage in Cells Treated with DEX Prior to Kaempferol Exposure Data Analysis. The average number of γ -H2AX foci of the treatments being compared are shown with the p-value from the comparison. A one-way ANOVA was used with Sidak's multiple comparisons test (**** $p < 0.0001$, *** $p < 0.001$, ** $p < 0.01$, * $p < 0.05$).

Compound	Comparison		Average Values		Difference	p-value	Significant
Kaempferol To Control	0h, 0 DEX	K	0.11	5.56	5.45	<0.0001	****
	1h, 200 DEX	K+ 1h, 200 DEX	1.78	9.16	7.38	<0.0001	****
	5h, 200 DEX	K+ 5h, 200 DEX	0.39	16.24	15.85	<0.0001	****
	K	K+ 1h, 200 DEX	5.56	9.16	3.61	<0.0001	****
	K	K+ 5h, 200 DEX	5.56	16.24	10.68	<0.0001	****
By DEX (h)	K+ 1h, 200 DEX	K+ 5h, 200 DEX	9.16	16.24	7.08	<0.0001	****

4.6 Dexrazoxane Cannot Reduce DNA Damage Induced by Combined Treatment of Bioflavonoids

To determine if DEX would be able to inhibit the appearance of γ -H2AX foci induced by combinatorial exposure to bioflavonoids, or if the additional activity of multiple bioflavonoids would overcome the available DEX. We hypothesized that a higher dose of DEX would be needed to possibly titrate out the bioflavonoids and thus used 200uM DEX for these experiments. For this, cells were treated with DEX and then exposed to 75uM of both genistein and quercetin or 50, 50, and 100 μ M genistein, quercetin and luteolin.

G/Q exposure alone induced an average 17.3 foci/cell that was slightly but significantly reduced by 18% to an average 14.2 foci/cell with 1h DEX treatment. By contrast, 5h DEX treatment did not lead to any reduction of observed foci compared to cells exposed to G/Q alone (Fig. 4.9 and Table 4.8). As shown above, DEX was not able to inhibit approximately half of the DNA damage that each of these bioflavonoids generated alone. Consistent with that, these results suggest that each of the two added bioflavonoids still generate half the DNA damage after DEX treatment and eliminated any observed impact of DEX treatment. These results further support the hypothesis that approximately half the DNA damage induced by genistein and quercetin is through Top2-independent mechanisms.

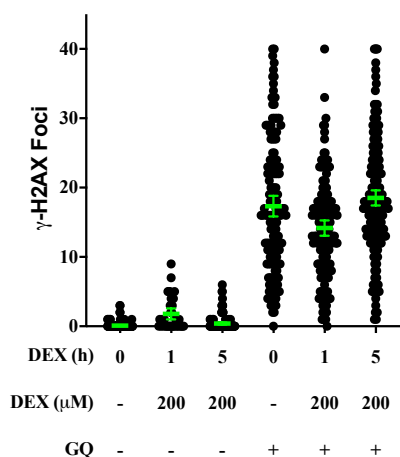


Figure 4.8: DNA Damage in Cells Treated with DEX Prior to Genistein/Quercetin Exposure. Cells were treated with 200 μM DEX for 1 or 5h before G/Q exposure (75/75 μM) for 1h. Each point represents the number of $\gamma\text{-H2AX}$ foci in a cell. Averages are represented in green with error bars showing the 95% confidence interval. At least 100 cells were counted for each treatment group/time point. For statistical analysis, see Table 4.8.

Table 4.8: DNA Damage in Cells Treated with DEX Prior to Genistein/Quercetin Exposure Data Analysis. The average number of γ -H2AX foci of the treatments being compared are shown with the p-value from the comparison. A one-way ANOVA was used with Sidak's multiple comparisons test (**** $p < 0.0001$, *** $p < 0.001$, ** $p < 0.01$, * $p < 0.05$).

Compound	Comparison	Average Values	Difference	p-value	Significant			
Genistein/ Quercetin	To Control	0h, 0 DEX	GQ	0.11	17.32	17.21	<0.0001	****
	1h, 200 DEX	GQ+ 1h, 200 DEX	1.78	14.16	12.38	<0.0001	****	
		5h, 200 DEX	GQ+ 5h, 200 DEX	0.39	18.51	18.12	<0.0001	****
	GQ	GQ+ 1h, 200 DEX	17.32	14.16	-3.16	<0.0001	****	
		GQ+ 5h, 200 DEX	17.32	18.51	1.19	0.3931	ns	
	By DEX (h)	GQ+ 1h, 200 DEX	GQ+ 5h, 200 DEX	14.16	18.51	4.34	<0.0001	****

G/Q/L exposure alone induced an average 17.8 foci/cell that could not be reduced with DEX treatment. The foci/cell remained constant at 18.8 foci/cell following 1h DEX. Additional DEX 5h did not reduce the DNA damage, but instead was significantly elevated by 30% or more to an average 24.1 foci/cell (Fig. 4.9 and Table 4.9). These data further support that genistein, quercetin, and luteolin induce DNA damage partially through Top2-independent mechanisms.

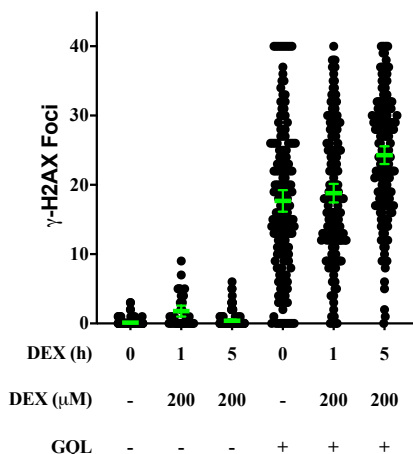


Figure 4.9: DNA Damage in Cells Treated with DEX Prior to Genistein/Quercetin/Luteolin Exposure. Cells were treated with 200 μ M DEX for 1 or 5h before G/Q/L exposure (50/50/100 μ M) for 1h. Each point represents the number of γ -H2AX foci in a cell. Averages are represented in green with error bars showing the 95% confidence interval. At least 100 cells were counted for each treatment group/time point. For statistical analysis, see Table 4.9.

Table 4.9: DNA Damage in Cells Treated with DEX Prior to Genistein/Quercetin/Luteolin Exposure Data Analysis. The average number of γ -H2AX foci of the treatments being compared are shown with the p-value from the comparison. A one-way ANOVA was used with Sidak's multiple comparisons test (**** $p < 0.0001$, *** $p < 0.001$, ** $p < 0.01$, * $p < 0.05$).

Compound	Comparison		Average Values	Difference	p-value	Significant		
Genistein/ Quercetin/ Luteolin	To Control	0h, 0 DEX	GQL	0.11	17.69	17.58	<0.0001	****
		1h, 200 DEX	GQL+ 1h, 200 DEX	1.78	18.82	17.03	<0.0001	****
		5h, 200 DEX	GQL+ 5h, 200 DEX	0.39	24.28	23.89	<0.0001	****
		GQL	GQL+ 1h, 200 DEX	17.69	18.82	1.13	0.6163	ns
		GQL	GQL+ 5h, 200 DEX	17.69	24.28	6.6	<0.0001	****
	By DEX (h)	GQL+ 1h, 200 DEX	GQL+ 5h, 200 DEX	18.82	24.28	5.47	<0.0001	****

4.7 Dexrazoxane Minimally Reduces DNA Damage Induced by Dipyrone

It has been hypothesized that dipyrone works to cause DNA damage through Top2-independent mechanisms⁶⁵. Thus, we hypothesized that DEX would have no impact on the amount of DNA damage. 100 μ M dipyrone exposure alone induced a small amount of DNA damage as observed by 5.26 foci/cell. Unexpectedly, 1h DEX treatment significantly reduced this DNA damage to low or undetectable levels similar to untreated controls. However, longer 5h DEX treatment did not impact the observed average foci/cell induced by dipyrone compared to no DEX as initially hypothesized (Fig. 10 and Table 10).

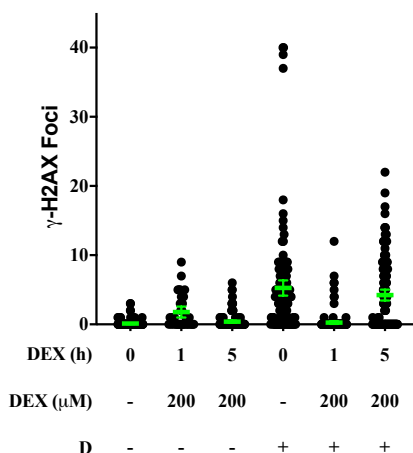


Figure 4.10: DNA Damage in Cells Treated with DEX Prior to Dipyrone Exposure. Cells were treated with 200 μ M DEX for 1 or 5h before dipyrone exposure (100 μ M) for 1h. Each point represents the number of γ -H2AX foci in a cell. Averages are represented in green with error bars showing the 95% confidence interval. At least 100 cells were counted for each treatment group/time point. For statistical analysis, see Table 4.3.

Table 4.10: DNA Damage in Cells Treated with DEX Prior to Dipyrone Exposure Data Analysis. The average number of γ -H2AX foci of the treatments being compared are shown with the p-value from the comparison. A one-way ANOVA was used with Sidak's multiple comparisons test (**** p<0.0001, *** p<0.001, ** p<0.01, * p<0.05).

Compound	Comparison		Average Values		Difference	p-value	Significant	
Dipyrone	To Control	0h, 0 DEX	D	0.11	5.26	5.15	<0.0001	****
		1h, 200 DEX	D+ 1h, 200 DEX	1.78	0.27	-1.51	0.1235	ns
		5h, 200 DEX	D+ 5h, 200 DEX	0.39	4.24	3.85	<0.0001	****
	By DEX (h)	D	D+ 1h, 200 DEX	5.26	0.27	-4.99	<0.0001	****
		D	D+ 5h, 200 DEX	5.26	4.24	-1.02	0.0964	ns
		D+ 1h, 200 DEX	D+ 5h, 200 DEX	0.27	4.24	3.97	<0.0001	****

4.8 Conclusions

Etoposide is known to cause damage through a Top2-dependent mechanism. As shown in this chapter, the DNA damage caused by etoposide is significantly reduced by pre-treatment with the Top2 inhibitor DEX in both a dose and time dependent manner. Therefore, these results validate that this system of measuring the impact of DEX treatment on the appearance of γ -H2AX foci can identify Top2-dependent damage. The data presented in this chapter further show that bioflavonoids act to induce DNA damage through both Top2-dependent and independent mechanisms.

These data support the hypothesis that the biochemical mechanism of Top2 poisoning is more predictive of a bioflavonoid's potential to induce DNA DSBs, than its subclass³². Exposure to etoposide and myricetin showed the most similar overall kinetics of DNA damage and repair (Chapter 3), as well as dependence on Top2. Etoposide and its metabolites act as both an interfacial (traditional) and as a covalent Top2 poison^{32,96}. Bandele et al. demonstrated that myricetin also works through these same mechanisms to poison Top2 in cell free systems. Results in chapter 3 showed that the appearance and resolution of DNA damage induced by myricetin was most similar to that induced by etoposide. Further, results in this chapter show that DNA damage induced by both

etoposide and myricetin is similarly and significantly inhibited. Although myricetin is in the same flavonol subclass as quercetin and kaempferol, each of these bioflavonoids had distinctly different results, suggesting the mechanisms by which these bioflavonoids work to cause DNA damage is not correlated with their biochemical sub-class. Future studies on bioflavonoids' potential to damage DNA could focus on the bioflavonoid's classification as a traditional or covalent Top2 poison instead of its structural classification.

The key to understanding the Top2-independent mechanisms of DNA damage induced by bioflavonoids will likely lie in investigating their pleiotropic effects. Bioflavonoids may lead to replication fork collapse, transcription machinery collision, oxidative stress, or early apoptotic triggers which can all lead to DSBs³⁷. Chapter 7 will propose future experiments to investigate what mechanisms caused the DNA observed in this chapter.

CHAPTER 5: BIOFLAVONOIDS INDUCE CHROMOSOMAL TRANSLOCATIONS THROUGH TOP2- DEPENDENT AND INDEPENDENT MECHANISMS

In the absence of DNA DSBs, chromosomal translocation events and other gross chromosomal rearrangements are unlikely to occur. However, DSBs and their illegitimate repair increase the frequency of translocations by at least 1000X⁹⁸. The purpose of these experiments was to understand the consequences of bioflavonoid-induced DSBs, the frequency that their repair can lead to a chromosomal translocation, and to determine if bioflavonoid-induced chromosomal translocations are Top2-dependent. Previous preliminary work of mine and colleagues in the Richardson lab used a genetically engineered cell reporter cell line to demonstrate that exposure to bioflavonoids or ROS can promote the formation of chromosomal translocations (Figure 2.1) although at a lower frequency than etoposide (Table 5.1).^{65,92} For the experiments in this chapter, these cells were treated with the catalytic inhibitor of Top2, DEX, for 5h preceding their treatment with bioflavonoids, and cells that contained chromosomal translocations identified⁶⁵.

5.1 Chromosomal Translocations Promoted by Bioflavonoid Exposure and Reduced by Dexrazoxane

These experiments used the MAG Reporter cell line described in chapter 2.1 to score chromosomal translocations between *MLL* and *AF9* transgenes that produce a GFP+ fluorescent cell colony (Figure 2.1). Therapy-related AML is a secondary form of cancer that develops after a cancer patient has been treated with a etoposide which induces a translocation between *MLL* and another gene partner (ex. *ENL*, *AF4*, *AF9*, & *AF6*)^{4,31,32}.

All experiments used 5h pre-treatment with 200uM DEX and 1h treatment with etoposide or bioflavonoids. As expected, exposure of MAG cells to 50uM etoposide led to the appearance of readily identifiable GFP+ fluorescent colonies calculated at a frequency of 8.46×10^{-6} . Following DEX pre-treatment the frequency of etoposide-induced translocations was significantly reduced by 3.4-fold to 2.47×10^{-6} (Table 5.1, Fig. 5.1A). Following DEX pre-treatment GFP+ colonies observed after myricetin exposure were calculated at a translocation frequency of 0.13×10^{-6} that was reduced 4.3-fold to 0.03×10^{-6} (Table 5.1, Fig. 5.1B). However due to the absolute low numbers of GFP+ colonies observed, this difference was not statistically significant.

By contrast, the formation of translocations induced by genistein or kaempferol exposure was not sensitive to Top2-inhibition. The calculated translocation frequency observed after genistein exposure was 1.23×10^{-6} and remained similar at 1.57×10^{-6} after DEX pre-treatment (Table 5.1, Fig. 5.1 C). DEX pre-treatment and kaempferol exposure resulted in 4.2-fold more GFP+ colonies with an initial translocation frequency of 0.38×10^{-6} to 1.57×10^{-6} (Table 5.1, Fig. 5.1D). The impact of dexrazoxane and Top2 inhibition of GFP+ chromosomal translocations was overall consistent with the observed γ -H2AX scoring.

Table 5.1: Inhibition of Top2 with Dexrazoxane Pre-treatment and Frequency of Bioflavonoid-induced Translocations.

Compound	Dose	Scored GFP+ Events		Average Frequency	
		-DEX	+DEX	-DEX	+DEX
Mock Treatment	n/a	0	0, 2, 4	$<0.007 \times 10^{-6}$	0.20×10^{-6}
Etoposide	50 μ M	80, 92, 68, 97	23, 25, 26	8.43×10^{-6}	2.47×10^{-6}
Myricetin	75 μ M	1, 1, 2	1, 0, 0	0.13×10^{-6}	0.03×10^{-6}
Genistein	75 μ M	15, 8, 14	11, 17, 19	1.23×10^{-6}	1.57×10^{-6}
Kaempferol	100 μ M	6, 2, 3, 4	10, 18, 19	0.38×10^{-6}	1.57×10^{-6}

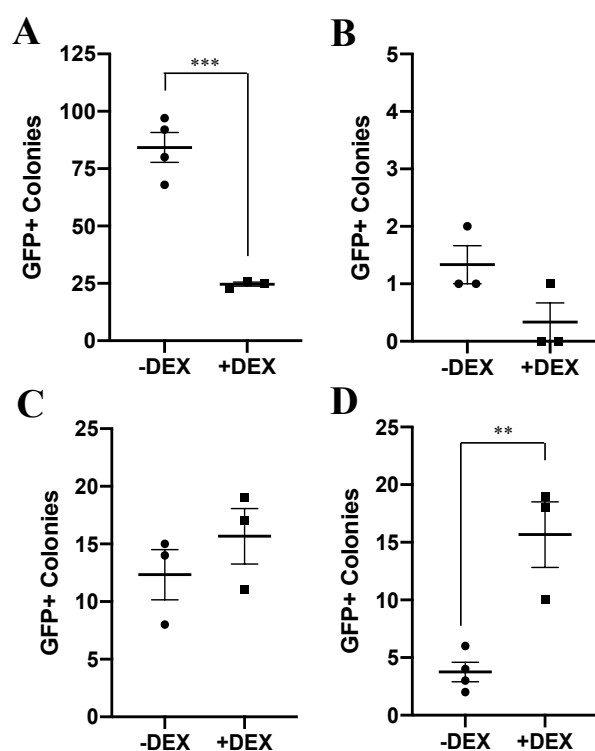


Figure 5.1: Quantification of Translocations in Bioflavonoid Treated Cells with Top2 Inhibited with Dexrazoxane. The MAG translocation reporter cell line was treated with 200 μ M dexrazoxane for 5h before 1h treatment with, A, etoposide (50 μ M), B, myricetin (75 μ M), C, genistein (75 μ M), or D, kaempferol (100 μ M). Number of GFP + colonies were counted after 5–7 days. Experiment was repeated in triplicate and compared to our previous reported data without dexrazoxane pre-treatment. The number of GFP+ colonies decreased with dexrazoxane pre-treatment for etoposide ($p = 0.0006$), increased for kaempferol ($p = 0.0058$) and remained statistically unchanged for untreated, genistein, and myricetin ($p = 0.272, 0.363, \text{ and } 0.101$, respectively).

5.2 Conclusions

The data presented in this chapter provide further support for the conclusions drawn in Chapter 4 that poisoning of Top2 with etoposide or a bioflavonoid causes DNA DSBs that are illegitimately repaired leading to chromosomal translocations. With dexrazoxane inhibition of Top2, the number of chromosomal translocations observed after etoposide or myricetin exposure is significantly reduced, in a manner similar to what was observed in Chapter 4 when measuring DNA DSBs. DEX and Kaempferol exposure also showed similar results to those of the previous chapter, with a significantly higher number of translocations observed after Top2 inhibition. DEX and genistein exposure lead to higher number of translocation events, though this was not significantly higher, these results are interesting when considering DEX pre-treatment in Chapter 4 lead to a reduction in the amount of DNA damage observed with genistein. Overall, these results support the idea that while Top2 poisoning does lead to chromosomal translocations, so does DNA damage caused by Top2-independent mechanisms.

These results also suggest that Top2-independent mechanisms of DNA damage may be more likely to cause translocations. The increase in DNA damage observed in Chapter 4 with dexrazoxane and kaempferol treatment was approximately 3-fold, however there was a more than 4-fold increase in the number of GFP+ colonies in this experiment, which could mean that the mechanisms by which the damage was caused may be more mutagenic or kaempferol may affect other proteins within the cell that increase the likelihood of mutagenic repair. The same can be said for genistein. In this set of experiments, genistein had a higher number of translocations with DEX pre-treatment, though Chapter 4 showed the amount of damage was reduced by approximately 50% with

5h 200 μ M DEX pre-treatment. Theoretically, with less DNA damage and a lower number of DSBs in the cell the likelihood of a translocation should decrease. Given this data and the observed higher number of translocations with DEX and kaempferol, it is possible that the other mechanisms or cellular pathways these bioflavonoids impact are more mutagenic. It is also possible that a Top2-independent activity of kaempferol or genistein leads to favored survival and proliferation of cells that contain translocations even if their statistically likelihood of occurring is not increased. Further exploration of this is necessary to suggest potential mechanisms that may be responsible for these results.

CHAPTER 6: CHRONIC, LOW DOSE EXPOSURE TO BIOFLAVONOIDS

The aim of these experiments was to determine if the risks of chromosomal translocations applied to cells treated with physiologically relevant low doses of bioflavonoids over a chronic extended time.

6.1 Detection of Chromosomal Translocations Induced by Chronic, Low Dose Bioflavonoid Treatment: Analysis of Cells After Paraformaldehyde Fixation

In this pilot experiment (n=1), MAG translocation Reporter cells⁶⁵ were treated with low doses of bioflavonoids (genistein, quercetin, luteolin, kaempferol, myricetin, genistein/quercetin and genistein/quercetin/luteolin) over the course of 20- 3 day cycles (see Chapter 2.6 for treatment scheme). After treatment cycles 7, 10, 15, and 20 cells were harvested and single cell suspensions fixed in paraformaldehyde. Samples were analyzed by flow cytometry (FACS ARIA) to detect GFP+ cells indicative of individual cells that contain a translocation within the populations sample. 2.5×10^6 events were recorded for each sample. No cells within the set GFP+ gate were sorted and further analyzed to determine if they were *bona fide* GFP+ cells with translocations.

A no treatment group was used as a baseline, and a DMSO treated group was used as a vehicle control. At all cycles, gating of GFP-/GFP+ events was set based on the no treatment group such that <0.01% of cells would be in the GFP+ gate. It was noted that throughout all 20 cycles of the no treatment group, gating parameters did not change (Fig. 6.1A). In the DMSO vehicle control group at cycle 7, approximately 0.23% of cells were within the GFP+ gate. However, at all other timepoints, no cells from the DMSO-treated

group were within the GFP+ gate (Fig. 6.1B). Cells were not sorted and further analyzed to determine if they were *bona fide* GFP+ cells with translocations.

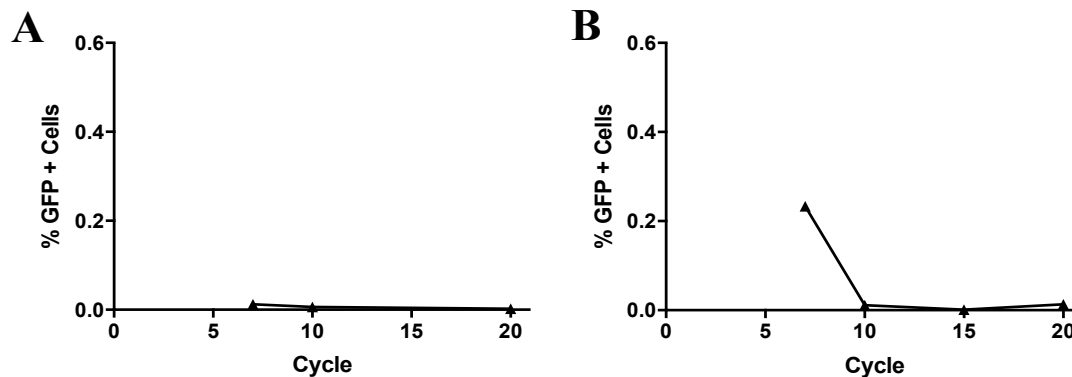


Figure 6.1: Percent of Fixed MAG Cells with Translocations in Control Groups Over 20 Cycles. Flow cytometry was utilized to analyze the percent of cells that were GFP+, which is indicative of a translocation event. Approximately 2.5 billion events were recorded in each sample, A, no treatment and B, DMSO(n=1). Events were recorded at cycles 7, 10, 15 and 20.

In samples treated with genistein, 0.46% of cells were within the GFP+ gate at cycle 7. By cycle 10, this population decreased to 0.07% and by cycle 15 there were almost no GFP+ cells. However, at cycle 20 the number of GFP+ cells increased again to 0.06%. These data suggest that prolonged, low dose genistein exposure leads to a persistent small population of cells with translocation events (Fig. 6.2A). When examining cells treated with both genistein/quercetin (G/Q) at low doses a similar trend was observed with 0.25% of cells within the GFP+ gate at cycle 7, and this population decreasing to an undetectable level at 15 cycles and then having a small secondary spike to 0.02% cells within the GFP+ gate cycle 20 (Fig. 6.2B). Cells were also treated with dipyrone. Cells that were within the GFP+ gate at cycle 7 were 0.05% before dropping through cycles 10 and 15, and then increasing slightly at cycle 20 (Fig. 6.2C).

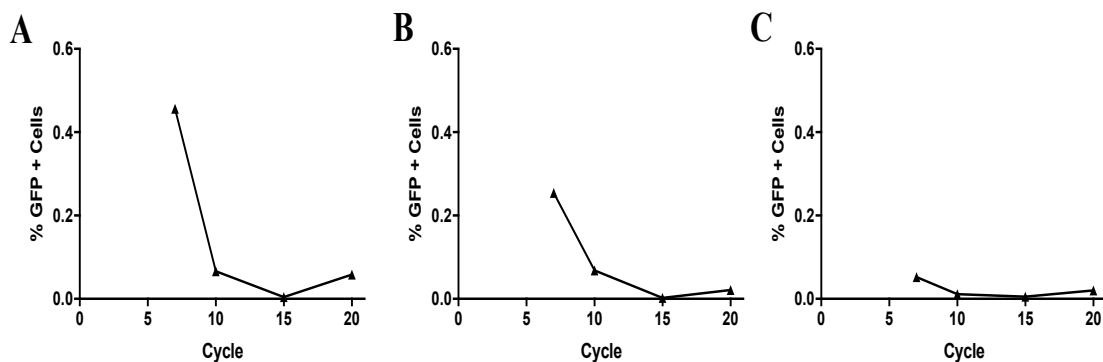


Figure 6.2: Percent of Fixed MAG Cells with Translocations in Genistein, Genistein/Quercetin and Dipyrone Groups Over 20 Cycles. Flow cytometry was utilized to analyze the percent of cells that were GFP+, which is indicative of a translocation event. Approximately 2.5 billion events were recorded in each sample, A, genistein, B, genistein/quercetin, and C, dipyrone (n=1). Events were recorded at cycles 7, 10, 15 and 20.

Analysis of cells treated with quercetin, luteolin and genistein/quercetin/luteolin showed a different trend. In these groups, the population of cells within the GFP+ gate remained consistent between cycles 7 and 10 (0.09% to 0.07%, 0.06% to 0.04%, and 0.07% to 0.07% for quercetin, luteolin and G/Q/L respectively) before decreasing at 15 cycles to undetectable levels (Fig. 6.3). At cycle 20 in all of these groups, a secondary spike of cells within the GFP+ gate (0.02%, 0.03%, and 0.13%) was observed.

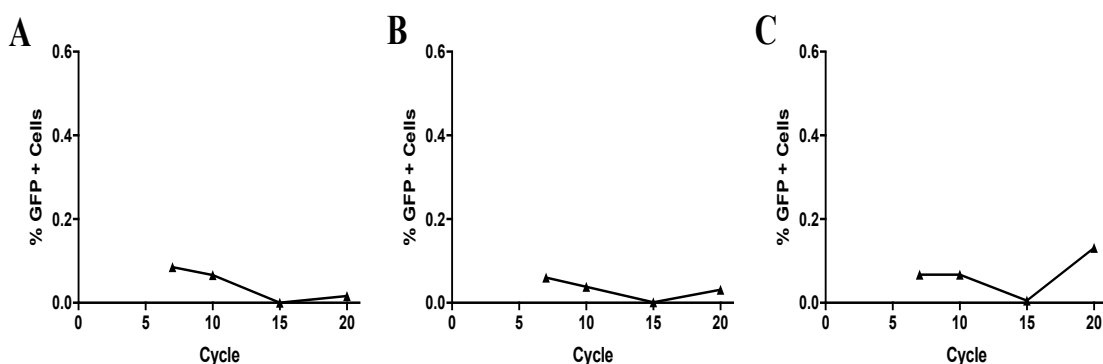


Figure 6.3: Percent of Fixed MAG Cells with Translocations in Quercetin, Luteolin, and Genistein/Quercetin/Luteolin Groups Over 20 Cycles. Flow cytometry was utilized to analyze the percent of cells that were GFP+, which is indicative of a translocation event. Approximately 2.5 billion events were recorded in each sample, A, quercetin, B, luteolin, and C, G/Q/L (n=1). Events were recorded at cycles 7, 10, 15 and 20.

Finally, in myricetin and kaempferol treated groups, a unique trend was observed. Only a baseline number of cells were observed in the GFP+ gate at cycle 7, and then at cycle 10, both treatment groups showed a peak of cells within the GFP+ gate with a 0.1% for myricetin and a 0.08% for kaempferol. The number of cells within the GFP+ gate decreased back down to baseline at later cycles for both groups (Fig. 6.4).

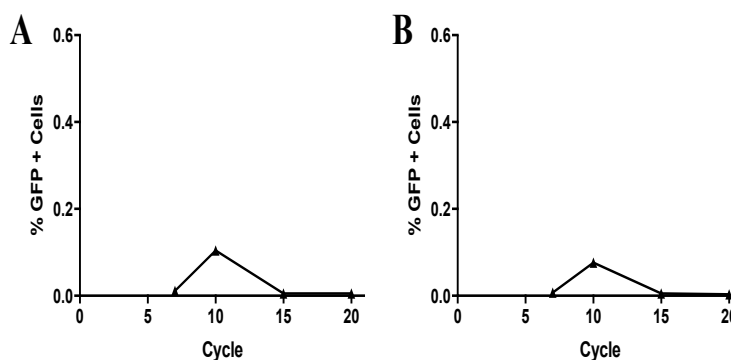


Figure 6.4: Percent of Fixed MAG Cells with Translocations in Myricetin and Kaempferol Groups Over 20 Cycles. Flow cytometry was utilized to analyze the percent of cells that were GFP+, which is indicative of a translocation event. Approximately 2.5 billion events were recorded in each sample, A, myricetin, and B, kaempferol (n=1). Events were recorded at cycles 7, 10, 15 and 20.

6.2 Detection of Chromosomal Translocations Induced by Chronic, Low Dose

Bioflavonoid Treatment: Analysis of Cells without Fixation

Given the results and trends observed in the one experiment that analyzed cells after paraformaldehyde fixation, subsequent replicates (n=2) were performed and cells analyzed by flow cytometry immediately after harvesting without fixation of cells. Again, MAG translocation Reporter cells⁶⁵ were treated with low doses of bioflavonoids (genistein, quercetin, luteolin, kaempferol, myricetin, genistein/quercetin and genistein/quercetin/luteolin) over the course of 20- 3 day cycles (see Chapter 2.6 for treatment scheme). After treatment cycles 1, 3, 5, 12, 15, 18 and 20, cells were harvested and single cell suspensions immediately analyzed by flow cytometry (FACS ARIA) to

detect GFP+ cells indicative of individual cells that contain a translocation within the populations sample. 2.5×10^6 events were recorded for each sample.

Gating of GFP-/GFP+ events was attempted to be set based on the no treatment group such that <0.01% of cells would be in the GFP+ gate, similar to the first experiment. However, in the no treatment group in the first replicate there appeared to be cells in a region that would normally be considered within a GFP+ gate. Thus, the gates were set based on the first experiment, but this resulted in data with GFP+ cells in the both the no treatment and DMSO treatment groups. No cells within the set GFP+ gate were sorted and further analyzed to determine if they were *bona fide* GFP+ cells with translocations. Since only two replicate experiments were performed no statistical analysis was run on these experiments.

In the no treatment group, no observable pattern was seen between the two replicates. In one no treatment replicate, the trend was similar to the DMSO-treated group, while the other had a group of cells within the GFP+ gate in cycles 1 and 5 (Fig. 6.5A). Luteolin similarly had one replicate with peaks of cells within the GFP+ gate at cycles 5 and 15 and another replicate with a similar trend to the quercetin and G/Q treated groups (Fig. 6.5B).

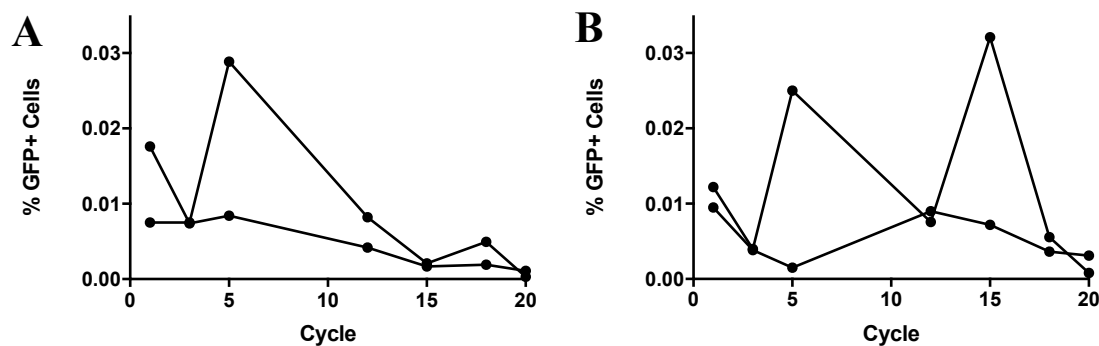


Figure 6.5: Percent of MAG Cells with Translocations in No Treatment and Luteolin Over 20 Cycles. Flow cytometry was utilized to analyze the percent of cells that were GFP+, which is indicative of a translocation event. Approximately 2.5 billion events were recorded in each sample, A, no treatment, and B, luteolin (n=2, both replicates displayed). Events were recorded at cycles 1, 3, 5, 12, 15, 18, and

The DMSO-treated and dipyrone-treated groups both showed low, persistent levels of cells within the GFP+ gate throughout the 20 cycles. The percent of cells within the GFP+ gate peaked around cycle 3 for the DMSO treated group with 0.0086% cells, and at cycle 5 in the dipyrone treated group with 0.0099% cells. By cycle 15, these populations reduced to 0.0024% and 0.0025% for DMSO and dipyrone treated groups, respectively, where they remained for the last 5 cycles (Fig. 6.6).

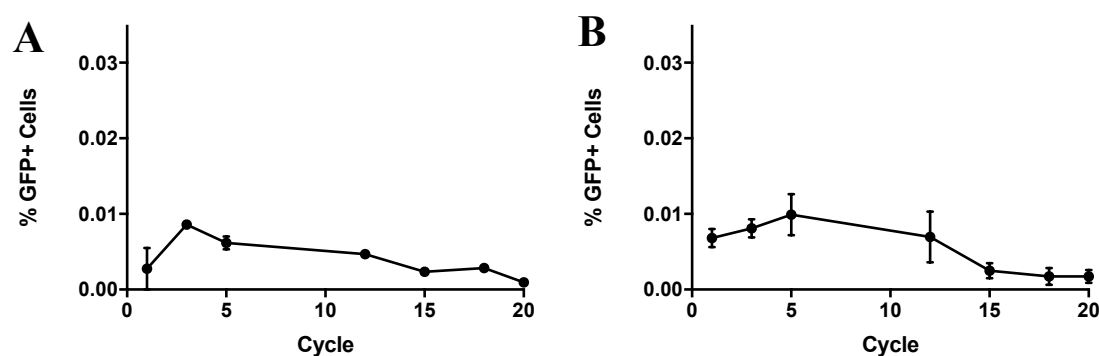


Figure 6.6: Percent of MAG Cells with Translocations in DMSO and Dipyrone Groups Over 20 Cycles. Flow cytometry was utilized to analyze the percent of cells that were GFP+, which is indicative of a translocation event. Approximately 2.5 billion events were recorded in each sample, A, DMSO, and B, dipyrone (n=2, mean represented with SEM). Events were recorded at cycles 1, 3, 5, 12, 15, 18, and 20.

The trends between the genistein, kaempferol, myricetin, and G/Q/L treated groups were similar. Genistein and kaempferol treated groups had peaks in the cells within the

GFP+ gates after 5 cycles with 0.0075% and 0.0074% respectively, while myricetin and G/Q/L treated groups had their peaks at cycle 12 with 0.009% and 0.0032%, respectively. After the peak in these groups the percent of cells within the GFP+ gate dropped by cycle 15 with a slight second wave in cycle 18 for all groups except G/Q/L (Fig. 6.7).

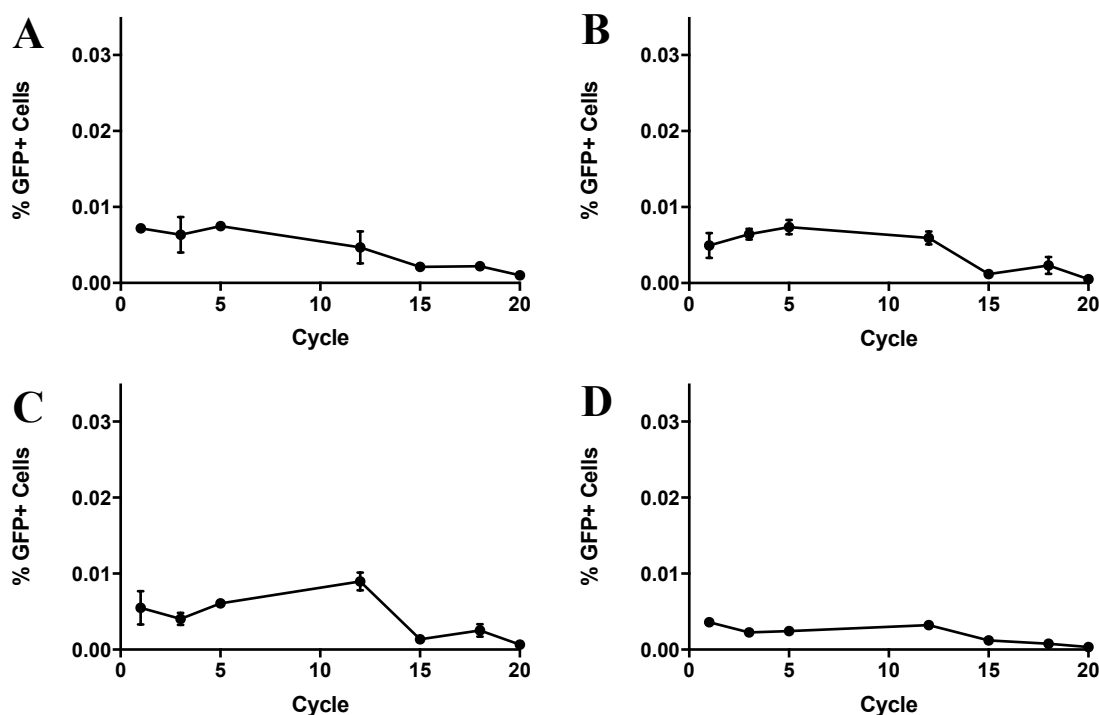


Figure 6.7: Percent of MAG Cells with Translocations in Genistein, Kaempferol, Myricetin, and G/Q/L Groups Over 20 Cycles. Flow cytometry was utilized to analyze the percent of cells that were GFP+, which is indicative of a translocation event. Approximately 2.5 billion events were recorded in each sample, A, genistein, B, kaempferol, C, myricetin, and D, G/Q/L (n=2, mean represented with SEM). Events were recorded at cycles 1, 3, 5, 12, 15, 18, and 20.

In the cells treated with quercetin and G/Q, a similar trend to the fixed genistein and G/Q groups from 6.1 was observed. These groups displayed a relatively large population of GFP+ cells in the initial cycles (0.017%, quercetin & 0.014%, G/Q), before decreasing in cycles 3 and 5. These groups then displayed a second wave of GFP+ cells at the 12 or 15 cycle mark before again decreasing at 20 cycles (Fig. 6.8).

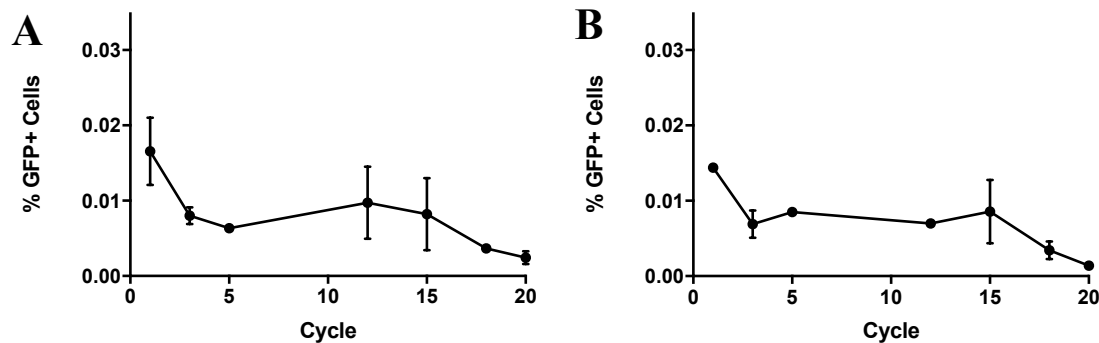


Figure 6.8: Percent of MAG Cells with Translocations in Quercetin and G/Q Groups Over 20 Cycles. Flow cytometry was utilized to analyze the percent of cells that were GFP+, which is indicative of a translocation event. Approximately 2.5 billion events were recorded in each sample, A, quercetin, and B, G/Q (n=2, mean represented with SEM). Events were recorded at cycles 1, 3, 5, 12, 15, 18, and 20.

6.3 Conclusions

The results from the first experiment analyzing fixed cells (Section 6.1) suggest that cells treated with chronic, low doses of bioflavonoids will lead to persistent, small populations of cells with chromosomal translocations that may be proliferating or dying off and newly appearing in waves over time. These data also suggest that some bioflavonoids may have different kinetics in causing these translocation events, since some genistein and G/Q treated groups showed an initial high population of GFP+ cells, while quercetin, luteolin, and G/Q/L treated cells had lower, but consistent, populations, and myricetin and kaempferol showed a later delayed peak of GFP+ cells.

The results from the second experiment two replicates analyzed immediately after collection were problematic and the results were very different as compared to the fixed cell experiment. The results for the no treatment and the luteolin groups were confounding without a designated trend between the two replicates, while the other treatments seemed to have consistent trends within the experiment. Though the trends of the other groups were consistent, the size of the populations of cells within the GFP+ gate in the bioflavonoid treated groups were very similar to the no treatment groups and if the differences were

significant at all with a third replicate, the number would likely be lower in the bioflavonoid groups compared to the control group. Overall it is difficult from these experiments to draw conclusions about how chronic, low doses of bioflavonoids impact cells.

In addition, it was noted over time that a change in the morphology of the cells treated with bioflavonoids occurred over time (Fig. 6.9). Cells appeared to lose their typical shape, which could indicate cellular senescence or epigenetic changes in gene expression. Future studies investigating these morphological differences are required.

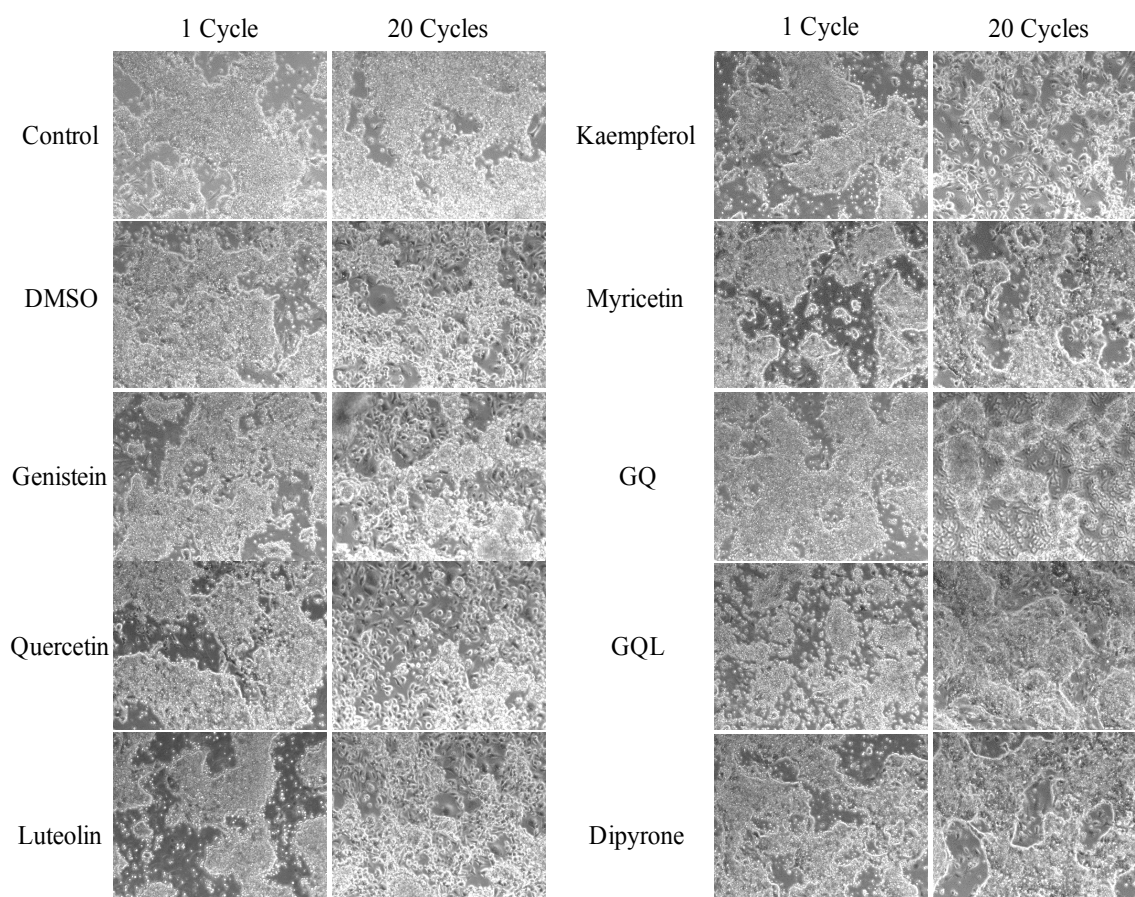


Figure 6.9: Representative Images of Morphological Changes in Cells with 20 Cycles of Bioflavonoid Treatment. Representative images captured after cycle 1 and 20 are shown for all treatment groups.

The conclusions that seem consistent are that chronic low doses of bioflavonoids may cause small persistent populations with chromosomal translocations, and these populations seem to appear in waves. Further research is necessary, potentially with repetition of these experiments, or with a different experimental design, or with single cell sorting of gated GFP⁺ events and further analysis and molecular characterization of them. Given the likely low translocation frequency promoted by chronic low doses and the need for frequent cell passaging, an *in vivo* mouse model may be better suited for this study.

CHAPTER 7: DISCUSSION AND FUTURE DIRECTIONS

7.1 Mechanistic Insights on Bioflavonoids as Top2 Poisons

To recapitulate the findings from these experiments, when quantifying the number of DSBs caused by bioflavonoid treatment in Chapter 3, differences in the kinetics of DSB resolution were observed based upon the classification of Top2 poison used. For treatments such as etoposide and myricetin, which act as both traditional/interfacial and covalent Top2 poisons, there was first an increase in the amount of DNA damage observed 1h post treatment before resolution of DSBs became observable at the latter time points. On the other hand, dipyrone, which is not a known Top2 poison or bioflavonoid, caused a very different kinetic pattern, with damage resolving instead of increasing before a second wave of damage occurred at the latest time point. Quercetin's kinetic trend was similar to dipyrone, suggesting that while quercetin is a known Top2 inhibitor, it is highly possible it has other cellular pathways through which it can cause DNA damage.

Genistein and luteolin's trends were similar to quercetin, with significant DSB resolution that continued through all time points, further supporting the conclusion that bioflavonoid classification as a Top2 poison is more predictive than the sub-class of the bioflavonoid in predicting the resolution kinetics of DSBs. However, this is not the complete picture and further research needs to be done focusing on covalent only poisons, given the results observed with kaempferol and both of the combination treatments. Kaempferol which has also been shown to only be a traditional poison had a similar kinetic trend to etoposide and myricetin, as did both combination treatments. This suggests kaempferol and potentially its metabolites have functions as a covalent poison, and that perhaps when genistein, quercetin and luteolin are combined their anti-inflammatory redox

mechanisms can impact the cell as a covalent poison that was not possible for them as individual treatments. This suggests that if their metabolites are covalent poisons, they are probably present in low quantities that would require very high doses, or combinations treatments to cause damage.

Chapter 4 gave further insights to the mechanism by which these bioflavonoids work to poison cells when Top2 was catalytically inhibited by dexrazoxane (DEX). With DEX inhibiting the Top2 from binding dsDNA with 1h pre-treatment or catalyzing the degradation of Top2 β with 5h pre-treatment, it was possible to consider if Top2-independent mechanisms were playing a role in the damage seen in Chapter 3. Etoposide, which is known to cause DNA DSBs through Top2 poisoning, expectedly saw significant decreases in DNA damage with increased dose and time of DEX pre-treatment. Myricetin, similarly to Chapter 3, showed the most similarity to etoposide treatment, with consistent decreases in the amount of damage seen back to control levels with the time and dose of DEX increased. This suggests myricetin has few, if any, Top2 independent mechanisms. However, given these findings, a different explanation is also possible. There is possibility the binding affinity for Top2 in traditional/interfacial and covalent poisons differ.

Covalent Top2 poisons, which bind to a distal site on the Top2 enzyme thereby causing a confirmation change keeping DSBs open after Top2 has caused them, could bind to the Top2 enzyme before it binds to DNA^{32,68}. In this situation it would not matter if cells were pre-treated with DEX before treatment with a covalent poison because the poison would be bound and unable to cause any pleiotropic cellular effects with or without DEX. This proposed hypothesis would explain the results seen in etoposide and myricetin treated cells. With both of these compounds, as time of pre-treatment and dose of DEX increased,

the amount of damage decreased because the etoposide metabolites (covalent poisons) and myricetin would bind to Top2 whether DNA was bound or not and therefore with increased dose of DEX there would be less myricetin free within the cell. Furthermore with 5h pre-treatment the myricetin and etoposide metabolites would be bound to Top2 β before it is degraded, thereby also degrading the bioflavonoid or metabolite.

In opposition, traditional poisons, which prevent the Top2 enzyme from religating the DSB back together acting as a “doorstop”, likely do not bind to or weakly bind Top2 if it has not already bound to two segments of dsDNA and created a DSB. However, once this traditional Top2 poison binds, it is highly possible that it stays bound to the enzyme until the stabilized Top2 cleavage complex is removed from DNA and all components including the poison are degraded. If a bioflavonoid has potential pleiotropic effects on the cell but is bound to Top2 and caught in a cleavage complex and then is degraded, the bioflavonoid would have a minimal impact, if any, on the cell outside of poisoning Top2. The exception to this would be if the bioflavonoid treatment was at a very high concentration, such that all Top2 active binding sites were bound.

As an example, in Chapter 4 when DEX was added to cells before kaempferol treatment, an increase in DNA DSBs was observed both with 1 and 5h DEX pre-treatment. Kaempferol, which is a traditional poison by Osheroff’s proposed rules, would not be able to bind to Top2 if it was not bound to DNA³². With the further increase seen with 5h DEX pre-treatment, it is possible any Top2 that was not inhibited 1h pre-treatment was inhibited with the increased pre-treatment, and furthermore if a traditional poison could weakly bind with non-DNA bound Top2, that would no longer be an option since Top2 β is degraded with 5h DEX pre-treatment. If kaempferol could no longer bind Top2, this would allow the

bioflavonoid to move throughout the cell, causing DSBs through other mechanisms. Based upon the kinetics of DSB resolution in Chapter 3, it is possible kaempferol has some potential as a covalent poison. However, given the results from these DEX experiments, it seems likely that Top2-independent mechanism in the cell may cause a majority of the DNA damage. This means Top2 may have a protective effect in cells exposed to kaempferol, especially given that there is an observed increase in chromosomal translocations seen in Chapter 5 with DEX + kaempferol treatment. These Top2-independent mechanisms may be more mutagenic than Top-dependent mechanisms given that the fold increase in translocations was higher than what was expected based upon the fold increase of γ -H2AX foci.

To further support these proposed hypotheses, genistein, quercetin and luteolin, which are known traditional poisons, but are also antioxidants and therefore could have byproducts that act as covalent poisons, as mentioned earlier this chapter, have unique patterns of DNA damage when DEX pre-treatment dose or time is increased. Genistein, for instance, does not show a decrease in damage until a higher dose, or increased pre-treatment time of DEX is given. This level of damage not decreasing with the lowest dose and time of DEX indicates genistein is acting primarily as a traditional poison, as it is known to be, but it may also have covalent properties. By binding any Top2-DNA complexes that were not impacted by the DEX, it can cause equal amounts of damage to the no DEX groups.

However, when Top2 activity is decreased further and the concentration is depleted by degrading Top2, approximately half of damage previously observed is still present. This indicates that genistein does have Top2-independent mechanisms to cause DNA damage,

but these are limited within the cells, either because the Top2-independent mechanisms can only cause DSBs in limited areas of the genome, or because genistein was degraded with Top2 because it was bound as a covalent poison. Given this data, it is proposed genistein has a high binding affinity to the Top2 active site, making it primarily a traditional poison, however when it cannot bind to the active site, genistein is able to bind to the distal site as a covalent poison, or act on other cellular pathways. In addition, while the number of γ -H2AX foci decreased with DEX treatment, there was a slight, though not significant, increase in the number of translocation events with DEX + genistein treatment, supporting that the Top2-independent mechanisms of damage may be more mutagenic. Quercetin may work in a similar manner given that approximately half of the initial damage seen without DEX treatment is still present with high doses and/or long pre-treatments of DEX.

Luteolin may have stronger Top2-independent mechanisms to cause damage, because with the low dose treatment the amount of damage drops significantly before increasing with extended DEX pre-treatment. This is a strong indicator that the Top2-dependent damage is mitigated with DEX, but that once Top2 is not present to bind luteolin, it has strong Top2-independent mechanisms by which to cause DNA damage. Therefore, as with kaempferol, Top2 may protect against luteolin-induced DNA damage. In the combination treatment group with genistein/quercetin, this trend is seen also. There is a slight decrease in damage seen with a high, but short DEX pre-treatment, suggesting some of the damage from these two bioflavonoids is because they have weak covalent properties, as previously proposed. This would be logical because with the higher treatment doses for combination treatments, there would be high competition for the active sites, leading to some covalent binding. This could also explain the results seen in the kinetic

experiments in Chapter 3 where both combination treatments resembled etoposide kinetics more than the individual treatment kinetics. With the high concentration of bioflavonoids competing for active Top2 sites since genistein, quercetin and luteolin are all primarily traditional poisons, there would be a surplus of free bioflavonoids to bind to the distal site as a covalent poison or act on other pathways in the cell.

The previous proposed hypotheses also support the observed similar increases in damage in the genistein/quercetin/luteolin group as to what was observed in the kaempferol group. Any bioflavonoids that bound to Top2 in a covalent manner were degraded with Top2 with 5h DEX pre-treatment, however given the concentration of bioflavonoids these cells were exposed to an increase in damage was observed because the genistein, quercetin and luteolin are free to act on the cell in other pathways that do not overlap creating increasing amounts of damage.

To summarize, these experiments have led to the generation of 5 new hypotheses (for a visual summary see Table 7.1):

1. The kinetic patterns of DNA damage resolution in cells treated with bioflavonoids, is dependent upon the bioflavonoid's ability to poison Top2 as a traditional or covalent poison, not its sub-group classification.
2. Genistein and quercetin have a primary binding affinity for the active site of Top2 when a DSB has been formed and therefore these bioflavonoids act as primarily traditional poisons. However, when this active site is not available due to Top2 inhibition or high competition, they can act as covalent poisons with a weak binding affinity for the distal Top2 site. Luteolin and kaempferol may also work in a similar manner with different binding predispositions.

3. Genistein, quercetin, luteolin and kaempferol all have Top2-independent mechanisms that can create DNA damage, though these are of varying strength. Therefore, if this is accurate Top2 may have a protective effect on cells, by binding poisons, to prevent them from causing further damage to the cell. The Top2-independent mechanisms of kaempferol and luteolin may cause more damage than genistein and quercetin.
4. Genistein and quercetin work through different Top2-independent mechanisms to cause DNA damage. It is a strong possibility that luteolin and kaempferol also work through different mechanisms than genistein or quercetin.
5. Top2-independent mechanisms in kaempferol are more mutagenic and cause more translocations than Top2-dependent mechanisms. This is possible of genistein's Top2 independent mechanisms also.

Though these data appear to support these hypotheses, further experiments are needed to determine the validity of these hypotheses or if any revisions are necessary.

Table 7.1: Visual Summarization of Hypothesized Mechanisms Bioflavonoids Utilize to Damage DNA. +, known mechanism; *, mechanism proposed by this research; ~, not enough data for conclusion; -, no support for this mechanism.

Compound	Top2-Dependent Mechanism		Top2-Independent Mechanism
	Traditional	Covalent	
Etoposide	+	+	-
Genistein	+	*	*
Quercetin	+	*	*
Luteolin	+	*	*
Kaempferol	+	~	*
Myricetin	+	+	-

7.2 Proposed Future Directions

7.2.1 Investigate Bioflavonoids that are Covalent Top2 Poisons

The bioflavonoids used for these experiments, except myricetin, are all classified as traditional/interfacial Top2 poisons according to the work done by Bandele, Clawson and Osheroff (Fig. 1.16) ³². Therefore, while the data support DNA damage resolution kinetics and Top2 inhibition patterns are not dependent on the sub-class of the bioflavonoid, without testing bioflavonoids with covalent Top2 poisoning capabilities the first new hypothesis is not fully supported by this research. To investigate if a bioflavonoid's Top2 poison classification determines the DNA damage resolution kinetics, the experiments performed in Chapter 3 would need to be performed with covalent Top2 poisons. Compounds that could be used in these experiments include 1,4-benzoquinone, a known covalent poison, and the two bioflavonoids, epigallocatechin gallate (EGCG) and delphinidin, which are classified as covalent poisons. By determining the kinetic DSB resolution of covalent Top2 poisons, the first new hypothesis could be supported and the second new hypothesis regarding genistein and quercetin having secondary abilities as covalent poisons could be considered.

The experiments done in Chapter 4 should be performed with covalent poisons also to determine if the patterns of DNA damage observed with DEX pre-treatment for the genistein, quercetin, luteolin, and kaempferol align with that of covalent poisons. In addition, these experiments could begin to investigate if Top2 has a protective effect on the cells as stated in hypothesis 3. If the covalent poisons binding to Top2 prevents them from causing other DNA damage within the cell, then with Top2 degraded, or if siRNA is used to deplete Top2 from cells, there should be an increase in the amount of damage seen

with bioflavonoid treatments. Phenanthriplatin would be an ideal control to test this hypothesis because this drug causes Top2 damage through Top2 poisoning, but it also acts as a potent DNA and RNA polymerase inhibitor by binding to DNA causing complex stalling⁹⁹.

7.2.2 Investigate Bioflavonoids that are Proposed Covalent Top2 Poisons

Additionally to investigate hypothesis 2, experiments performed in cell free systems with the incubation of bioflavonoids with Top2 before adding in DNA as done by Bandele, Clawson, and Osheroff³² could be done. All bioflavonoids from the experiments shown in these experiments, plus the covalent compounds 1,4-benzoquinone, EGCG, and delphinidin, would be incubated with Top2 α/β prior to addition to a DNA mixture. As observed in the Bandele paper, the longer myricetin was incubated with Top2 α prior to DNA addition, the less ability Top2 had to cleave DNA. Based upon this evidence, it appears that covalent poisons can bind to Top2 without DNA present and that once the poison binds to Top2 without DNA, the poison instead acts as an inhibitor.

In that same experiment by Bandele, quercetin demonstrated a reduced ability to cause DNA cleavage when it was incubated with Top2 prior to the addition of DNA, unlike kaempferol, which showed no decreases in DNA cleavage with pre-incubation. This supports that quercetin may have covalent poisoning capabilities and that this system would be a promising way to determine if other bioflavonoids, such as genistein and luteolin have such abilities also. Additionally, in these experiments, the reducing agent DTT was added to the bioflavonoids before addition of the Top2 α enzyme. DTT prevented the covalent poison from binding to Top2, therefore when DNA was added after the Top2

incubation period the reduced cleavage from myricetin and quercetin was not seen. If the other known covalent poisons and compounds being tested demonstrate the same reduction in ability to cleave DNA with Top2 pre-incubation and the DTT reverses this inability to cleave the DNA, it is highly probable that those compounds have the ability to poison Top2 covalently, which may lead to the need to redefine covalent versus traditional Top2 poison classifications.

7.2.3 Investigate Bioflavonoids Top2-Independent Mechanisms of DNA Damage

To investigate hypotheses 3-5 and determine what Top2-independent mechanisms bioflavonoids use to cause DNA damage, the new technique developed by the Nussenzweig lab called END-seq could be utilized^{49,100}. Though incomplete the Richardson lab in collaboration with Drs. Jennifer Weller and Robert Reid have begun troubleshooting and modifying the END-seq protocol to suit these experiments. For a preliminary protocol, see Appendix B. The END-seq technique allows the researcher to detect where DSBs specifically occur across the genome through the capture and sequencing of DSBs. This technology has been shown to reproducibly detect DSBs through the genome caused by etoposide through Top2 poisoning and can even distinguish between clean DSBs and DSBs with unresolved Top2 cleavage complexes attached to DNA by poisoning.

For these experiments, the DSBs across the entire genome caused by the bioflavonoid panel used in these experiments will be compared to the DSBs caused by etoposide. The hypothesis for these experiments being that regions with overlapping DSBs are caused by Top2-dependent mechanisms, while DSBs unique to the bioflavonoids are

caused by their Top2 independent mechanisms. By comparing the DSBs caused by these treatments to one another, it will be possible to determine which bioflavonoids have unique mechanisms to cause DNA damage allowing for the evaluation of new hypothesis 4. This data will also allow for the prediction of what Top2-independent mechanisms are used to cause this damage by bioflavonoids. For instance, genistein is a known estrogen-mimic, meaning that it causes the activation of specific gene transcription. If an increase in DSBs are seen within those regions of newly active transcription, it can be concluded that the increased transcription through those estrogen-activated genes is one cause of Top2-independent breaks. This can be applied to other break sites also. If the other bioflavonoids tested have increased DSBs in specific regions of the genome, increased transcription of those regions could be tested through quantitative PCR. In addition, if the region of increased DSBs is relative to specific regions of the genome, such as CpG islands, or protein scaffolding sites, investigation of bioflavonoids in relation to the proteins known to interact with these regions would be possible.

END-seq could also be performed with DEX pre-treatment or the use of siRNA to knockdown Top2 to verify DSBs that are Top2-independent. This would allow for the evaluation of hypothesis 3; if in the absence of Top2 the amount of damage caused by Top2-independent mechanisms increases, then Top2 does play a protective role against Top2-independent damage.

7.2.4 Determine Potential Mechanisms Bioflavonoids Use to Cause Translocations

In addition to determining the Top2 independent mechanisms by which bioflavonoids cause DSBs, investigating the mechanism by which chromosomal

translocations are promoted by these compounds may be beneficial to understanding their impact on the cell. Many bioflavonoids have been shown to impact signal transduction pathways and there are example of bioflavonoids modulating the expression of DNA repair proteins^{21,65,69}. END-seq will show where DSBs occur across the genome, it would be of particular interest if DSBs localized at DNA repair gene sequences, preventing their transcription. Other experiments could treat cells with bioflavonoids and then utilize mRNA microarray technology to determine if the panel of bioflavonoids examined cause changes to the mRNA levels of DNA repair proteins.

Another pleiotropic bioflavonoid effect that could impact DNA repair is the modulation of epigenetic markers^{72,75-79}. Since specific patterns of epigenetic markers are associated with different types of DSB repair⁵ and cause gene transcription changes, it is possible bioflavonoid induced epigenetic changes modulate repair pathway choice. Therefore, evaluation by ChIP-seq of open chromatin markers and markers associated with specific types of DSB repair may allow for observation of patterns of epigenetic modulation caused by bioflavonoid treatment.

7.3 Implications of this Research

This research and the future experiments described above may provide insights into the mechanisms by which bioflavonoids cause DNA damage and chromosomal translocations. If the DNA damaging and mutating mechanisms of a panel of different bioflavonoids is elucidated, it could allow scientists and medical professionals to discuss the potential for using bioflavonoids as an alternative for etoposide and other anti-cancer agents⁵⁸. Especially since bioflavonoids seem to impact more rapidly dividing cell

populations with translocation events, thereby making it possible that bioflavonoids would have a very minor impact on non-cancerous cells within the body⁶⁵. The data from these experiments could be utilized to determine the potential ideal bioflavonoid/dose or combination therapy that would maximize the amount of DNA damage that occurs while minimizing the risk of translocations occurring. These investigations could also help to determine what tests and experiments are essential to determining future bioflavonoid or other Top2 poisoning compounds that would be ideal for anti-cancer treatments.

Additionally, if the mechanisms by which bioflavonoids and other Top2 poisoning compounds is understood, the prevention of chromosomal translocations may be possible. This information could be essential to decreasing the rate of infant leukemia. Currently epidemiological data suggests that bioflavonoid rich diets in pregnant women increases the likelihood of infant leukemia^{30,31,101}. The current solution is that pregnant women should avoid intake of bioflavonoid rich foods or supplements. However, there are health benefits to bioflavonoids and the foods rich in bioflavonoids are an essential part of the diet, making it difficult to determine what foods should be avoided. This is especially true when many of the epidemiological studies focused on bioflavonoid take struggle to find the best way to quantify bioflavonoid intake based on a subject's self-reporting of their diet^{59,61}. Therefore, if these future studies can determine the bioflavonoids and the concentrations of bioflavonoids that put pregnant women at the most risk, or if they could determine a mechanism to prevent translocations from occurring, the risk of infants developing leukemia could be diminished.

REFERENCES

1. Ranjha, L., Howard, S. M. & Cejka, P. Main steps in DNA double-strand break repair: an introduction to homologous recombination and related processes. *Chromosoma* **127**, 187–214 (2018).
2. Rouse, J. & Jackson, S. P. Interfaces between the detection, signaling, and repair of DNA damage. *Science (80-.)*. **297**, 547–551 (2002).
3. Heijink, A. M., Krajewska, M. & Van Vugt, M. A. T. M. The DNA damage response during mitosis. *Mutat. Res. - Fundam. Mol. Mech. Mutagen.* **750**, 45–55 (2013).
4. Pendleton, M., Lindsey, R. H., Felix, C. A., Grimwade, D. & Osheroff, N. Topoisomerase II and leukemia. *Ann. N. Y. Acad. Sci.* **1310**, 98–110 (2014).
5. Thomas *et al.* Comprehensive Mapping of Histone Modifications at DNA Double-Strand Breaks Deciphers Repair Pathway Chromatin Signatures. *Mol. Cell* 250–262 (2018). doi:10.1016/j.molcel.2018.08.020
6. Bariar, B., Vestal, C. G. & Richardson, C. Long-Term Effects of Chromatin Remodeling and DNA Damage in Stem Cells Induced by Environmental and Dietary Agents. *J. Environ. Pathol. Toxicol. Oncol.* **32**, 307–327 (2013).
7. Gong, F. & Miller, K. M. Histone methylation and the DNA damage response. *Mutat. Res. Mutat. Res.* 0–1 (2017). doi:10.1016/j.mrrev.2017.09.003
8. Sancar, A., Lindsey-Boltz, L. A., Ünsal-Kaçmaz, K. & Linn, S. Molecular Mechanisms of Mammalian DNA Repair and the DNA Damage Checkpoints. *Annu. Rev. Biochem.* **73**, 39–85 (2004).
9. Zhou, B. B. & Elledge, S. J. The DNA damage response: putting checkpoints in

- perspective. *Nature* **408**, 433–9 (2000).
10. Harper, J. W. & Elledge, S. J. The DNA Damage Response: Ten Years After. *Mol. Cell* **28**, 739–745 (2007).
 11. Ciccia, A. & Elledge, S. J. The DNA Damage Response: Making It Safe to Play with Knives. *Mol. Cell* **40**, 179–204 (2010).
 12. Jasin, M. & Rothstein, R. Repair of strand breaks by homologous recombination. *Cold Spring Harb. Perspect. Biol.* **5**, 1–18 (2013).
 13. Wright, W. D., Shah, S. S. & Heyer, W. D. Homologous recombination and the repair of DNA double-strand breaks. *J. Biol. Chem.* **293**, 10524–10535 (2018).
 14. Byrne, M. *et al.* Mechanisms of oncogenic chromosomal translocations. *Ann. N. Y. Acad. Sci.* **1310**, 89–97 (2014).
 15. Nussenzweig, A. & Nussenzweig, M. C. Origin of chromosomal translocations in lymphoid cancer. *Cell* **141**, 27–38 (2010).
 16. Pommier, Y., Sun, Y., Huang, S. Y. N. & Nitiss, J. L. Roles of eukaryotic topoisomerases in transcription, replication and genomic stability. *Nat. Rev. Mol. Cell Biol.* **17**, 703–721 (2016).
 17. Nambiar, M. & Raghavan, S. C. How does DNA break during chromosomal translocations? *Nucleic Acids Res.* **39**, 5813–5825 (2011).
 18. Wray, J. *et al.* PARP1 is required for chromosomal translocations. *Blood* **121**, 4359–4365 (2013).
 19. Ferguson, D. O. *et al.* David O., PNAS, 2000.pdf. (2000).
 20. Gómez-Herreros, F. *et al.* TDP2-Dependent Non-Homologous End-Joining Protects against Topoisomerase II-Induced DNA Breaks and Genome Instability in

- Cells and In Vivo. *PLoS Genet.* **9**, (2013).
21. Charles, C., Nachtergaeel, A., Ouedraogo, M., Belayew, A. & Duez, P. Effects of chemopreventive natural products on non-homologous end-joining DNA double-strand break repair. *Mutat. Res. - Genet. Toxicol. Environ. Mutagen.* **768**, 33–41 (2014).
 22. Chang, H. H. Y., Pannunzio, N. R., Adachi, N. & Lieber, M. R. Non-homologous DNA end joining and alternative pathways to double-strand break repair. *Nature Reviews Molecular Cell Biology* **18**, (2017).
 23. Libura, J., Ward, M., Solecka, J. & Richardson, C. Etoposide-initiated MLL rearrangements detected at high frequency in human primitive hematopoietic stem cells with in vitro and in vivo long-term repopulating potential. *Eur. J. Haematol.* **81**, 185–95 (2008).
 24. Zhang, Y. & Jasin, M. An essential role for CtIP in chromosomal translocation formation through an alternative end-joining pathway. *Nat. Struct. Mol. Biol.* **18**, 80–4 (2011).
 25. Nambiar, M., Kari, V. & Raghavan, S. C. Chromosomal translocations in cancer. *Biochim. Biophys. Acta - Rev. Cancer* **1786**, 139–152 (2008).
 26. Alexander, F. E. *et al.* Transplacental chemical exposure and risk of infant leukemia with MLL gene fusion. *Cancer Res.* **61**, 2542–2546 (2001).
 27. Zheng, J. Oncogenic chromosomal translocations and human cancer (Review). *Oncol. Rep.* **30**, 2011–2019 (2013).
 28. Ashour, M. E., Atteya, R. & El-Khamisy, S. F. Topoisomerase-mediated chromosomal break repair: An emerging player in many games. *Nat. Rev. Cancer*

- 15**, 137–151 (2015).
29. Sung, P. A., Libura, J. & Richardson, C. Etoposide and illegitimate DNA double-strand break repair in the generation of MLL translocations: New insights and new questions. *DNA Repair (Amst)*. **5**, 1109–1118 (2006).
 30. Spector, L. G. *et al.* Maternal Diet and Infant Leukemia: The DNA Topoisomerase II Inhibitor Hypothesis: A Report from the Children's Oncology Group. *Cancer Epidemiol. Biomarkers Prev.* **14**, 651–655 (2005).
 31. Strick, R., Strissel, P. L., Borgers, S., Smith, S. L. & Rowley, J. D. Dietary bioflavonoids induce cleavage in the MLL gene and may contribute to infant leukemia. *Proc. Natl. Acad. Sci.* **97**, 4790–4795 (2000).
 32. Bandele, O. J., Clawson, S. J. & Osheroff, N. Dietary polyphenols as topoisomerase II poisons: B ring and C ring substituents determine the mechanism of enzyme-mediated DNA cleavage enhancement. *Chem. Res. Toxicol.* **21**, 1253–1260 (2008).
 33. Tan, J., Muntean, A. G. & Hess, J. L. PAFc , a Key Player in MLL-rearranged Leukemogenesis. **1**, 461–465 (2010).
 34. Marschalek, R. Mechanisms of leukemogenesis by MLL fusion proteins. *Br. J. Haematol.* **152**, 141–154 (2011).
 35. Meyer, C. *et al.* New insights to the MLL recombinome of acute leukemias. *Leukemia* **23**, 1490–1499 (2009).
 36. Muntean, A. G. & Hess, J. L. The Pathogenesis of Mixed-Lineage Leukemia. *Annu. Rev. Pathol. Mech. Dis.* **7**, 283–301 (2012).
 37. Betti, C. J. *et al.* Cleavage of the MLL gene by activators of apoptosis is

- independent of topoisomerase II activity. *Leukemia* **19**, 2289–2295 (2005).
38. Nitiss, J. L. & Nitiss, K. C. Tdp2: A Means to Fixing the Ends. *PLoS Genet.* **9**, 2–4 (2013).
 39. Nitiss, J. L. DNA topoisomerase II and its growing repertoire of biological functions. *Nat. Rev. Cancer* **9**, 327–37 (2009).
 40. Dewese, J. E. & Osheroff, N. The DNA cleavage reaction of topoisomerase II: Wolf in sheep's clothing. *Nucleic Acids Res.* **37**, 738–748 (2009).
 41. Berger, J. M. Type II DNA topoisomerases. *Curr. Opin. Struct. Biol.* **8**, 26–32 (1998).
 42. Schoeffler, A. J. & Berger, J. M. DNA topoisomerases: Harnessing and constraining energy to govern chromosome topology. *Q. Rev. Biophys.* **41**, 41–101 (2008).
 43. Smart, D. J. *et al.* Assessment of DNA double-strand breaks and γ H2AX induced by the topoisomerase II poisons etoposide and mitoxantrone. *Mutat. Res. - Fundam. Mol. Mech. Mutagen.* **641**, 43–47 (2008).
 44. Nitiss, K. C., Nitiss, J. L. & Hanakahi, L. A. DNA Damage by an essential enzyme: A delicate balance act on the tightrope. *DNA Repair (Amst)*. **82**, 102639 (2019).
 45. Atkin, N. D., Raimer, H. M. & Wang, Y. H. Broken by the Cut: A Journey into the Role of Topoisomerase II in DNA Fragility. *Genes (Basel)*. **10**, (2019).
 46. Aparicio, T., Baer, R., Gottesman, M. & Gautier, J. MRN, CtIP, and BRCA1 mediate repair of topoisomerase II-DNA adducts. *J. Cell Biol.* **212**, (2016).
 47. Schellenberg, M. J. *et al.* ZATT (ZNF451)–mediated resolution of topoisomerase

- 2 DNA-protein cross-links. *Science* (80-.). **357**, 1412–1416 (2017).
48. Ledesma, F. C., El Khamisy, S. F., Zuma, M. C., Osborn, K. & Caldecott, K. W. A human 5'-tyrosyl DNA phosphodiesterase that repairs topoisomerase-mediated DNA damage. *Nature* **461**, 674–678 (2009).
49. Canela, A. *et al.* Topoisomerase II-Induced Chromosome Breakage and Translocation Is Determined by Chromosome Architecture and Transcriptional Activity. *Mol. Cell* **75**, 252–266.e8 (2019).
50. Zagnoli-Vieira, G. & Caldecott, K. W. TDP2, TOP2, and SUMO: What is ZATT about? *Cell Res.* **27**, 1405–1406 (2017).
51. Gómez-Herreros, F. *et al.* TDP2 protects transcription from abortive topoisomerase activity and is required for normal neural function. *Nat. Genet.* **46**, 516–521 (2014).
52. Lee, K. C. *et al.* Effect of TDP2 on the level of TOP2-DNA complexes and SUMOylated TOP2-DNA complexes. *Int. J. Mol. Sci.* **19**, (2018).
53. Hall, S. R. & Goralski, K. B. ZATT , TDP2 , and SUMO2 : breaking the tie that binds TOP2 to DNA. **7**, 439–444 (2018).
54. Gómez-Herreros, F. *et al.* TDP2 suppresses chromosomal translocations induced by DNA topoisomerase II during gene transcription. *Nat. Commun.* **8**, 1–9 (2017).
55. Rao, T. *et al.* Novel TDP2-ubiquitin interactions and their importance for the repair of topoisomerase II-mediated DNA damage. *Nucleic Acids Res.* **44**, 10201–10215 (2016).
56. Jiang, N., Doseff, A. I. & Grotewold, E. Flavones: From biosynthesis to health benefits. *Plants* **5**, 1–1256 (2016).

57. Manach, C., Scalbert, A., Morand, C., Rémésy, C. & Jiménez, L. Polyphenols: Food sources and bioavailability. *Am. J. Clin. Nutr.* **79**, 727–747 (2004).
58. Spagnuolo, C. *et al.* Genistein and cancer: current status, challenges, and future directions. *Adv. Nutr.* **6**, 408–19 (2015).
59. Esch, H. L., Kleider, C., Scheffler, A. & Lehmann, L. *Isoflavones: Toxicological Aspects and Efficacy. Nutraceuticals: Efficacy, Safety and Toxicity* (2016).
doi:10.1016/B978-0-12-802147-7.00034-6
60. Pollastri, S. & Tattini, M. Flavonols: Old compounds for old roles. *Ann. Bot.* **108**, 1225–1233 (2011).
61. Aherne, S. A. & O'Brien, N. M. Dietary Flavonols: Chemistry, Food Content, and Metabolism CHEMISTRY AND STRUCTURE OF THE FLAVONOIDS. *Nutrition* **18**, 75–81 (2002).
62. D'Andrea, G. Quercetin: A flavonol with multifaceted therapeutic applications? *Fitoterapia* **106**, 256–271 (2015).
63. Devi, K. P. *et al.* Kaempferol and inflammation: From chemistry to medicine. *Pharmacol. Res.* **99**, 1–10 (2015).
64. Kumar, S. & Pandey, A. K. Chemistry and biological activities of flavonoids: an overview. *ScientificWorldJournal.* **2013**, 162750 (2013).
65. Bariar, B. *et al.* Bioflavonoids promote stable translocations between MLL - AF9 breakpoint cluster regions independent of normal chromosomal context : Model system to screen environmental risks. *Environ. Mol. Mutagen.* (2018).
doi:10.0.3.234/em.22245
66. Biechonski, S. *et al.* Quercetin alters the DNA damage response in human

- hematopoietic stem and progenitor cells via TopoII- and PI3K-dependent mechanisms synergizing in leukemogenic rearrangements. *Int. J. Cancer* **140**, 864–876 (2017).
67. Schroder-van der Elst, J. P., van der Heide, D., Rokos, H., Morreale de Escobar, G. & Kohrle, J. Synthetic flavonoids cross the placenta in the rat and are found in fetal brain. *Am J Physiol* **274**, E253-6 (1998).
 68. Bandele, O. J. & Osheroff, N. Bioflavonoids as poisons of human topoisomerase II α and II β . *Biochemistry* **46**, 6097–6108 (2007).
 69. Nambiar, D. K. *et al.* Silibinin Preferentially Radiosensitizes Prostate Cancer by Inhibiting DNA Repair Signaling. *Mol. Cancer Ther.* **14**, 2722–2734 (2015).
 70. Zandvliet, D. W. J. *et al.* Analysis of foetal expression sites of human type II DNA topoisomerase α and β mRNAs by in situ hybridisation. *Biochim. Biophys. Acta - Gene Struct. Expr.* **1307**, 239–247 (1996).
 71. Todaka, E. *et al.* Fetal exposure to phytoestrogens—The difference in phytoestrogen status between mother and fetus. *Environ. Res.* **99**, 195–203 (2005).
 72. Kim, H. J., Kim, S. H. & Yun, J. M. Fisetin inhibits hyperglycemia-induced proinflammatory cytokine production by epigenetic mechanisms. *Evidence-based Complement. Altern. Med.* **2012**, (2012).
 73. Jones, E. A., Shahed, A. & Shoskes, D. A. Modulation of apoptotic and inflammatory genes by bioflavonoids and angiotensin II inhibition in ureteral obstruction. *Urology* **56**, 346–351 (2000).
 74. Aalinkeel, R. *et al.* The dietary bioflavonoid, quercetin, selectively induces apoptosis of prostate cancer cells by down-regulating the expression of heat shock

- protein 90. *Prostate* **68**, 1773–1789 (2008).
75. Lee, J. H., Shu, L., Fuentes, F., Su, Z.-Y. & Kong, A.-N. T. Cancer Chemoprevention by Traditional Chinese Herbal Medicine and Dietary Phytochemicals: Targeting Nrf2-Mediated Oxidative Stress/Anti-Inflammatory Responses, Epigenetics, and Cancer Stem Cells. *J. Tradit. Complement. Med.* **3**, 69–79 (2013).
76. Malireddy, S. *et al.* Phytochemical Antioxidants Modulate Mammalian Cellular Epigenome: Implications in Health and Disease. *Antioxid. Redox Signal.* **17**, 327–339 (2012).
77. Russo, G. L. *et al.* Dietary polyphenols and chromatin remodeling. *Crit. Rev. Food Sci. Nutr.* **57**, 2589–2599 (2017).
78. Shankar, S., Kumar, D. & Srivastava, R. K. Epigenetic modifications by dietary phytochemicals: Implications for personalized nutrition. *Pharmacol. Ther.* **138**, 1–17 (2013).
79. Wu, D. Sen *et al.* Epigallocatechin-3-gallate and trichostatin A synergistically inhibit human lymphoma cell proliferation through epigenetic modification of p16 INK4a. *Oncol. Rep.* **30**, 2969–2975 (2013).
80. Cho, S. *et al.* Quercetin suppresses proinflammatory cytokines production through MAP kinases and NF- κ B pathway in lipopolysaccharide-stimulated macrophage. *Mol. Cell. Biochem.* **243**, 153–160 (2003).
81. Gerritsen, M. E. *et al.* Flavonoids inhibit cytokine-induced endothelial cell adhesion protein gene expression. *Am J Pathol* **147**, 278–292 (1995).
82. Gohil, K. & Packer, L. Bioflavonoid-rich botanical extracts show antioxidant and

- gene regulatory activity. *Ann. N. Y. Acad. Sci.* **957**, 70–77 (2002).
83. Ishikawa, Y., Sugiyama, H., Stylianou, E. & Kitamura, M. Bioflavonoid quercetin inhibits interleukin-1-induced transcriptional expression of monocyte chemoattractant protein-1 in glomerular cells via suppression of nuclear factor-kappaB. *J. Am. Soc. Nephrol.* **10**, 2290–6 (1999).
84. Phillips, P. A. *et al.* Myricetin induces pancreatic cancer cell death via the induction of apoptosis and inhibition of the phosphatidylinositol 3-kinase (PI3K) signaling pathway. *Cancer Lett.* **308**, 181–188 (2011).
85. Tang, S. N. *et al.* The dietary bioflavonoid quercetin synergizes with epigallocatechin gallate (EGCG) to inhibit prostate cancer stem cell characteristics, invasion, migration and epithelial-mesenchymal transition. *J. Mol. Signal.* **5**, 1–15 (2010).
86. Singh, B. N., Shankar, S. & Srivastava, R. K. Green tea catechin , epigallocatechin-3-gallate (EGCG): Mechanisms , perspectives and clinical applications Catechin backbone. *Biochem. Pharmacol.* **82**, 1807–1821 (2011).
87. Horn-Ross, P. L. *et al.* Phytoestrogen consumption and breast cancer risk in a multiethnic population: The bay area breast cancer study. *Am. J. Epidemiol.* **154**, 434–441 (2001).
88. Mulligan, A. A., Welch, A. A., McTaggart, A. A., Bhaniani, A. & Bingham, S. A. Intakes and sources of soya foods and isoflavones in a UK population cohort study (EPIC-Norfolk). *Eur. J. Clin. Nutr.* **61**, 248 (2006).
89. Ross, J. A. & Kasum, C. M. Dietary flavonoids : Bioavailability , metabolic effects , and safety Reproduced with permission of the copyright owner . Further

- reproduction prohibited without permission . *Annu. Rev. Nutr.* **22**, 19–34 (2002).
90. Doetschman, T. C., Eistetter, H. & Katz, M. The in vitro development of blastocyst-derived embryonic stem cell lines: Formation of visceral yolk sac, blood islands and myocardium. *J. Embryol. Exp. Morphol.* **VOL. 87**, 27–45 (1985).
91. Hooper, M., Hardy, K., Handyside, A., Hunter, S. & Monk, M. HPRT-deficient (Lesch-Nyhan) mouse embryos derived from germline colonization by cultured cells. *Nature* **326**, 292–5
92. Richardson, C., Yan, S. & Vestal, C. G. Oxidative stress, bone marrow failure, and genome instability in hematopoietic stem cells. *Int. J. Mol. Sci.* **16**, 2366–2385 (2015).
93. Yi, L. L. *et al.* Topoisomerase II β -mediated DNA double-strand breaks: Implications in doxorubicin cardiotoxicity and prevention by dexrazoxane. *Cancer Res.* **67**, 8839–8846 (2007).
94. Deng, S. *et al.* Dexrazoxane may prevent doxorubicin-induced DNA damage via depleting both Topoisomerase II isoforms. *BMC Cancer* **14**, 1–11 (2014).
95. Shaikh, F. *et al.* Cardioprotection and second malignant neoplasms associated With dexrazoxane in children receiving anthracycline chemotherapy: A systematic review and meta-Analysis. *J. Natl. Cancer Inst.* **108**, (2016).
96. Smith, N. A., Byl, J. A. W., Mercer, S. L., Dewese, J. E. & Osheroff, N. Etoposide quinone is a covalent poison of human topoisomerase II β . *Biochemistry* **53**, 3229–3236 (2014).
97. Chou, T.-C. Theoretical Basis, Experimental Design, and Computerized Simulation of Synergism and Antagonism in Drug Combination Studies.

- Pharmacol Rev* **58**, 621–81 (2006).
98. Richardson, C. & Jasin, M. Frequent chromosomal translocations induced by DNA double-strand breaks. *Nature* **405**, 697 (2000).
 99. Riddell, I. A., Agama, K., Park, G. Y., Pommier, Y. & Lippard, S. J. Phenanthriplatin Acts As a Covalent Poison of Topoisomerase II Cleavage Complexes. *ACS Chem. Biol.* **11**, 2996–3001 (2016).
 100. Canela, A. *et al.* DNA Breaks and End Resection Measured Genome-wide by End Sequencing. *Mol. Cell* **63**, 898–911 (2016).
 101. Tower, R. L. & Spector, L. G. The epidemiology of childhood leukemia with a focus on birth weight and diet. *Crit. Rev. Clin. Lab. Sci.* **44**, 203–242 (2007).

APPENDIX I: CURRENT CURRICULUM VITAE

Education and Advancement:

Doctorate of Philosophy, Candidate in Biological Sciences, University of North Carolina at Charlotte, 2015 - 2020

Non-Thesis Masters, Biological Sciences, University of North Carolina at Charlotte, 2019

Graduate Certificate, University and College Teaching, University of North Carolina at Charlotte, 2018

Bachelor of Science, Biology, Queens University of Charlotte, 2014; Minor: Psychology

Professional Experience:

2018 - 2020 Teaching Assistant, University of North Carolina Charlotte, Dept. of Biological Sciences, *Cell Biology, Genetics, & Anatomy and Physiology I Lab*

2016 - 2017 Research Assistant, University of North Carolina Charlotte, Dept. of Biological Sciences

2015 - 2016 Teaching Assistant, University of North Carolina Charlotte, Dept. of Biological Sciences

2014 - 2015 Student Intern, Carolinas Healthcare System; Carolinas Medical Center, General Surgery Research

2013 - 2014 Independent Study, Queens University of Charlotte, Dept. of Biology

2013 Independent Study, Queens University of Charlotte, Dept. of Chemistry

2013 Laboratory Assistant, Queens University of Charlotte, Dept. of Biology

Research Interests and Skills:

- DNA damage and repair, cancer development, progression, metastasis and treatment, epigenetic gene regulation, neurodegeneration, immune response in cancer, and therapeutic delivery platforms
- Confocal Microscopy, Flow Cytometry, Immunocytochemistry, Mammalian Tissue Culture, Animal Handling (Rat and limited mouse), Plasmid Design, Cellular Transformation/Transfection, PCR, Western Blotting, ELISAs, GraphPad PRISM

Peer Reviewed Publications:

1. Lalwani K, **Goodenow D.**, Richardson C, *Eukaryotic Recombination: Initiation by Double-strand Breaks. In eLS, (Ed.). Under review.*

2. **Goodenow D.**, Emmanuel F., Berman C., Sahyouni M., & Richardson C. Bioflavonoids cause chromosome breaks and translocations through topoisomerase II-dependent and -independent mechanisms. *Mutation Research – Genetic Toxicology and Environmental Mutagenesis*. 2020 Jan; 849:503144 PMID: 32087851

3. Bariar B., Vestal C.G., Deem B., **Goodenow D.**, Ughetta M., Engledove R.W., Sahyouni M., and Richardson C. Bioflavonoids promote stable translocations between MLL-AF9 breakpoint cluster regions independent of normal chromosomal context: Model system to screen environmental risks. *Environmental and Molecular Mutagenesis*. 2019 Mar; 60(2):154-167 PMID:30387535.

4. Powell R.D., Raynor N.E., **Goodenow D.A.**, Jacobs D.D., & Stallion A. Examining the role of follow-up skeletal surveys in non-accidental trauma. *American Journal of Surgery*. 2017 Apr; 213(4):606-610. PMID: 28007317
5. Powell R.D., **Goodenow D.A.**, Mixer H.V., McKillop I.H., & Evans S.L. Cytochrome c limits oxidative stress and decreases acidosis in a rat model of hemorrhagic shock and reperfusion injury. *Journal of Trauma and Acute Care Surgery*, 2017 Jan; 82(1):35-41. PMID: 27602909
6. Powell R.D., **Goodenow D.A.**, Christmas A.B., McKillop I.H., & Evans S.L. Effect of systemic triphenylphosphonium on organ function and oxidative stress. *The American Surgeon*. 2018 Jan; 84(1):36-42. PMID: 29428024

Funding and Awards Received:

- | | |
|------|---|
| 2019 | Environmental Mutagenesis and Genomics 50 th Annual Meeting, 1 st place Student Platform Presentation |
| 2019 | Environmental Mutagenesis and Genomics 50 th Annual Meeting, Student Travel Award |
| 2019 | Graduate School Summer Fellowship, UNC Charlotte |
| 2018 | UNC Charlotte 3 Minute Thesis Competition, 2 nd Place |
| 2018 | 1 st Southern Genome Maintenance Conference, Best Student Oral Presentation |
| 2018 | Graduate Research Symposium, 3 rd place in Oral Presentation, Physical and Natural Sciences |

Research Presentations and Posters:

- | | |
|------|--|
| 2019 | Goodenow D.A. , Richardson C. Bioflavonoids induce DNA Double-Strand Breaks by Topoisomerase II-dependent and –independent Mechanisms. <i>Environmental Mutagenesis and Genomics Society Meeting. Sept. 2019. Washington, D.C. USA. Platform Presentation.</i> |
| 2019 | Goodenow, D.A. , Richardson C. Characterization of both topoisomerase II-dependent and –independent induction of DNA double-strand breaks, damage signaling pathways, and chromosomal translocations by sub-groups of bioflavonoids. <i>AACR: Environmental Carcinogenesis: Potential Pathway to Cancer Prevention. June 2019. Charlotte, North Carolina, USA. Poster Presentation.</i> |
| 2018 | Goodenow, D.A. , Richardson C. <i>Bioflavonoids induce persisting DNA double strand breaks and chromosomal translocations. 1st Southern Genome Maintenance Conference. Oct. 2018. Mobile, Alabama, USA. Oral and Poster Presentation.</i> |
| 2018 | Goodenow, D.A. , Richardson C. <i>Bioflavonoids cause sustained DNA damage in a drug- and dose-dependent manner that correlates with the promotion of chromosomal translocations. Environmental Mutagenesis and Genomics Society Meeting. Sept. 2018. San Antonio, Texas, USA. Poster Presentation and Flash Talk.</i> |
| 2018 | Goodenow, D.A. , Richardson C. Biting off more than your DNA can handle: Bioflavonoids' impact on DNA damage. <i>Graduate Research Symposium: UNC Charlotte. April 2018. Charlotte, North Carolina, USA. Oral Presentation</i> |
| 2018 | Goodenow, D.A. , Richardson C. Examining the Negative Impacts of Bioflavonoids on DNA Repair Mechanisms in Mouse Embryonic Stem Cells. <i>24 Hours of Stem Cells. November 2017. Virtual Event. Oral Presentation.</i> |
| 2015 | Powell, R. D., Goodenow, D. A. , McKillop, I. H., & Evans, S. L. Triphenylphosphonium (TPP) is not an Inert Mitochondrial Delivery Mechanism. |

- SHOCK Society Annual Meeting. June 2015. Denver, Colorado, USA. Poster Presentation.*
- 2015 Powell, R. D., **Goodenow, D. A.**, McKillop, I. H., & Evans, S. L. Physiological Response to MitoQ After HSR is Organ Specific and Highly Varied. *SHOCK Society Annual Meeting. June 2015. Denver, Colorado, USA. Poster Presentation.*
- 2015 Powell, R.D., **Goodenow D.A.**, Fetcko, K.M., McKillop, I.H., & Evans, S.L. MitoQ Upregulation of Glutathione Peroxidase Activity is Associated with a Tissue Specific Decrease in Inflammation following Hemorrhage. *Keystone Symposia Conference: Mitochondria, Metabolism and Heart Failure. January 2015. Santa Fe, New Mexico, USA. Poster Presentation.*
- 2014 **Goodenow D.A.**, Koplas P., & Thomas, J. Why Did You Die? A Post-Mortem Analysis of Avian Tissues. *Annual Association of Southeastern Biologists Conference. April 2014. Spartanburg, South Carolina, USA. Poster Presentation.*

Service:

- 2019 - 2020 Student Activity Fees Commission**, University of North Carolina Charlotte, *Committee Chair*
- 2019 - 2020 Student Union Advisory Board**, University of North Carolina Charlotte, *Committee Chair*
- 2018 - 2019 Association of Biological Sciences Graduate Students**, University of North Carolina Charlotte, *President*
- 2018 - 2019 Student Activity Fees Commission**, University of North Carolina Charlotte, *At-Large Committee Member*
- 2018 Graduate and Professional Student Government**, University of North Carolina Charlotte, *Chair of Elections Committee*
- 2016 – 2019 UNC Chapel Hill**, *Annual NC DNA Day Ambassador*
- 2016 - 2017 Graduate and Professional Student Government**, University of North Carolina Charlotte, *Vice President*
- 2016 - 2017 Graduate Research Symposium Committee**, University of North Carolina Charlotte, *Committee Chair*
- 2015 - 2016 Graduate Research Symposium Committee**, University of North Carolina Charlotte, *Co-Chair of Sessions*
- 2015 - 2016 Graduate and Professional Student Government**, University of North Carolina Charlotte, *Finance Committee*
- 2014 - 2016 Undergraduate Research Consultant**, Queens University of Charlotte

Professional Memberships:

American Association for the Advancement of Science
 American Association for Cancer Research
 Environmental Mutagenesis and Genomics Society
 Graduate Women in Science

APPENDIX II: END-SEQ PRELIMINARY PROTOCOL

To determine where DNA DSBs occur across the genome, the Nussenzweig lab developed the molecular technique termed END-seq. Since this technique was developed in 2016, it has been improved upon to differentially detect between protein-bound and protein-free DSBs. The basic technique involves suspending cells treated with DNA damaging agents into agarose plugs. After these plugs have solidified, they are treated with lysis buffer, proteinase K and RNase. The plugs are then treated with exonucleases to blunt DSB ends to allow for DNA adaptors to be ligated to the broken ends. After ligation, the agarose plugs are digested to retrieve the DNA for shearing into lengths of approximately 170bp. The DNA is then purified and the sheared ends are ligated to a second DNA adaptor. PCR is then utilized to amplify the DNA bound by the two adaptors for sequencing. Once the data is sequenced the signals are analyzed and overlaid to the whole genome to determine where the DSBs occur.

This technique can be utilized by our lab to determine where DSBs occur in cells treated with bioflavonoids. The DSB signals could then be compared to where etoposide causes breaks and the treatment groups could also be compared to one another. I hypothesize that DSBs that overlap with etoposide DSB signals are occurring due to Top2-dependent mechanisms. It is also possible traditional poisons will have peaks in DSBs in areas of the genome distinctive from covalent poisons, since the kinetics of DSBs appear dependent upon poison type. I also predict this technique could potentially give insight on the Top2-independent mechanisms that bioflavonoids use to cause DSBs based upon the breakpoints detected. I hypothesize that DSB signals may overlap between different bioflavonoids, indicating bioflavonoids utilize similar Top2-

independent mechanisms. This technique has the potential to clarify and quantify the number and potential mechanisms bioflavonoids use to damage DNA.

Detailed Procedure and Current Progress

This section details the current progress made modifying END-seq protocol, described in Nussenzweig 2016, to our lab at UNC Charlotte.

Clean cut agarose from the CHEF Genomic DNA Plug Kit (170-3591) was melted in a 50C water bath, while MAG cells were trypsinized. 5×10^6 cells per plug were treated with etoposide (50 μM) or quercetin (100 μM) for 1h. After treatment, cells were washed with 1X PBS twice, centrifuged and supernatant discarded. 53 μL of cold cell suspension buffer was added for every count of 5×10^6 cells. This cell suspension was brought to room temperature for 5 minutes, after which 38 μL of melted agarose was added per plug. The solution was gently mixed to avoid air bubbles, then 100 μL of the solution was quickly added to the plug molds on ice. After solidifying for 20 minutes on ice, lysis buffer (2.5 mL) with Proteinase K (170 μL) was added. The Eppendorf Thermomixer C was utilized to heat the samples to 50C for 1h then 37C for 7h with intermittent mixing (15 seconds at 400rpm once every 15 minutes). After the samples were rinsed 3 times with 10mM Tris pH 8, 50mM EDTA (Wash buffer) and the samples were left at room temperature overnight in the Wash buffer.

Plugs were then rinsed with 10 mM Tris pH 8.0, 1mM EDTA (TE buffer). This TE buffer was then used to wash the plugs twice for 15 minutes on a platform mixer

130rpm at room temperature. TE buffer (2.5 mL) with 50 μ L of RNaseA for 1h at 37C with intermittent mixing (15 seconds at 400rpm once every 15 minutes). After RNaseA treatment, Wash buffer was used to wash plugs 4 times for 15 minutes on a platform mixer. Plugs were left in Wash buffer at 4C for up to 3 months.

Next Steps

Next, we will be blunting the DSB ends by washing the plugs in 15ml EB buffer (10 mM Tris pH 8.0) 4 times for 15 minutes on a horizontal platform mixer at 180rpm at room temperature. Plugs will then be equilibrated twice for 15 minutes in 1 ml NEB Exonuclease VII buffer in a rotator at room temperature before treatment with 50 units of Exonuclease VII in 100 μ l of NEB Exonuclease VII buffer for 1 hour at 37C with continuous mixing. After Exonuclease VII digestion, equilibration of plugs twice for 15 minutes in 1 ml NEBuffer 4 in a rotator will occur at room temperature. Treatment with 25 units of Exonuclease T in 100 μ l of NEBuffer 4 for 45 minutes at 25°C with continuous mixing will then occur. Finally, plugs will be washed 3 times for 15 minutes in 15ml EB buffer (10 mM Tris pH 8.0) on horizontal platform mixer at 180rpm at room temperature.

After blunting the DSBs, plugs will be equilibrated 3 times for 15 minutes in 1 ml NEBNext dA-Tailing reaction buffer in a rotator at room temperature. Each plug will be treated with 30 units of Klenow fragment exo- (NEB) in 100 μ l of NEBNext dA-Tailing reaction buffer. Plugs will then be washed in 1 ml NEBuffer 2 for 15 minutes in a rotator. After a-tailing, plugs will be added to 125 μ l NEB Quick Ligation buffer with 8,000 U of

NEB Quick ligase and 0.4 μ M of END- seq adapter 1 (*5'-Phos-GATCGGAAGAGCGTCGTGTAGGGAAAGAGTGUU[Biotin-dT]U[BiotindT]UUACACTCTTCCCTACACGACGCTCTTCCGATC*T-3' [*phosphorothioate bond]*) for 1 hour at 25°C with continuous mixing. Then plugs will be washed 4 times for 15 minutes in 1 ml of Wash buffer (Tris pH 8.0, 50mM EDTA) in a rotator at room temperature. Plugs will be equilibrated overnight in 45 ml of Wash buffer at 23°C in a ThermoMixer C (Eppendorf) with intermittent mixing (15 minutes without mixing, 15 seconds 400 rpm mixing).

Next the DNA will need to be sheared by sonication. To accomplish this, plugs will be washed 4 times for 15 minutes in 15 ml of TE buffer on a horizontal platform mixer at 180rpm at room temperature. Plugs will then be melted at 70°C for 2 minutes and equilibrate for 5 minutes in a water bath at 43°C. Digestion of plugs with with 0.4U of Agarase () for 45 minutes at 43°C will then occur. Freed DNA will be cleaned by drop-dialysis (dialysis membranes 0.1 μ m VCWP04700 Millipore, MA, USA) against 15ml TE buffer for 1 hour. 0.1% of SDS will then be added to the DNA and treatment with 80 μ g of proteinase K (Ambion) for 15 minutes at 50°C will occur. The total volume of the solution will then be brought to a volume of 130 μ l with TE buffer. DNA will be sheared with a Covaris S220 sonicator for 4 min at 10% duty cycle, peak incident power 175, 200 cycles per burst in a water bath maintained at 4°C (Sonication under these conditions resulted in DNA fragments with a median shear length of 170bp) in Covaris microTUBE AFA Fiber Pre-Slit Snap-Caps (6 \times 16mm). DNA from the same sample in different plugs will then be combined. DNA will be recipitated with 1 μ l of glycogen (Roche, 20 mg/ml) 0.1 volumes of 3M NaOAc pH5.2 and 2.5 volumes of 100% ethanol in dry ice for 15

minutes. Next, centrifugation at full speed in a standard microcentrifuge at 4 degrees for 15 minutes will occur. The pellet will be washed twice with 70% ethanol and solubilized in 70 μ l of TE low EDTA (10mM TrisHCl pH 8.0, 0.1mM EDTA).

We will purify the DNA from solution by washing 35 μ l of Dynabeads (MyOne Streptavin C1 Beads, ThermoFisher #650-01) twice with 1 ml Binding and Wash Buffer (1 \times BWB) (10 mM Tris-HCl pH8.0, 1 mM EDTA, 1 M NaCl, 0.1% Tween20) by pipetting up and down 6 times. Recovery of the beads will be done using a DynaMag-2 magnetic separator (12321D, Invitrogen). Washed beads will be resuspended in 70 μ l 2 \times Binding and Wash Buffer (2 \times BWB) (10 mM Tris-HCl pH8.0, 2 mM EDTA, 2 M NaCl) combined with 70 μ l of DNA from the 'Sonication and Shearing' steps and incubated at 24 $^{\circ}$ C for 30 minutes in a ThermoMixer C at 400 rpm (tubes vortexed every 10 minutes).

Bead bound biotinylated DNA will be washed the 3 times with 1 ml 1 \times BWB, twice with 1 ml EB buffer, once with 1 ml T4 ligase reaction buffer (NEB). Next, beads will be added to 50 μ l of end-repair reaction with T4 ligase reaction buffer, 0.4 μ M of dNTPs, 2.7 U of T4 DNA polymerase (NEB), 9 U of T4 Polynucleotide Kinase (NEB) and 1 U of Klenow fragment (NEB) and incubated at 24 $^{\circ}$ C for 30 minutes in a ThermoMixer C at 400 rpm (tubes vortexed every 10 minutes). After collecting beads with a magnetic separator, beads will be washed once with 1 ml 1 \times BWB, twice with 1 ml EB buffer, once with 1 ml NEBNext dA-Tailing reaction buffer (NEB).

The sheared DNA end will then be a-tailed by resuspending the beads in 50 μ l of A-tailing reaction with NEBNext dA-Tailing reaction buffer (NEB) and 20 U of Klenow fragment exo- (NEB). Incubation at 37 $^{\circ}$ C for 30 minutes in a ThermoMixer C at 400 rpm (tubes vortexed every 10 minutes) will then occur. Beads will be washed once with 1 ml

NEBuffer 2, then resuspended in 115 μ l of Ligation reaction with Quick Ligase buffer (NEB), 6,000 U of Quick Ligase (NEB) and 13 nM of END-seq adaptor 2 and incubated at 25°C for 30 minutes in a ThermoMixer C at 400 rpm.

(ENDseq-adaptor-2, 5'-Phos-

*GATCGGAAGAGCACACGTCUUUUUUUAGACGTGTGCTCTTCCGATC*T-3'*

*[*phosphorothioate bond], HPLC purified, 10 μ M oligo dissolved in NEB T4 DNA ligase reaction buffer was self-annealed by incubating it on a floater on 1L of water at 95°C that was left to cool to room temperature, diluted to 0.5 μ M and aliquoted)*

Beads will be washed 3 times with 1 ml 1 \times BWB, 3 times with 1 ml EB buffer, and resuspended in 8 μ l of EB and added to 10 μ l of USER reaction (containing 8 μ l of 2X Kapa HiFi HotStart Ready mix (Kapa Biosciences) and 2 μ l USER enzyme mix 1U/ μ l (NEB)) to digest hairpins on adapters. This solution will then be incubated at 37°C for 30 minutes and mixed with 1.5 μ l of 50 μ M TruSeq barcoded primer (5'-

CAAGCAGAAGACGGCATAACGAGATNNNNNN

GTGACTGGAGTTCAGACGTGTGCTCTTCCGATC*T-5'), 1.5 μ l of 50 μ M TruSeq

multiplex primer (5'-

AATGATACGGCGACCACCGAGATCTACACTCTTCCCTACACGACGCTCTTCC

GATC*T-3' * represents a phosphothiorate bond and NNNNNN a Truseq index

sequence, 20 μ l of 2X Kapa HiFi HotStart Ready mix (Kapa Biosciences) and 17 μ l of H₂O. Then PCR amplification will be performed (45 s at 98 C followed by 16 cycles of 15 s at 98°C, 30 s at 63°C, 30 s at 72°C followed by a final 5 min extension at 72°C).

Dynabeads will be removed and PCR reactions cleaned with Agencourt AMPure XP beads (Beckman Coulter). Products will be run on a 2% agarose gel and DNA at a distribution of 200–400bp will be gel purified using a QIAquick Gel Extraction Kit (Qiagen). DNA concentrations will be determined with KAPA Library Quantification Kit for Illumina Platforms (Kapa Biosystems). Sequencing with Illumina Nextseq500 (75bp single end reads) will be done according to the manufacturer's specifications.

These steps will be performed in collaboration with Dr. Jennifer Weller and Dr. Robert Reid, who will be helping with analysis of the sequencing result. If these preliminary experiments analyzing untreated cells, etoposide and quercetin treated cells, appear accurate and consistent with expectations, other bioflavonoids, doses and treatments with dexrazoxane can be performed. If not, troubleshooting will occur to determine how to optimize this procedure for our lab.